IN-20
216 088

Final Report

for

NASA-Marshall Grant NAG8-1302

Launch Vehicle Systems Analysis

Covering the Period June 3, 1996 to September 30, 1998

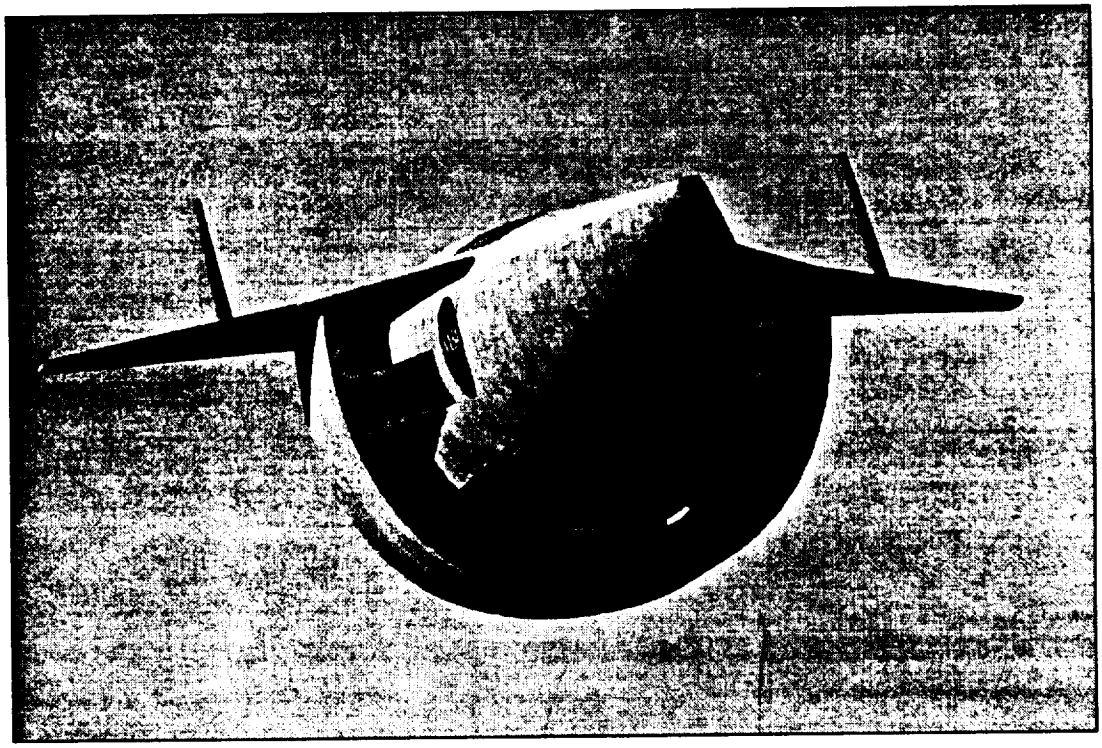

Submitted By:

Dr. John R. Olds, Project PI
Georgia Institute of Technology
Space Systems Design Lab
School of Aerospace Engineering
Atlanta, GA 30332-0150

Date Submitted:

January 27, 1999

Georgia Institute of Technology

School of Aerospace Engineering
Atlanta, Georgia 30332-0150 U.S.A.
PHONE 404-894-3000
FAX 404-894-2760

January 27, 1999

Mr. Uwe Hueter
Manager, ARTT Program
Mail Code PS03
NASA Marshall Space Flight Center
Huntsville, AL 35812

Dear Mr. Hueter,

Attached are the final report materials for NASA Grant NAG8-1302 entitled "Launch Vehicle Systems Analysis" that was conducted by the Space Systems Design Laboratory (SSDL) at the Georgia Institute of Technology during the period June 3, 1996 to September 30, 1998. The final report includes a summary of grant activities, copies of technical papers written during this grant, and presentation-style charts highlighting major grant activities.

In addition to providing generic RBCC design tool and process support to MSFC's Preliminary Design office (PD), our research under this grant was divided into four main topics. First, we have developed a new performance analysis tool for Rocket-Based Combined-Cycle engines. The new tool is called SCCREAM, and it is available to users on the World Wide Web. Second, we have conducted an independent Vision Vehicle design exercise to evaluate ejector scramjet RBCC propulsion for advanced HTHL launch vehicles. Our vehicle design is called *Hyperion*. Third, we actively supported Marshall's Bantam-X program to explore low cost, low payload launch vehicle designs. Georgia Tech developed and evaluated two RBCC concepts for Bantam-X – *Stargazer* and *Bantam Argus*. Lastly, we supported MSFC's Mars Exploration team during the summer of 1998 by evaluating several interplanetary trajectory options for a potential human mission.

I would like to thank you for your continued support of our research and educational activities in advanced space transportation system design. Partly with the support of this grant, the Space Systems Design Lab has grown from only 2 graduate students in 1996 to a more fully developed and capable research lab of 11 graduate students in 1998. Thanks to its sponsors, SSDL is becoming a unique resource for training students in the tools and methods of advanced vehicle design. We look forward to working with you and your organization on future projects.

Sincerely,

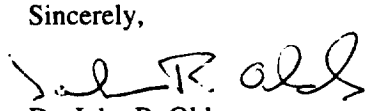

Dr. John R. Olds
School of Aerospace Engineering
Director, Space Systems Design Lab
Georgia Institute of Technology
Atlanta, GA 30332-0150
404-894-6289
john.olds@ae.gatech.edu

Final Summary of Grant Activities

Launch Vehicle Systems Analysis

Grant NAG8 –1302, NASA – Marshall Space Flight Center

For the period June 3, 1996 – September 30, 1998

Grant Background:

This report summaries the key accomplishments of Georgia Tech's Space Systems Design Laboratory (SSDL) under NASA Grant NAG8-1302 from NASA – Marshall Space Flight Center. The report consists of this summary white paper, copies of technical papers written under this grant, and several viewgraph-style presentations. The period of performance of this grant was June 3, 1996 to September 30, 1998.

Summary of Grant Accomplishments:

During the course of this grant, there were four main tasks completed by the PI and student members of the SSDL. These tasks were,

1) SCCREAM – A new computer analysis tool for predicting the performance of various RBCC engine configurations was originally developed and later improved under this grant. SCCREAM (Simulated Combined-Cycle Rocket Engine Analysis Module) is an object-oriented code written in C++. Version 5 (the latest version) is also accessible from the web at http://atlas.cad.gatech.edu/~jebradfo. SCCREAM is capable of quickly predicting thrust and Isp of a given RBCC engine configuration over a range of flight conditions and engine operating modes (ejector, ramjet, fan-ramjet, etc.). Unlike other airbreathing engine codes, SCCREAM is uniquely suited for use in a conceptual vehicle design environment — particularly where POST is used to perform trajectory optimization. This work was carried out by John Bradford, a graduate student in SSDL, from September 1996 to September 1998. He plans to continue improving SCCREAM and adding new capabilities under a NASA GSRP Fellowship that started in September 1998. SCCREAM is currently being used by NASA – MSFC personnel in PD and EP (George Kearns and D. R. Komar). Copies of SCCREAM technical papers are included as attachments to this report.

2) *Hyperion* – In support of its RBCC ground test program, NASA's ARTT office also solicited advanced launch vehicle designs from the various ARTT engine contractor teams. These RBCC Vision Vehicles were to be single-stage LOX/LH2 vehicles capable of

delivering 25,000 lb. payloads to the International Space Station orbit. Under this grant, Georgia Tech developed and refined an RBCC SSTO vehicle design based partially on the Vision Vehicle requirements. The Georgia Tech design is called *Hyperion*. It is a horizontal take-off, horizontal landing vehicle powered by 5 RBCC ejector scramjet engines. A set of ducted fans is also included for powered landing and loiter operations. Two versions of Hyperion were investigated — a baseline version capable of delivering 11,000 lb. to Space Station, and a Vision Vehicle version capable of delivering 25,000 lb. to Space Station. Both designs used non-proprietary tools and databases and the results were made available in the open literature. The *Hyperion* design was analyzed and refined over the period of this grant by a team of several graduate students in SSDL lead by John Bradford. Team skills and disciplines included aerodynamics, propulsion, trajectory optimization, mass properties, operations, configuration and packaging, cost analysis, and business simulation. The latest results from the *Hyperion* design are included as attachments to this report. Other grant-supported presentations made on *Hyperion* or RBCC Vision Vehicle mission requirements are also attached.

3) Bantam-X Support - In the late spring of 1998, a $25k supplement was added to this grant for an SSDL design team to address Bantam-X vehicle configurations. Bantam is a small payload mission (about 300 lb. to LEO) with a very aggressive launch price goal of less than $1M - $1.5M per launch. A team of several Georgia Tech students and the PI worked with NASA MSFC personnel (primarily D. R. Komar of EP) to develop a Bantam-class TSTO launch vehicle design called *Stargazer*. *Stargazer* uses a wedge shaped, reusable, flyback booster powered by 4 LOX/LH2 ejector scramjet RBCC engines and a LOX/RP expendable upper stage (with a Fastrac-derived engine). The Georgia Tech team performed a conceptual assessment of *Stargazer* including weight, performance, and cost. A second concept, *Bantam Argus*, was also briefly evaluated. The preliminary results for both designs are included as an attachment to this report. In addition, this grant supplement sponsored a summer internship at MSFC for Laura Ledsinger, a graduate student in SSDL. While at MSFC the summer of 1998, Ms. Ledsinger continued to make refinements to the *Stargazer* concept and provided various forms of trajectory support to PD and EP. A copy of Laura Ledsinger's summer research results are attached. She currently serves as the team leader for on-going *Stargazer* trade studies being conducted under a new NASA grant.

4) Interplanetary Trajectory Support - A second grant supplement in the amount of $6k was added in the summer of 1998 to support trajectory analysis for interplanetary human Mars missions being conducted by MSFC's Exploration office. This supplement supported a summer internship for Tara Poston, an undergraduate student in SSDL. Ms. Poston worked primarily with Larry Kos in PD evaluating various trajectory options and opportunities for Human Mars missions (e.g. departure dates, stay times, aerobrake vs. propulsion capture, and preliminary launch vehicle stack sizing). A summary presentation of Ms. Poston's summer research activities is included as an attachment.

Secondary Goal - Knowledge Transfer:

When initiated, one of the secondary purposes of this grant was to increase the cooperation between MSFC's advanced space vehicle design organizations (primarily the Preliminary Design office and some elements of the Advanced Space Transportation Program office) and Georgia Tech's Space Systems Design Lab. As the grant continued, this underlying cooperation was developed and maintained in the form of information exchange, design tool development, and "on-site" residency of the Georgia Tech PI at NASA during parts of the summers of 1997 and 1998. Also, the PI and the students in the SSDL at Georgia Tech often served as a remote resource for Preliminary Design (PD) in areas specifically related to RBCC launch vehicle design. SSDL has performed several conceptual RBCC launch vehicle designs using tools similar to those available to engineers in PD, and the NASA COTR had hoped by that SSDL would help to build a new capability to analyze and design RBCC launch vehicles within PD.

While good working relationships have developed between both organizations, actual transfer of RBCC vehicle design capabilities has not been entirely successful. At the end of this grant, it is still not clear that NASA MSFC has the capability to fully perform a complete conceptual design of an RBCC launch vehicle. The tools and computer resources are in place to do so (most were existing already, only GT's new SCCREAM and CABAM tools were added to the toolset). What then is the reason for lack of success in this area? While it is not the purpose of this report to recommend possible solutions to NASA, three areas are highlighted that, in the opinion of the PI, are keys to any successful design organization.

1) Management – A successful design organization depends on quality technical management. Management must provide motivation for the team, establish expectations of performance and schedule, monitor the team's progress, and initiate corrections as needed. In particular, management is responsible for assembling a team of personnel capable and willing to perform a given design task. Management must also establish a clear reward system based upon each employee's performance in the design environment. As a particular suggestion in this case, NASA management should also move to more fully integrate cost analysis into PD advanced design projects.

2) Lead Engineers/Systems Engineers – Lead engineers are the most critical component of a design team. They manage the flow of information between members of a team, set schedules, call meetings, and provide technical decision making. Lead engineers are knowledgeable of all of the individual disciplines within a process (cross-trained) and fully understand the data flow between them. They have considerable design experience and are typically promoted from within an organization. A good design organization will have 3-4 lead engineers so that more than one design project can be conducted simultaneously. PD

currently has a lack of lead engineers and a lack of disciplinary engineers even willing to serve as a lead engineer, partly because there is no organizational-level reward to progressing into that position. Also, previous lead engineers have often been given responsibility for a given project, without also being given the authority to manage his or her team members. A formal, continuous training program for lead engineers would also be beneficial.

3) Disciplinary Skills – Most design organizations will be at least "two deep" in every discipline. PD buyouts, retirements, and transfers have left its advanced design organization without trained, motivated personnel in several of the key engineering disciplines required to conduct a conceptual RBCC vehicle design. MSFC often asks its most motivated young engineers to handle two or three disciplines in an effort to cover the design space. Necessary computing tools are either in place or easily obtained. PD should be allowed to recruit new personnel to its advanced design organization. RBCC propulsion, aerodynamics, configuration, and mass properties are in particular need of additional depth.

Students Supported:

During the period of this grant, three Georgia Tech graduate students were directly supported with graduate research assistantship (GRA) monthly stipends and tuition reimbursement. An undergraduate student was also partially supported.

1) John E. Bradford (graduate student, GRA supported from 9/96 – 6/98)

2) Laura A. Ledsinger (graduate student, GRA, supported from 6/98 – 9/98)

3) Jeffery A. Scott (graduate student, GRA, supported from 6/98 – 9/98)

4) Tara Poston (undergraduate student, supported 6/98 – 8/98)

John Bradford was supported by the original grant. Laura Ledsinger and Jeff Scott were part of the Bantam-X Stargazer team and were supported by the Bantam-X grant supplement. Tara Poston was supported during her 1998 summer internship by the Exploration grant supplement.

Degrees Awarded:

One advanced degree was awarded during the period of this grant based partially on research work performed on tasks outlined above.

1) John E. Bradford, Master of Science in Aerospace Engineering, December 1997.

After earning his MS AE in December of 1997, Mr. Bradford is continuing his research on SCCREAM and is currently a Ph.D. student in AE at Georgia Tech. He has been supported by a NASA GRSP Fellowship since September of 1998. Jeff Scott, who was supported by this grant for several months during the summer of 1998 as part of the *Stargazer* team, earned an MS in AE in December 1998 (just after the grant concluded).

Travel & Summer Activities:

The following travel was taken in support of activities related to this grant.

1) Dr. John Olds spent four weeks at NASA MSFC during the summer of 1997. This time was spent working with PD (primarily Steincamp, Brady, and Pannell) to improve the RBCC design process, understand tools, review PD designs, etc.

2) John Bradford spent eight weeks at NASA MSFC during the summer of 1997 working on SCCREAM and conducting *Hyperion* trade studies. During this time he worked with Bill Pannell in PD and was supported by the NASA Academy program.

3) Dr. John Olds and John Bradford attended the 37th AIAA Joint Propulsion Conference in Seattle, WA in July 1997 to present a technical paper on SCCREAM (AIAA 97-2760).

4) Dr. John Olds, John Bradford, David McCormick, and David Way attended a NASA RBCC Workshop and Review held at UAH in Huntsville, February 1998.

5) Dr. John Olds spent fours weeks at NASA MSFC during the summer of 1998. Part of this time was spent working with engineers in PD (Swalley), and part of the time was spent in AST. The primary goal was to improve PD's RBCC design process and provide assistance as necessary with design tools.

6) Laura Ledsinger spent eight weeks at NASA MSFC on an internship during the summer of 1998. She worked primarily with PD (Swalley), but also worked closely with D. R. Komar from EP. Her primary task was to continue *Stargazer* trade studies and assess branching trajectories.

7) Tara Poston spent nine weeks on an undergraduate internship at NASA MSFC during the summer of 1998. She conducted trajectory analyses for PD's Exploration team (Kos).

8) Dr. John Olds and John Bradford attended the 38th AIAA Joint Propulsion Conference in Cleveland, OH in July 1998 to present a technical paper on SCCREAM improvements (AIAA 98-3775).

Papers Published & Presented:

Two AIAA papers were published during this grant based on the research program outlined above. Copies of these papers are included as attachments to this final report.

1) Olds, J. R. and J. Bradford., "SCCREAM (Simulated Combined-Cycle Rocket Engine Analysis Module): A Conceptual RBCC Engine Design Tool," AIAA 97-2760, 33rd AIAA/ASME/SAE/ASEE Joint Propulsion Conference and Exhibit, Seattle, WA, July 1997.

2) Bradford, J. E. and Olds, J. R., "Improvements and Enhancements to SCCREAM, A Conceptual RBCC Engine Analysis Tool," AIAA 98-3775, 34th AIAA/ASME/SAE/ASEE Joint Propulsion Conference and Exhibit, Cleveland, OH, July 12 - 15, 1998.

In addition to these two papers that have already been published, two new papers are currently being written that document *Hyperion* and *Stargazer* vehicle design results. These papers will be presented at an upcoming AIAA Spaceplanes conference.

Plans for Continuing Space Transportation Research:

Our Space Systems Design Lab team is fortunate to have been selected for a new three-year grant by NASA's Advanced Space Transportation Program (ASTP) office. This new grant will allow us to continue our research and education program in the areas related to advanced space transportation including propulsion, performance, cost, and mass properties.

"Launch Vehicle Systems Analysis"

NAG8 – 1302

Final Report Attachments

NAG8-1302 Report Attachments

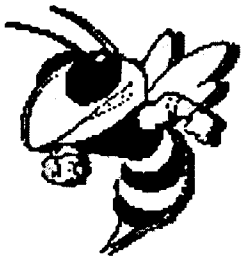

- SCCREAM Development
  - SCCREAM summary slides (Bradford, 1998 AIAA JPC)
  - 1998 and 1997 technical papers (Bradford/Olds)
- *Hyperion* Vehicle
  - Current *Hyperion* status slides (SSDL team/Bradford, 1/99)
  - RBCC vehicle "Honest Assessment" slides (Olds, 2/98 RBCC Workshop)
  - RBCC vehicle "Better Direction" slides (Olds, 1998 NASA summer stay)
  - 1997 *Hyperion* trade studies (Bradford, 1997 summer internship)
- 1998 Bantam-X Support
  - 1998 LOX/LH2 *Stargazer* overview slides (SSDL team/Ledsinger, 1/99)
  - *Stargazer* staging Mach number trade study (Ledsinger, 1998 summer internship)
  - 1998 *Bantam Argus* overview slides (SSDL team/Way, 6/98)
- 1998 Mars Exploration Support
  - Mars Mission trajectory evaluation slides (Poston, 1998 summer internship)

SCCREAM

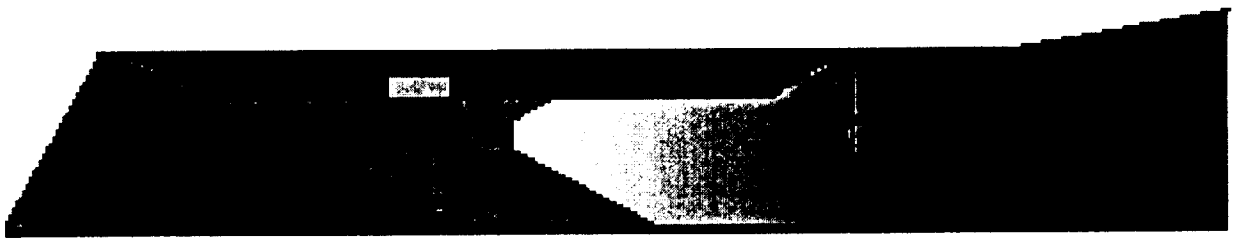

Simulated Combined Cycle Rocket Engine Analysis Module

John E. Bradford
Dr. John R Olds
Space Systems Design Lab
Georgia Institute of Technology
Atlanta, Georgia

What is RBCC Propulsion?

- Combines elements of rocketry and air-breathing engines into single unit
- Capable of many different mission scenarios
- Provide loiter, fly-back, and abort capability
- Many different operating modes (ducted rocket, ramjet, scramjet, rocket)

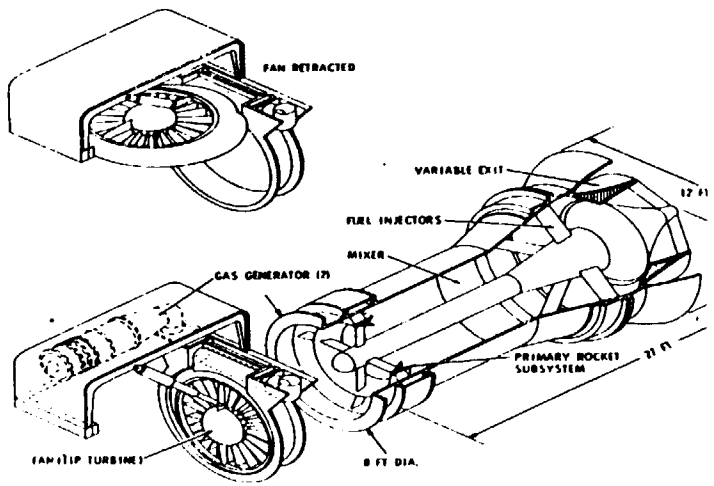

Supercharged Ejector Ramjet (SERJ)

History of SCCREAM

- Initially spreadsheet based tool started by
- Dr. John Olds (NCSU) as part of PhD dissertation work
- Further expanded by Greg Saks (GT) in 1995 to include fan-ramjet and ramjet mode analysis
- Current format began in 1996 as Master's degree research work at Georgia Tech
- Under development for 2 years with funding by NASA MSFC

GT

Research Rationale

- Need a quick, accurate tool for modeling RBCC and airbreathing engine performance, suitable for use in the conceptual launch vehicle design environment
- Need to allow trade studies for:
  - Transition Mach numbers - Engine Geometry
  - Dynamic pressure boundary - Forebody Shape
  - Secondary to primary flow ratio

GT

What is SCCREAM?

- Written in ANSI C++ and executes on Unix workstation
- Analyzes all modes of engine operation for H_2/O_2 RBCC engine configurations
- Generates engine performance at 100's of flight conditions in under a minute
- Provides formatted POST engine deck

GT

Modeling Assumptions

- Quasi 1-D flow using conservation equations: mass, momentum, energy
- Inlet modeled using curve fit for total pressure recovery
- Efficiency factors used to account for friction, heat loss, and poor mixing
- Complete combustion with fuel efficiency factor
  - Species Considered: H_2, O_2, H_2O, N_2, Ar

Engine Station Identification

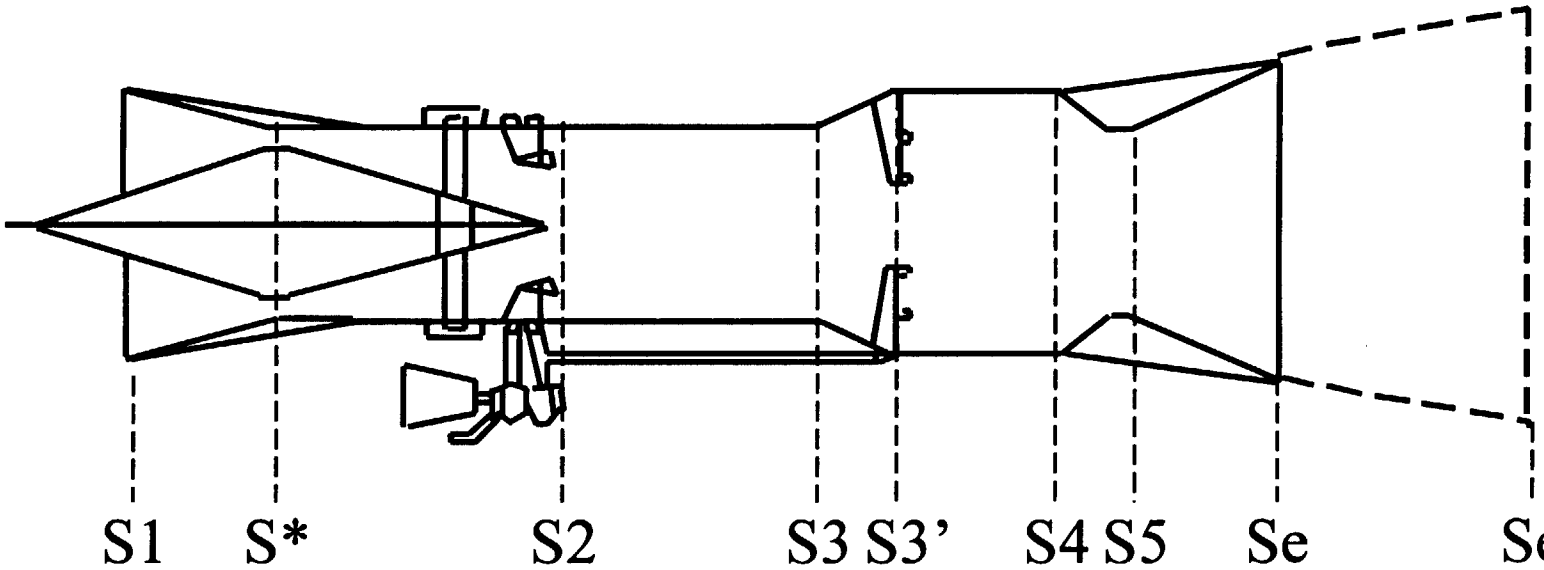

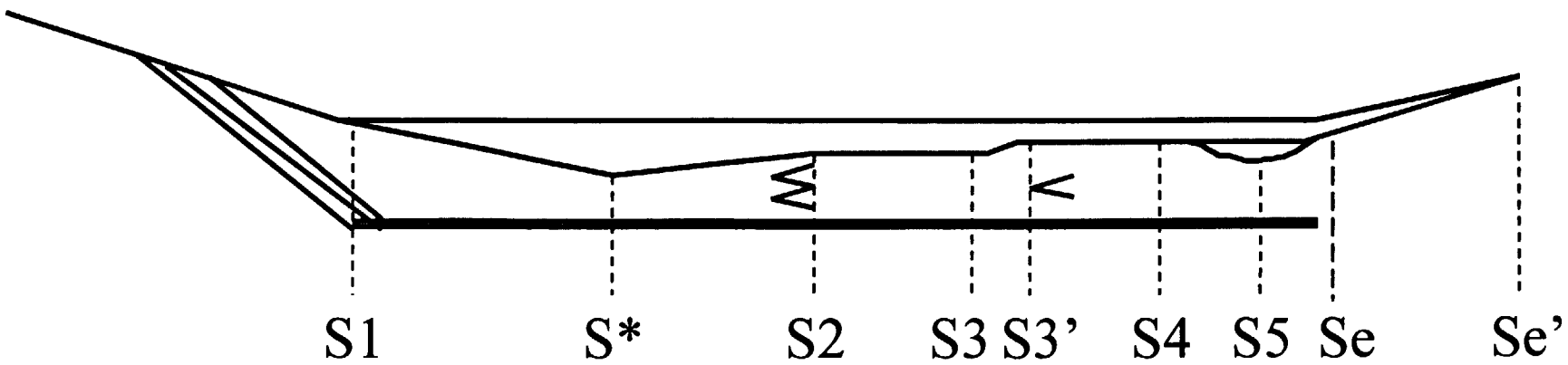

Previous Version Limitations

- No scramjet analysis capability
- Only stoichiometric, ideal H_2/O_2 rocket primary
- Simplified conical forebody analysis
- Used specific heat values for each species based on a fixed hot/cold flow temperature
- Text-based user interface

Recently Added Capabilities

- Scramjet mode analysis
- Higher fidelity rocket primary combustion process
- Hydrogen-Peroxide (H_2O_2) rocket primary at 3 different concentrations
- Web-based user interface
- 2-D conical forebody analysis
- Additional POST deck information

GT

Web Interface

http://atlas.cad.gatech.edu/~jebradfo

INPUTS

- engine configuration
- inlet (cowl) area
- required thrust or mp
- forebody type and angle
- primary characteristics
- engine area ratios
- engine efficiencies

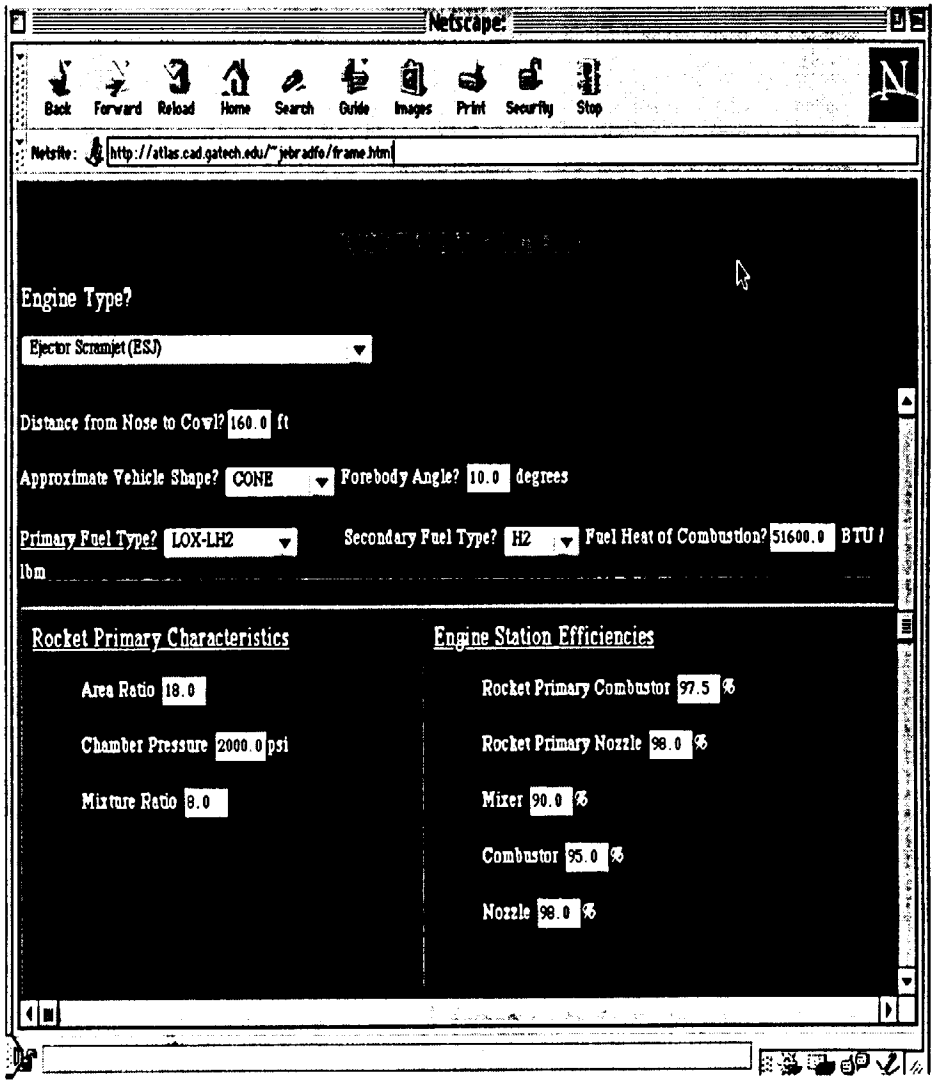

Trajectory Supplied Output

- Thrust, thrust coefficient, maximum static pressure is provided for each engine mode
- Rocket Mode Thrust and Isp

```
$tblmlt genv6m= 2938.36, tvc1m= 8,tvc2m=  1,  5hgenv5, tvc3m=1,
 $
l$tab table=5htvc1t,2,4hmach,6haltito,31,17,8*1,
 0,
          0,        150000,
        0.1,         148073,
        0.2,         147205,
        0.3,         147353,
        0.4,         148499,
        0.5,         150652,
        0.6,         153847,
        0.7,         158143,
        0.8,         163626,
        0.9,         170407,
```

rbcc.dat file

Rocket Primary Subsystem

- Mole fractions, total temperature, and specific heat ratio determined from RSE's

  $X = a*Pc + b*Pc2 + c*MR*Pc + d*MR + e*MR2$

- SCCREAM modified to handle non-stoichiometric primary
- Can specify H_2O_2 monopropellant in concentrations of 85%, 90%, and 98%

GT

Comparisons With RJPA

- RJPA ran to compare with new SCCREAM scramjet results
- 10° forebody, dynamic pressure 2000 psf
- Inlet mass capture matched with SCCREAM
- Same inlet efficiency and engine geometry
- Maximum Phi=1 (minimum 0.5)
- Nozzle efficiency 98%
- Frozen-to-Equilibrium ratio 0.667

GT

SCCREAM vs. RJPA
Thrust Coefficient

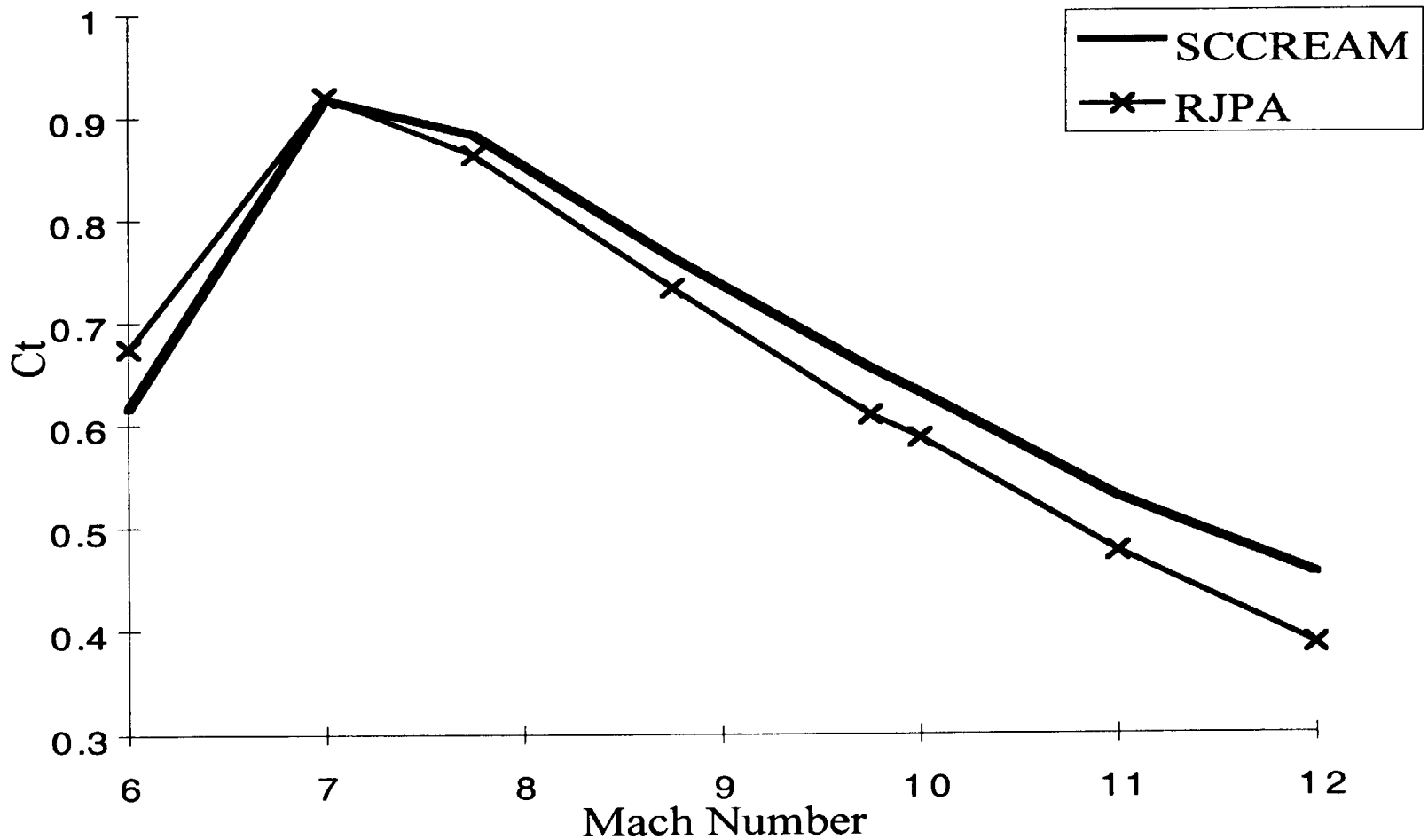

SCCREAM vs. RJPA
Specific Impulse

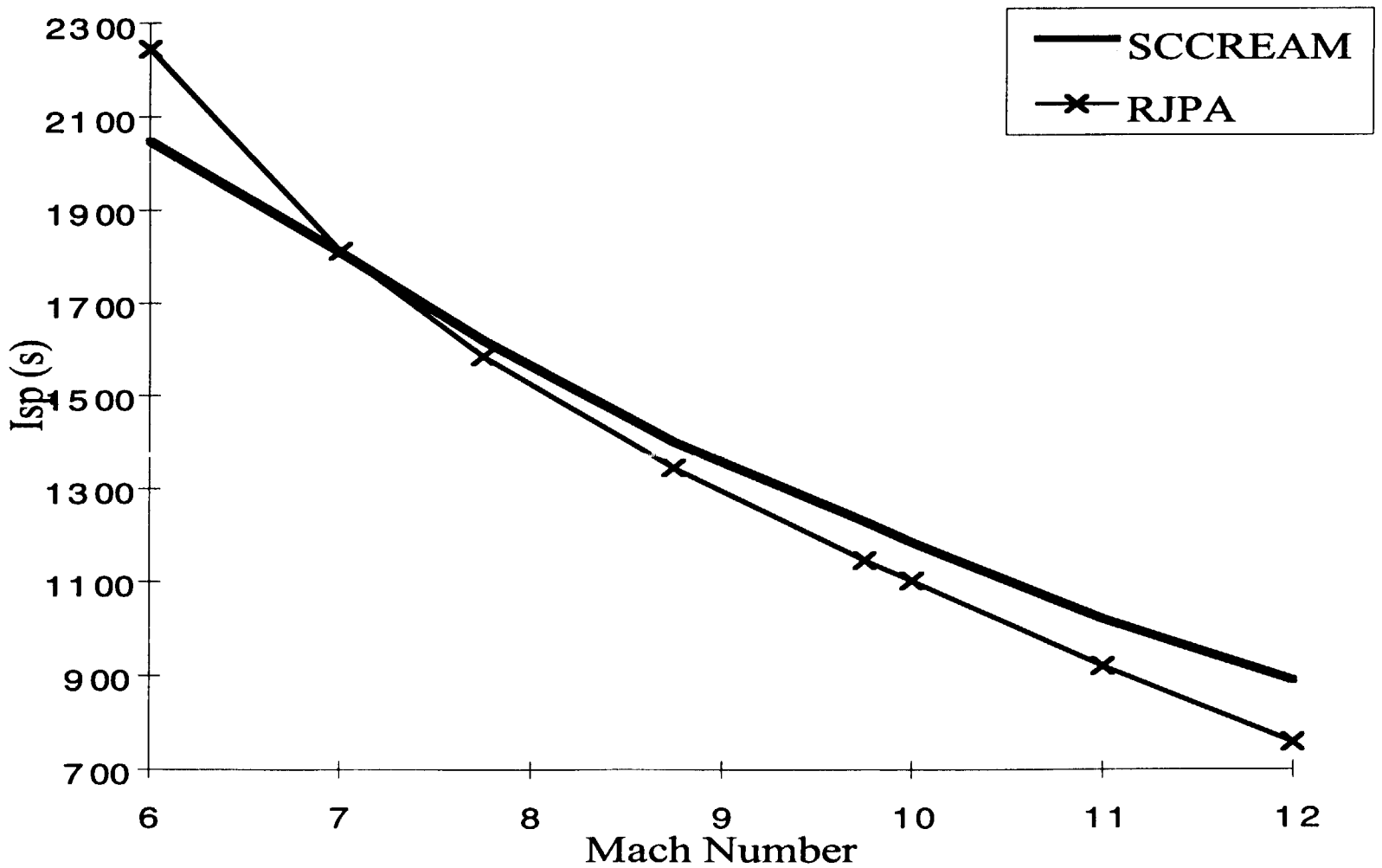

Specific Run Data

		Mach 6		Mach 8.75		Mach 10	
	Flow Property	*SCCREAM*	*RJPA*	*SCCREAM*	*RJPA*	*SCCREAM*	*RJPA*
Diffuser Exit	Mach	3.74	4.11	5.03	5.24	5.27	5.56
	Ps (psi)	3.54	3.70	2.83	2.59	2.39	2.14
	Ts (R)	605.1	722.5	768.8	1004.0	927.3	1188.60
Combustor Exit	Mach	1.21	1.09	1.96	1.87	2.36	2.31
	Ps (psi)	25.16	36.47	17.68	19.09	11.94	12.36
	Ts (R)	3195.4	4009.3	4713.9	4906.3	4792.2	4847.20
	Gamma	1.281	1.267	1.245	1.250	1.245	1.25
	Mol. Wgt	26.45	26.55	24.31	23.81	24.31	23.76
Nozzle Exit	Mach	3.17	3.12	3.49	3.43	3.84	3.80
	Ps (psi)	1.10	1.41	1.23	1.25	0.91	0.92
	Ts (R)	1643.7	1933.4	2831.1	2776.8	2908.2	2813.30
	Gamma	1.328	1.315	1.270	1.282	1.272	1.28

Reference Concept for Comparisons

- 'Hyperion' SSTO Vision Vehicle
- 9.2° conical forebody
- 5 ESJ engines with thrust,sls = 90 klbs ea.
- Dynamic pressure
  - 1500 psf in ramjet mode to Mach 5.5
  - 2000 psf in scramjet mode to Mach 10

GT

Hyperion Color Slide

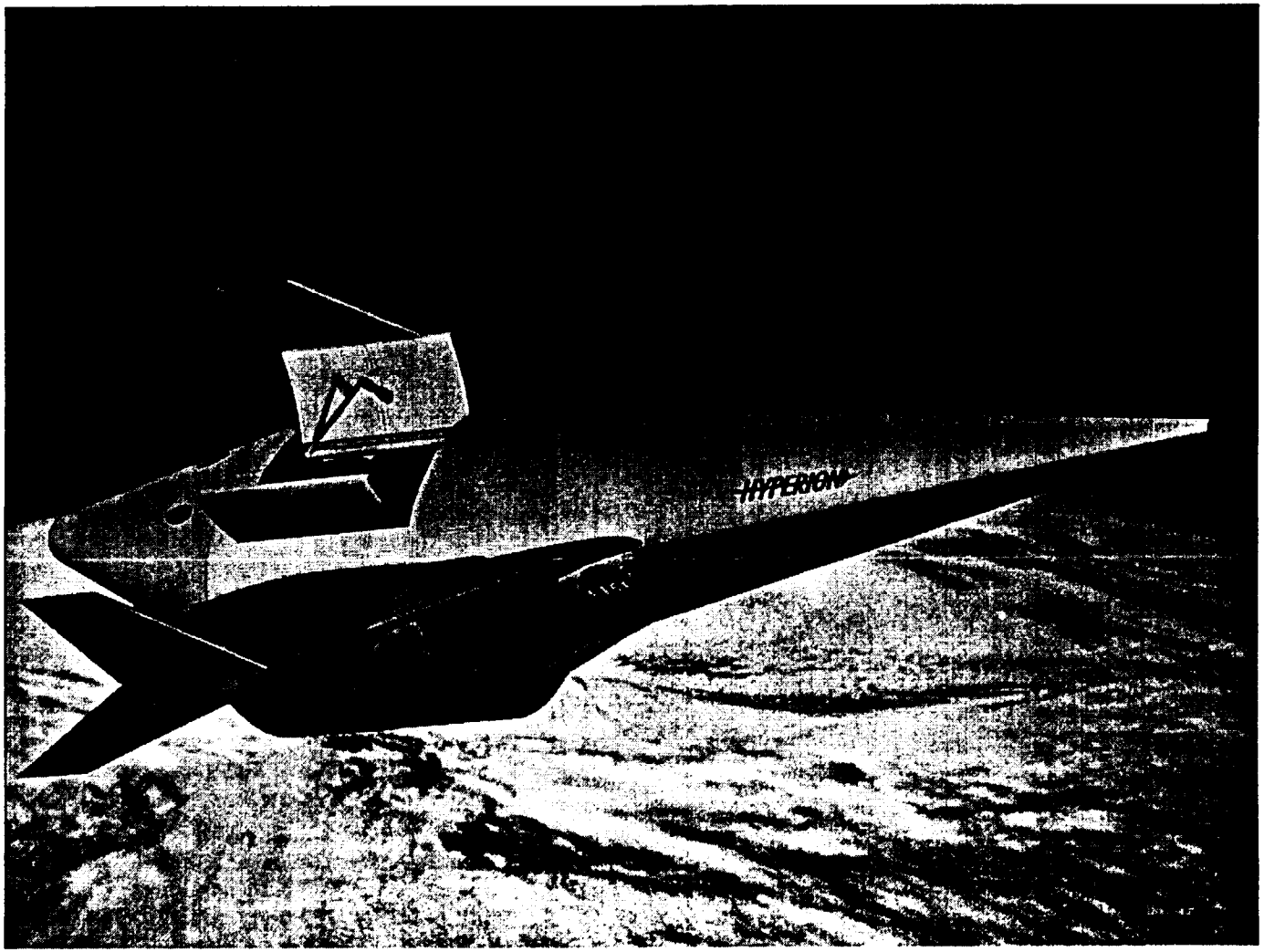

Comparisons With Other Codes

- RJPA data from previous results
- RAMSCRAM data for ramjet and scramjet modes for similar geometry, mass capture, and flight path as Hyperion concept
- SRGUL data for pure scramjet configuration with 5° conical forebody

GT

Thrust Coefficient

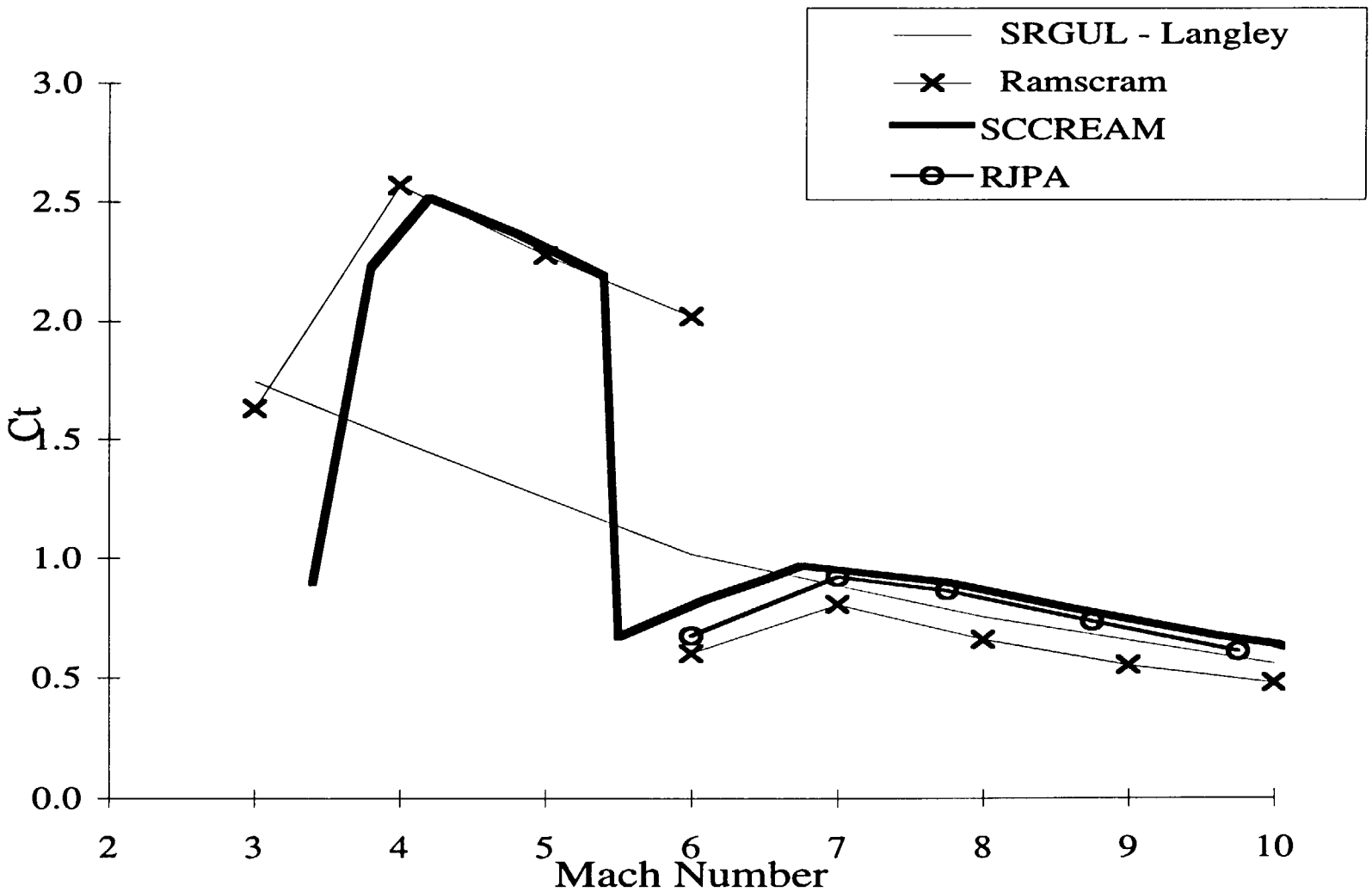

Specific Impulse

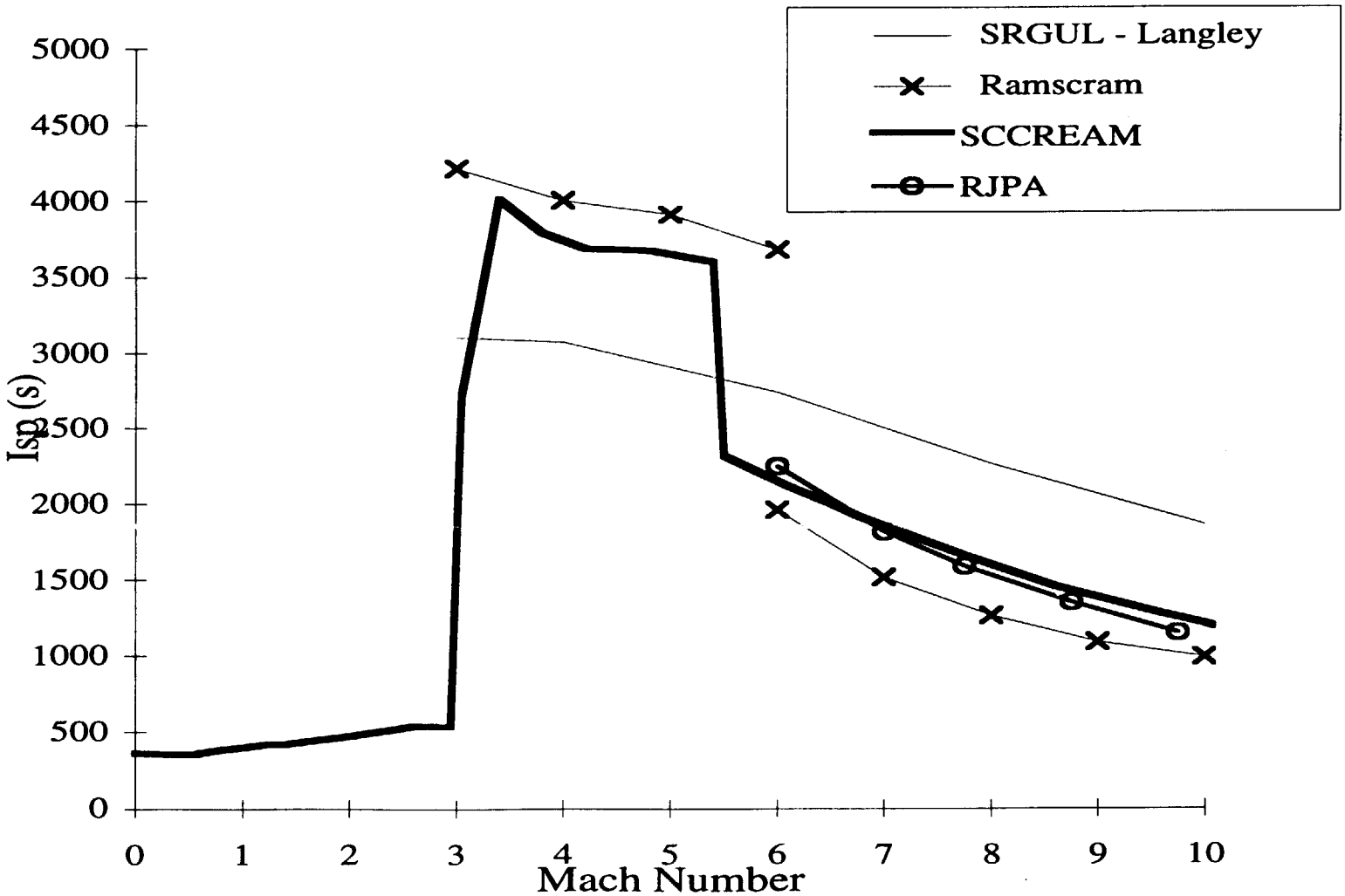

Comparisons with Historical Data

- NAS7-377 Marquardt Results from study in 1960's for ERJ and ESJ configurations with 8° conical forebody and q=1500 psf trajectory
- Astronautics Corporation data from 1988 for ESJ engines on vehicle with 6° wedge forebody

Thrust Coefficient

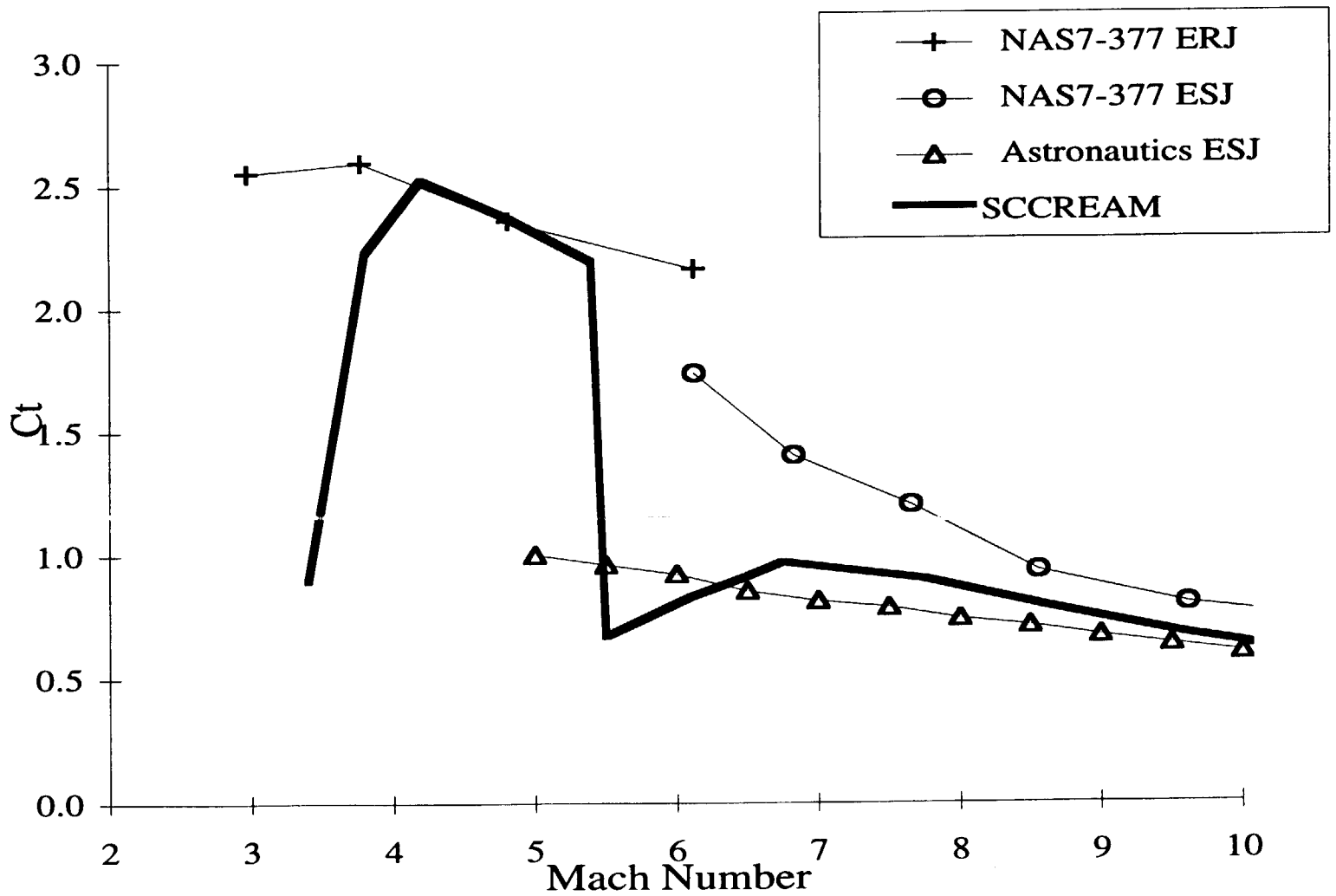

Specific Impulse

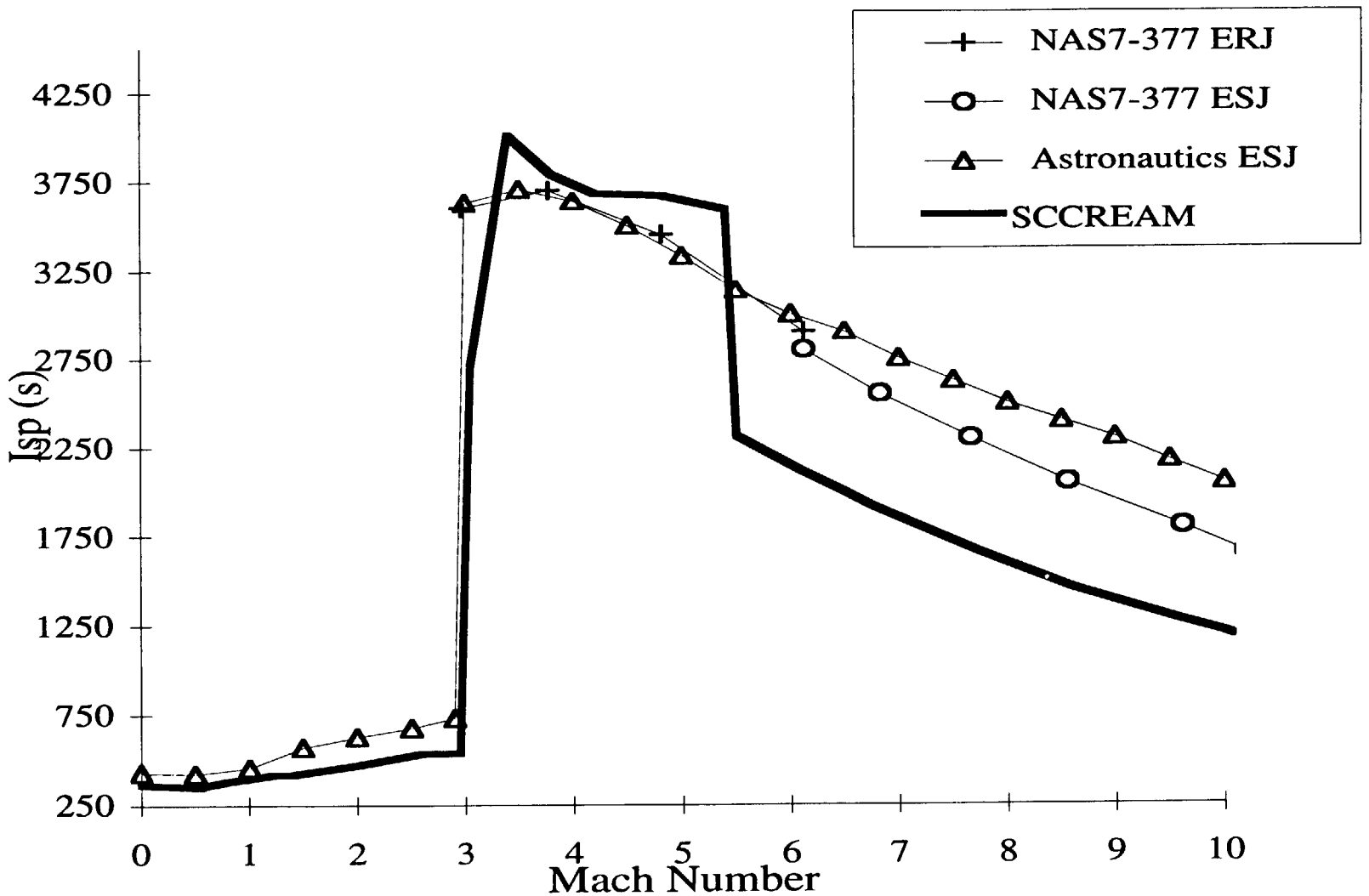

Future Work

- New combustor model with diverging area, friction, and heat loss effects
- Multiple forebody compression ramps
- Angle of attack effects on inlet performance
- Addition of scram-rocket mode for thrust augmentation at high Mach numbers
- Hydrocarbon fuels in primary and afterburner

GT

Improvements and Enhancements to SCCREAM, A Conceptual RBCC Engine Analysis Tool

John E. Bradford[†]
Dr. John R. Olds[*]
Space Systems Design Lab
School of Aerospace Engineering
Georgia Institute of Technology, Atlanta, GA

ABSTRACT

A rocket based combined-cycle engine analysis tool suitable for use in the conceptual design environment has recently been established. While this tool was being used in the design environment, new analysis capabilities were desired and areas for improvement were noted.

This paper will detail the recent improvements made to the conceptual design tool, SCCREAM, and present the results generated by the added capabilities. The improvements range from an additional engine analysis mode, alternate propellant combinations, and a new user-interface which enables remote execution.

The improvements and added capabilities to SCCREAM will be discussed and the program methodology will be examined in detail when appropriate. Results generated by SCCREAM's new scramjet analysis mode are then shown to compare very well with an industry standard code, RJPA. Engine performance generated by SCCREAM for a single stage to orbit launch vehicle are then compared with historical airbreathing engine performance data, and other industry common analysis codes.

NOMENCLATURE

A_c	normalizing area for thrust coefficient (ft^2)
A_i	engine cross-sectional area at station *i* (ft^2)
Ar	argon
C_p	constant pressure specific heat (BTU/slg-R°)
C_t	thrust coefficient (thrust/q*A_c)
H_2O_2	hydrogen peroxide
H	monatomic hydrogen
H_2	hydrogen
I_{sp}	specific impulse (sec)
K	kelvin
LH2	liquid hydrogen
LOX	liquid oxygen
MR	propellant mixture ratio
N_2	nitrogen
O	monatomic oxygen
O_2	oxygen
OH	hydroxyl radical
P_c	chamber pressure (psi)
P_t	total pressure (psi)
phi	combustor equivalence ratio
q	freestream dynamic pressure (lb/ft^2)
V_r	radial velocity component
V_θ	normal velocity component
γ	ratio of specific heats
θ	ray angle from cone centerline

RBCC BACKGROUND

Rocket Based Combined-Cycle (RBCC) represents a new approach for providing routine access to space. By integrating the elements of rocketry and air-breathing systems into a single unit, RBCC tries to exploit the best qualities of each. The rocket primary is used for providing the high level of thrust required at

takeoff conditions and for acceleration until ramjet takeover speeds can be obtained. Once ramjet operation is feasible, the rocket primary is shut off to conserve fuel. The airbreathing modes of ramjet and scramjet are then used to accelerate the vehicle through the portions of the atmosphere where free oxygen is available. As the vehicle climbs and increases its speed, a point will be reached at which the ramjet or scramjet is no longer providing enough thrust to sufficiently accelerate the vehicle. For single stage to orbit (SSTO) configurations, it is at this point that the rocket primary is re-ignited and the vehicle proceeds directly to orbit.

RBCC is not a new concept. Originating in the 1960's, a variety of basic concepts were developed considerably under a joint effort by the Marquardt Corporation, U.S. Air Force, and Lockheed[1]. Due to budget constraints at the time and technical challenges required for full implementation, RBCC quickly fell to the sidelines, and the less complex rocket engine received full attention for space applications.

During the 1980's, significant gains were made in the area of airbreathing propulsion. The National Aerospace Plane program, or NASP, made major technological gains for airbreathing systems. NASP identified the major difficulties associated with this form of propulsion and many new technologies in the areas of thermal protection, inlet design, and supersonic combustion were enabled. Despite the technology advances, the unbelievable and overwhelming task of airbreathing to speeds above Mach 15 prevented a feasible vehicle design from being obtained.

It has been only recently that interest has been renewed in RBCC systems. By merging two previously independent systems, RBCC can offer a number of advantages for launch vehicle designers. In terms of engine performance, RBCC offers higher trajectory averaged specific impulse (I_{sp}) than pure rocket engines, and higher engine thrust-to-weight ratios than pure airbreathing engines. But, these gains come at the expense of a higher vehicle dry weight and increased vehicle complexity. The real advantage from RBCC is in the high flight rates and mission flexibility that these engines enable. RBCC is suitable for missions that include: earth-to-orbit, pop-up trajectory maneuvers, and high speed point-to-point missions. RBCC also promises increased loiter and abort options. These capabilities will be required on future space transportation systems.

A number of very attractive vehicle concepts for future launch systems have already been designed[2]. Many of the most promising of these concepts utilize RBCC propulsion, and the feasibility of these systems is almost unquestioned. The primary challenge now is in designing an economically viable system. With total program development costs ranging in the billions of dollars, robust designs that ensure success are mandatory.

RBCC propulsion appears to have a very promising future, and may provide the key to affordable, routine, and safe access to space.

PREVIOUS RESEARCH

Engineers in a conceptual RBCC launch vehicle design environment needed to be able to assess engine performance at each point in the ascent trajectory. That is, for a given altitude, flight velocity, and engine operating mode, what thrust and I_{sp} are produced by the engine? This data is typically used in a trajectory optimization code to determine a minimum fuel flight path to orbit.

Due to computing speed limitations, the required engine data is commonly generated off-line for a range of expected altitudes and flight speeds. The resultant database is formatted into a tabular form. Data is interpolated from the tables as needed by the trajectory optimization code.

The current engine analysis tool, SCCREAM, is a descendant of tools generated under earlier research efforts[3]. SCCREAM (Simulated Combined-Cycle Rocket Engine Analysis Module), is an object-oriented code written in C++. The code executes on a UNIX workstation, runs a full range of flight conditions and engine modes in under 60 seconds, and will output a properly formatted POST[4] engine table. SCCREAM is not intended to be a high-fidelity propulsion tool suitable for analyzing a particular RBCC engine concept in great detail, although its results compare

very well with those generated from more detailed codes. It was created to be a conceptual design tool capable of quickly generating a large number of reasonably accurate engine performance data points in support of early launch vehicle design studies.

SCCREAM OVERVIEW

SCCREAM has the capability to model the performance of four types of RBCC engines. One is the configuration identified in the Marquardt study —the supercharged ejector ramjet (SERJ). The other three are the (non-supercharged) ejector ramjet (ERJ), the ejector scramjet (ESJ), and the supercharged ejector scramjet (SESJ). Additionally, SCCREAM can model pure ramjet and pure scramjet configurations.

SCCREAM operates by solving for the fluid flow properties (velocity, temperature, pressure, mass flow rate, gamma, specific heat capacity, etc.) through the various engine stations for each of the engine operating modes. Equations for conservation of mass, momentum, and energy are used. This process is often iterative at a given engine station or between a downstream and an upstream station. The flow properties are calculated using quasi-1D flow equations. Engine cross-sectional area is the only geometry variable along the stream direction. Component efficiencies are used to simulate losses of total pressure in the mixer and nozzle, and reduced enthalpy in both the rocket primary and main combustor. The inlet is simulated by a simple total pressure recovery schedule. Thrust and I_{sp} are determined using a control volume analysis of the entering and exiting fluid momentum and the static pressures at the inlet and exit planes.

Most internal areas in SCCREAM are determined based on ratios to the inlet/cowl cross-sectional area. Default area ratios are supplied, so typically a user enters only the inlet area. The size of the rocket primary unit is primarily based on a user-entered propellant mass flow rate for the rocket primary. These two independent variables can be varied to produce an engine with a desired sea-level static thrust and secondary-to-primary mass flow ratio. In practice, however, the inlet area is often limited by overall vehicle geometry or shock-on-lip conditions. Optionally, the user can enter a desired sea-level static thrust and inlet area, and SCCREAM will iterate to determine the primary mass flow rate required.

In order to generate a POST engine table, a candidate engine's performance is evaluated over a range of altitudes and Mach numbers. These Mach number and altitude ranges can be set by the user. For example, a ramjet's operational Mach numbers might be set from 2 to 5.5, with altitude ranges from 30,000 feet to 150,000 feet. Overlapping Mach numbers and altitudes between various operating modes allows POST to select optimum engine mode transition points if desired. Default Mach number and velocity ranges are provided for each mode.

Performance in pure rocket mode is determined by analyzing a high expansion ratio rocket engine operating in a vacuum. A user-entered nozzle efficiency is used to account for losses associated with the expansion of the primary exhaust through the engine and then onto the aftbody.

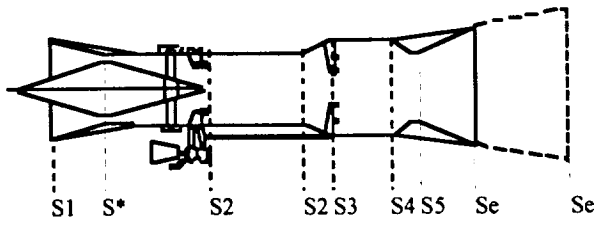

Figure 1 - Axisymetric Engine Station Locations

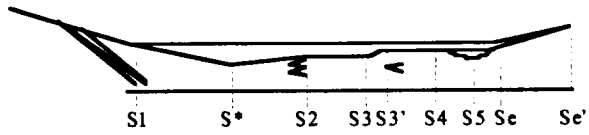

Figure 2 - 2-D Engine Station Locations

Figure 1 shows the station numbers and reference locations for by SCCREAM for an axisymetric RBCC engine configuration. Figure 2 shows station locations for a 2-D engine configuration. The 2-D engine layout is more common for vehicles with scramjet capability. Station 1 is at the inlet plane of the engine. Freestream flow conditions at station 'infinity' are modified by a single shock wave to simulate any precompression effects of the vehicle forebody on the engine. The forebody shape (wedge or cone) and the forebody angle are entered by the user.

Therefore the flow conditions at station 1 are typically not the same as the freestream flight conditions.

The inlet performance is modeled by a curve fit of the total pressure recovery and is a function of the Mach number at the inlet face. Variable geometry at the inlet throat is assumed.

Station 2 is at the location of the rocket primary and scramjet fuel injectors. For ejector mode, station 2 to 3 is a constant area mixing process between the entrained air stream and primary exhaust.

From station 3 to 3' an isentropic expansion of the flow is performed. This is generally beneficial for ramjet performance, but tends to penalize the scramjet performance.

From station 3' to 4, the hydrogen fuel is injected at a specified equivalence ratio and allowed to burn. Upon exiting the combustor, the flow is passed through a converging-diverging nozzle to the exit plane of the engine (station e or e').

For a more complete description of the flow process, the reader is referred to Reference 3.

IMPROVEMENTS

The following is a list of the improvements made to SCCREAM that will be discussed next.

1. Scramjet analysis capability
2. Rocket primary combustion
3. Rocket primary propellants
4. Detailed forebody analysis
5. New POST output deck format
6. Remote operation

Some of the improvements have already been mentioned while discussing the general operation of the code. Each will now be discussed in detail.

Scramjet Analysis

As stated earlier, the previous version of SCCREAM lacked a scramjet mode analysis capability. Results from an earlier study by Shaughnessey[5] were hard-wired into SCCREAM for this mode. The scramjet capability is undoubtedly the most signif cant and important improvement made.

Modeling of scramjet performance involved allowing a supersonic flow to pass completely through the engine without choking in the inlet throat, combustor, and nozzle sections. The conservation equations for mass, momentum, and energy were employed n a similar manner to that from the subsonic flow (ejector, fan-ram, and ramjet modes) cases. By careful arrangement of the iteration routines, the supersonic solution which satisfies the 3 conservation equations can always be obtained.

The entire mass flow at the inlet face is always ingested by the engine. The flow at station 1 is passed through the inlet and oblique shock system (not actually modeled in detail). A curve fit for the total pressure recovery of a supersonic inlet, based on the Mach number at station 1 replaces the subsonic inlet curve fit. Figure 3 shows the subsonic and the new supersonic pressure recovery schedules.

The conditions at the location of the rocket-primary (station 2) are then determined. This is a simple iteration procedure and as long as the area blockage from the rocket-primary is not too large, then a supersonic Mach number at station 2 can be obtained. If the area downstream of the inlet is too small, a common occurrence for RBCC configurations with oversized primaries, the downstream primary blockage will choke the flow to subsonic conditions. For these cases, a solution is not obtained.

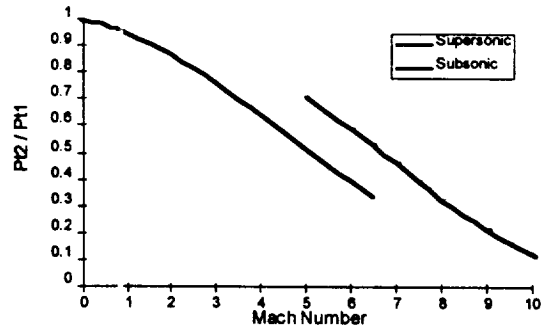

Figure 3 - Inlet Total Pressure Recovery

The hydrogen fuel is injected and mixed from station 2 to station 3, without any reaction occurring

(no heat addition). This is done to simulate injecting the fuel further upstream, as often required for supersonic combustion to allow adequate mixing. The added fuel changes the molecular weight and specific heat of the flow. This slightly affects the static conditions at station 3. A total pressure loss is simulated in the mixer section by defining an efficiency factor.

When solving for the static conditions at station 3, a new iteration procedure is required. Recall that for the subsonic flow cases, the assumption was that the static temperature is close to the total temperature. The mixture specific heat capacity was then calculated using the total temperature. This allowed for a much simpler iteration routine involving Mach number, which can easily be bounded between Mach 0 and Mach 1. For supersonic flow, the assumption of the static temperature being close to the total temperature is poor. A new routine has been devised that now includes the specific heat in the determination of the static conditions.

The static temperature at station 3 is iterated upon instead of the Mach number. This creates some problems because of the difficulty in setting upper and lower bounds on the temperature that will always ensure a supersonic solution is obtained. The exact problems encountered will be discussed later.

With an assumed static temperature and known flow composition, the mixture specific heat can be obtained. JANNAF based curve fits of the specific heat for each species a function of temperature is used by SCCREAM. A mass averaging technique is then used to determine the specific heat of the mixture.

Once the specific heat is obtained, the specific heat ratio can then be easily calculated since the molecular weight is known. The total enthalpy of the flow at station 3 is the same as that a station 2, thus the total temperature can be obtained dividing the total enthalpy by the specific heat value.

The known quantities are now static temperature, total temperature, and specific heat ratio. From these, the Mach number at 3 can be obtained using the conservation of energy equation. From the definition of Mach number, the flow's velocity can then be obtained. The continuity equation, or conservation of mass, is then used to determine the static pressure at station 3.

It is now necessary to obtain a new value for the static temperature to confirm the guessed value. This new temperature is obtained from the momentum equation. It is assumed that the added fuel has no contribution to the momentum balance.

The new and guessed temperatures are then compared and a new estimate for the static temperature, based upon a bisection routine, is determined. This process is repeated until convergence is obtained.

As previously mentioned, convergence problems can be encountered from iterating on the static temperature. If the guess is to high, the flow can have a subsonic Mach number at station 3. But, this condition can also result if too much fuel is added at station 2. A series of checks is used to either adjust the guess for the temperature or reduce the amount of fuel being added.

After a solution at station 3 is reached, the flow is isentropically expanded to the area at station 3'. This process will accelerate the flow since it is supersonic and the area is increasing.

From station 3' to station 4, the fuel that was added in at station 2 is now burned. The combustion process is modeled as a frictionless, one-dimensional heat addition process. A routine similar to that used from station 2 to 3 is applied again. At station 4, a minimum Mach number at or above sonic conditions can be set, with the SCCREAM default being Mach 1.15. If thermal choking occurs, or the minimum Mach number constraint is violated, the amount of fuel added (based on user defined phi) is automatically reduced, and the analysis restarts at station 2. Complete combustion is assumed, with the combustor efficiency accounting for the unburned fuel and resulting oxygen content. Species accounted for in the combustion process are: N_2, H_2O, Ar, O_2, and H_2.

After station 4, the flow is expanded out the diverging portion of the nozzle to the exit plane of the engine (station e) or aftbody of the vehicle (station e'), depending upon the current flight altitude. Since the

flow is supersonic, there is not a converging section in the nozzle. The flow composition from the combustor is frozen, and the specific heats are again included in the iteration procedure to account for the decreasing static temperature from the accelerating flow.

It should also be noted that SCCREAM can also be used to model a pure ramjet or pure scramjet engine now. These are non-RBCC engines configurations that do not have an ejector-mode nor the accompanying blockage at station 2 in the engine.

Rocket Primary

Previously, the user had large number of input parameters that had to be defined in order to properly model and size the rocket primary. These parameters included the total temperature, molecular weight, specific heat ratio, expansion ratio, and chamber pressure. SCCREAM was able to accurately determine the primary nozzle exit area and product exhaust velocity, but only after the user had over-defined the primary. Once in the engine, the flow was then assumed to be composed of 100% H_2O and the user-defined value for the molecular weight was overridden and set to 18.0, corresponding to a pure steam exhaust. Thus, even after defining all these inputs, the rocket primary could still only be modeled at stoichiometric conditions upon entering the main engine.

To eliminate this discrepancy and relieve the user of the extraneous input parameters, Response Surface Equation's (RSE's) were used to model the chamber temperature and exhaust product mole fractions. RSE's model complex systems with simple algebraic equations. These equations can yield very accurate results for non-discrete models, as well as save valuable computation time.

In all, 8 RSE's were generated as a function of the chamber pressure and mixture ratio. The first two equations were for the total temperature and specific heat ratio(γ). The remaining 6 were used for the mole fractions of: H_2, O_2, H_2O, O, H, and OH.

The well established Chemical Equilibrium and Applications program, or CEA[6], from the NASA Lewis Research Center was used for determining the equilibrium composition in the rocket chamber. For the analysis performed by CEA, the rocket propellants (oxygen and hydrogen) were both assumed to be in gaseous form at 298 K. The input parameters, chamber pressure and mixture ratio, were varied from 500 to 3,000 psia and from 4 to 12 respectively. A total of 64 different cases were analyzed.

After all of the runs were completed, a statistical analysis program , JMP[7], was then used for setting up the RSE's. The general form of each RSE generated is:

$$X = \alpha * P_c + \beta * P_c^2 + \chi * MR * P_c + \delta * MR + \varepsilon * MR^2 \quad (1)$$

where P_c is the chamber pressure, MR is the primary mixture ratio, and α through ε are constants. A residual analysis of the RSE fits show excellent correspondence with the results from CEA.

With the mole fractions now known, the molecular weight of the mixture can be determined. The flow composition is frozen and then expanded to match the user-defined expansion ratio. Basic rocket analysis equations are used for solving for the throat area, exit pressure, and exit velocity.

SCCREAM was then modified to track all of the primary exhaust products throughout the rest of the engine. In doing so, operation of a non-stoichiometric rocket primary is enabled.

Primary Propellants

An additional rocket primary propellant, hydrogen peroxide (H_2O_2), has been added. Concentrations of 85%, 90%, and 98% H_2O_2 can be selected and modeled. The non-H_2O_2 percentage in the concentrations is pure water. The user is simply required to select the desired concentration, then enter the chamber pressure and expansion ratio for the primary subsystem.

Hydrogen peroxide is a mono-propellant that reacts when brought into contact with a catalyst like platinum or copper. For a given concentration, the decomposition temperature is fixed, thus the expected temperatures for the 3 concentrations are hard-wired into SCCREAM. The decomposition of H_2O_2 results in a mixture composed of 43% O_2 and 57% H_2O by

weight, not including any initial H_2O present. Benefits of H_2O_2 are the design simplicity resulting from having only a single working fluid, as well as a lower combustion temperature. The lower combustion temperature allows for increased chamber pressures. Typical values for P_c are from 500-5000 psi. These benefits come at the cost of a lower specific impulse and exhaust velocity.

SCCREAM will analyze the performance and size the rocket primary for the H_2O_2 configurations. Industry data has shown that 100% decomposition is nearly obtainable, so a primary combustion efficiency is not used for these cases. The O_2 and H_2O exhaust products are then tracked through the mixer and into the combustor. The excess O_2 from the primary is added to the oxygen content of the air stream. The total oxygen mass flow is then used with the equivalence ratio to determine the amount of fuel added in the combustor.

Forebody Analysis

SCCREAM allows the user to define either a conical or 2-D wedge shaped forebody to account for compression effects. In SCCREAM version 1.0, both the cone and wedge shapes used closed form solutions for solving for the flow properties behind the bow shock. For conical flow, this closed form solution will accurately predict the properties behind the shock, but not behind the shock at the surface of the vehicle and at the cowl lip. To obtain a more accurate estimate of the mass flow at the inlet, a more rigorous analysis is now performed.

For determining the properties behind the bow shock of a cone, a system of 3 ordinary differential equations must be solved. They are shown here in their more familiar (spherical coordinates) form:

$$V_\theta = \frac{dV_r}{d\theta} \tag{2}$$

$$\frac{dV_\theta}{d\theta} = \left[\frac{a^2}{(V_\theta^2 - a^2)}\right](2 * V_r + V_\theta * \cot\theta - \frac{V_r V_\theta^2}{a^2}) \tag{3}$$

$$\frac{dp}{d\theta} = \left(\frac{-\rho V_\theta a^2}{(V_\theta^2 - a^2)}\right) * (V_r + V_\theta \cot\theta) \tag{4}$$

where a is the speed of sound, θ is the ray angle, V_r is the radial velocity component, V_θ is the normal velocity component perpendicular to the radial component, p is the static pressure, and ρ is the density of the flow.

The reverse procedure of guessing a shock angle, as recommended by Anderson[8], is implemented to solve these equations.

Additional information about the inlet is required from the user (these input values are not necessary for a wedge shaped forebody). These new inputs are the length from the nose of the vehicle to the inlet lip and the height of the inlet.

When equations (2)-(4) are solved, the flow field behind the bow shock is completely defined. A streamline that intersects the cowl lip can be determined using the additional input parameters. The mass flux is then determined along this streamline and averaged with the mass flux at the vehicle's surface. This value is then used as the mass flow rate seen across the entire inlet at station 1.

Output Deck

The static pressures inside an airbreathing engine can be substantial and will significantly effect the weight of an engine. The trajectory flown by the vehicle will have the strongest influence on the maximum internal pressures that will be experienced by the engine. For freestream dynamic pressures (q) greater than 1500 psf, ramjet mode static pressures in excess of 200 psi can easily develop as the flight Mach number is increased. This can significantly increase the weight of an engine, and this information needs to be supplied to the engine weight model.

Figure 4 shows the maximum static pressures experienced by an Ejector Scramjet configuration for a typical constant-q, single stage RBCC vehicle. Note that from Mach 4 to 5.5, the pressure increases very rapidly, especially for the q=2000 psf trajectory. At Mach 5.5, the q=1500 path has a maximum pressure of only 220 psi, while the q=2000 path experiences over 300 psi. These effects are indeed significant and must be accounted for in the overall vehicle design.

To allow for tracking of these engine pressures, a new table has been included in the POST engine deck produced by SCCREAM. This table contains the maximum static pressure experienced by the engine at every flight condition. This information can easily be monitored during the trajectory, and can be passed to an engine weight estimation code (WATES[9]) during each iteration while closing a design. Alternatively, a maximum static pressure limit can be set in the trajectory model. POST can be constrained not to exceed this value for the static pressure over the course of the trajectory.

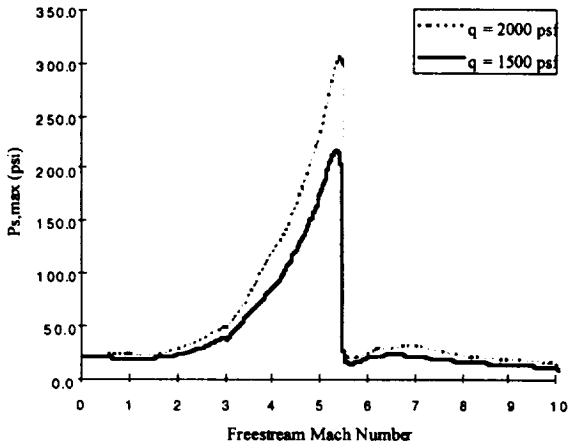

Figure 4 - Maximum Internal Static Pressures

Remote Operation

In the interest of allowing easy access and operation of SCCREAM, a web based interface has been created. This interface allows for execution and retrieval of the results from SCCREAM over the web from any computing platform. The user must simply have access to an Internet browser (Netscape, Internet Explorer, etc.). The web interface also allows for any user to easily access the most current version of SCCREAM without the hassle of obtaining and installing the newest version. Currently, access to SCCREAM is unrestricted. The web address for SCCREAM is:

http://atlas.cad.gatech.edu/~jebradfo

In addition to remote operation, the new interface allows for easy error checking before program execution. Hyper-links for each variable are set up to provide a brief description of each input parameter and give typical ranges. Sample engine configurations for a variety of RBCC vehicles have also been included on the page.

The web interface is composed of three different programming languages. They are the common Hyper Text Markup Language (HTML), JavaScript, and Practical Extraction Report Language (PERL).

The HTML portion utilizes the form 'post' method for transferring data to the machine hosting the SCCREAM executable. The 'post' method is preferable over the 'get' method when transferring more than one piece of information. The web page itself consists of radio buttons, pull-down menus, and text fields for the SCCREAM input parameters. This allows for easy configuration changes and updating of the engine model. Figure 5 provides a partial screen shot of the user interface for Version 4.0 of SCCREAM.

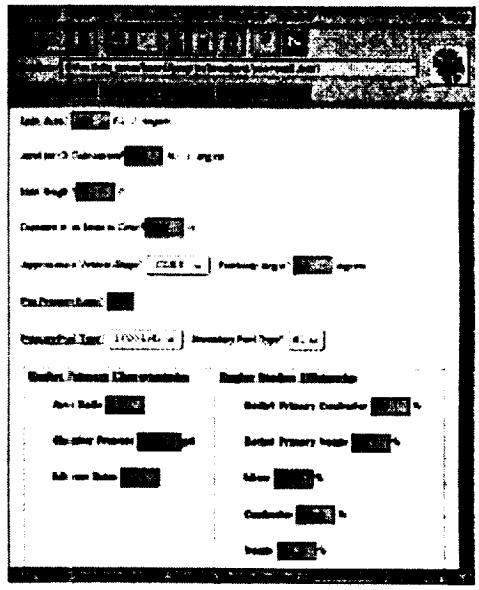

Figure 5 - Web-based user interface

The JavaScript routines perform error and range checking of the user inputs. This helps limit the possibility of errors being generated when SCCREAM executes. For example, if the user accidentally puts in a nozzle efficiency greater than 100%, a JavaScript warning message will be displayed. This message will identify the name of the variable with the infeasible input value and provide the allowable ranges for the

particular variable. The JavaScript also creates a more dynamic page, with default input values automatically changing based upon a user's selections. As an example, if a non-supercharging RBCC engine (no fan) is selected, the fan pressure ratio automatically changes to 1.0, for no total pressure rise. If the user selects the pure-ramjet option, all input fields associated with the rocket primary subsystem are eliminated.

Once all of the input parameters have been checked and verified by the JavaScript, an estimate of the total run time required is displayed. The web form is then processed by execution of a Common Gateway Interface (CGI) script. This script is located on the server for the SCCREAM host, and is written in PERL. This PERL script opens and writes to the 6 text based input files, runs SCCREAM, and then displays the results back to the user's web browser. It should be noted that the original text input files are still in place and the SCCREAM source code has not been altered to be compatible with the web interface. Therefore, SCCREAM can still be executed on a stand-alone platform that does not have Internet access.

After execution of SCCREAM is completed, the user can simply download the results by selecting the hyper-links to the main output file and POST deck. The browser 'Save As' option will retrieve the results and place them in the user's local directory.

RESULTS

Comparison with RJPA

The Ramjet Performance Analysis Code[10], RJPA, was developed at Johns Hopkins University in the mid-1960's. The Fortran based code uses a one-dimensional integral analysis approach and is applicable to a wide variety of airbreathing and rocket propulsion concepts. The combustor uses the NOTS equilibrium code for determining the chemical composition of the flow. Frozen and equilibrium flow analysis options can be selected.

The RJPA engine model is divided into 4 main components: the inlet, diffuser, combustor, and nozzle sections.

For comparison runs with SCCREAM, only scramjet performance was analyzed for Mach numbers from 6 to 12. A generic scramjet engine configuration with moderate internal area contraction and exit flow expansion was selected.

For establishing the inlet flow conditions, the static conditions for temperature, velocity, and pressure behind the bow shock were specified for each case. These values were obtained from SCCREAM for a conical forebody with a half-angle of 9.2°. The physical area of the inlet at the cowl was 51 ft^2.

The diffuser section consisted of defining the exit area, total pressure recovery, and initial guesses for the specific heat ratio. The exit area from the diffuser corresponded with the area at station 3' in SCCREAM, and was set to a value of 33 ft^2. The total pressure recovery was made to correspond to the value used by SCCREAM, at each flight condition. Heat losses in the diffuser were ignored.

For the combustor model, a constant area process was desired, so the exit area from the combustor was 33 ft^2. Skin friction and heat transfer in the combustor were neglected. The equivalence ratio and initial guesses for the static pressure at the exit plane were also defined in RJPA. For cases below Mach 7.25, the equivalence ratio had to be reduced in order to prevent choking due to the heat addition in the combustor. If the specified phi is too high in RJPA, a solution cannot be obtained. For these same cases, SCCREAM automatically throttled back the fuel flow rate from the maximum value defined by the user. The phi determined by SCCREAM provided starting points for determining an allowable phi in RJPA. It should be noted that the allowable fuel flow rate from SCCREAM was slightly higher than the value allowed by RJPA. To ensure a fair comparison, SCCREAM was run again with the same phi used by RJPA.

For the nozzle expansion, an efficiency of 98% and an exit area of 204 ft^2 was defined. A frozen-to-equilibrium nozzle flow ratio of 0.667 was also used for determining the thrust and I_{sp} values. RJPA performs the nozzle analysis for both frozen and equilibrium flow. The frozen flow case should have

lower thrust and I_{sp}, when compared to the equilibrium case. Real nozzle performance is somewhere in between these to bounds, with kinetic models suggesting it is closer to the frozen flow results. By defining a frozen-to-equilibrium ratio of 2/3, RJPA computes a 'real' flow performance by averaging 2/3 of the frozen flow results with 1/3 of the equilibrium flow results. The performance results presented are for the 'real' flow case.

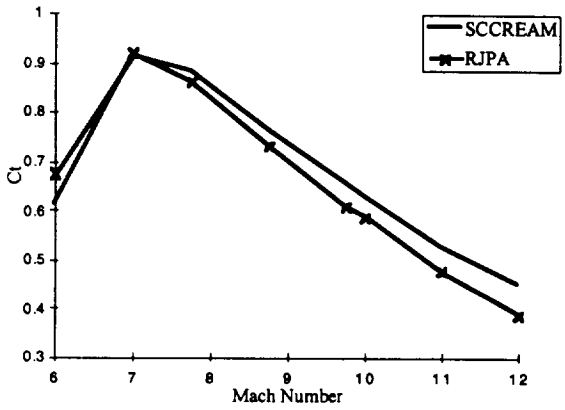

Figure 6 - C_t versus Mach Number

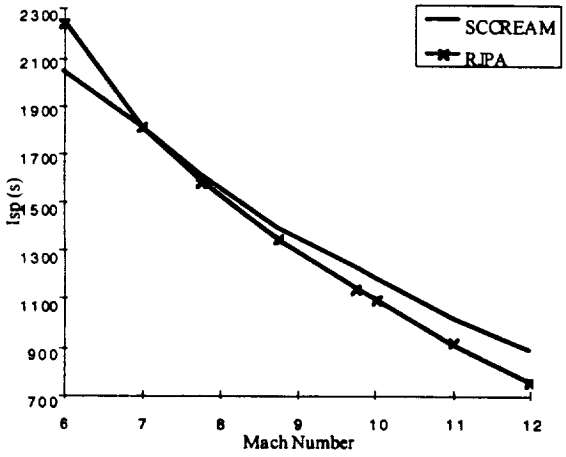

Figure 7 - I_{sp} versus Mach Number

Figure 6 provides the comparative results for the thrust coefficient versus freestream Mach number. The cowl area of 51 ft^2 was used to normalize the thrust coefficient. The dynamic pressure for most cases was approximately 2000 psf.

In the Mach number range of 7 to 10, SCCREAM and RJPA match very well. At the lower Mach numbers, it appears SCCREAM underpredicts the thrust level predicted by RJPA. This is currently being attributed to SCCREAM not modeling the pre-combustion static pressure rise (the PSPCI term in RJPA) from the shock train. This pressure rise results in different flow conditions at the start of the combustion process, which in turn effect the flow conditions exiting the combustor. Table 1 provides more detailed information on the static conditions at this low Mach number condition. Notice from the table the static pressure and temperature differences exiting the combustor. These differences diminish at the Mach 8.75 and Mach 10 conditions, where the effect of the shock train pressure rise also diminishes. This lends support as to the theory of why the differences are occurring, but determining the exact mechanism will require further investigation.

At Mach numbers above 10, the differences between RJPA and SCCREAM appear to be slowly increasing. As the Mach number and energy of the flow increases, the exact composition of the flow becomes more important. Of particular consequence is the fact the SCCREAM does not account for the hydroxyl species (OH). The presence of the hydroxyl molecule will effect the molecular weight and specific heat of the flow. These in turn affect the static conditions. Since this is not modeled by SCCREAM, a higher thrust value than RJPA could result at increased Mach numbers due to different static conditions at the exit plane.

Figure 7 provides the I_{sp} versus Mach number. As expected based on the thrust coefficient trends, SCCREAM slightly underpredicts the I_{sp} predicted by RJPA at the lower, reduced phi, Mach numbers. From Mach 7 to 10, very good correspondence between the two codes is displayed again. Above Mach 10, SCCREAM has a higher I_{sp} in a similar manner as the thrust profile.

Table 1. Flow Property Comparison for SCCREAM and RJPA

		Mach 6		Mach 8.75		Mach 10	
	Flow Property	*SCCREAM*	*RJPA*	*SCCREAM*	*RJPA*	*SCCREAM*	*RJPA*
Diffuser Exit	Mach	3.74	4.11	5.03	5.24	5.27	5.56
	Ps (psi)	3.54	3.70	2.83	2.59	2.39	2.14
	Ts (R)	605.1	722.5	768.8	1004.0	927.3	1188.60
Combustor Exit	Mach	1.21	1.09	1.96	1.87	2.36	2.31
	Ps (psi)	25.16	36.47	17.68	19.09	11.94	12.36
	Ts (R)	3195.4	4009.3	4713.9	4906.3	4792.2	4847.20
	Gamma	1.281	1.267	1.245	1.250	1.245	1.25
	Mol. Wgt	26.45	26.55	24.31	23.81	24.31	23.76
Nozzle Exit	Mach	3.17	3.12	3.49	3.43	3.84	3.80
	Ps (psi)	1.10	1.41	1.23	1.25	0.91	0.92
	Ts (R)	1643.7	1933.4	2831.1	2776.8	2908.2	2813.30
	Gamma	1.328	1.315	1.270	1.282	1.272	1.28

Comparison with Other Codes

The *Hyperion* concept's ejector scramjet (ESJ) engine performance has been reanalyzed using the current SCCREAM (Version 4.0) model. *Hyperion* is a single stage to orbit vehicle that flies on a constant q boundary of 2,000 psf in scramjet mode up to Mach 10. The vehicle is design to carry 20,000 lbs to low earth orbit from Kennedy Space Center (KSC) in Florida. The forebody is a conical shape with a half-angle of 9.2°. The reader is encouraged to obtain reference 3 for more details on the *Hyperion* concept.

As previously documented, RAMSCRAM[3,11] data has been generated based upon a similar Hyperion engine geometry and flight path. It should be noted that a ramjet to scramjet transition Mach number of 6 was used for the RAMSCRAM data, but *Hyperion* now transitions at Mach 5.5.

SRGUL was used by Shaughnessey[5] to generate ramjet and scramjet performance for a vehicle with a 5° half-cone angle for NASA-Langley. These results are for a non-RBCC engine with a different engine geometry and inlet efficiency.

The RJPA results presented here are for the conditions previously stated in the direct comparison cases. The engine geometry is very similar to *Hyperion's* engine design.

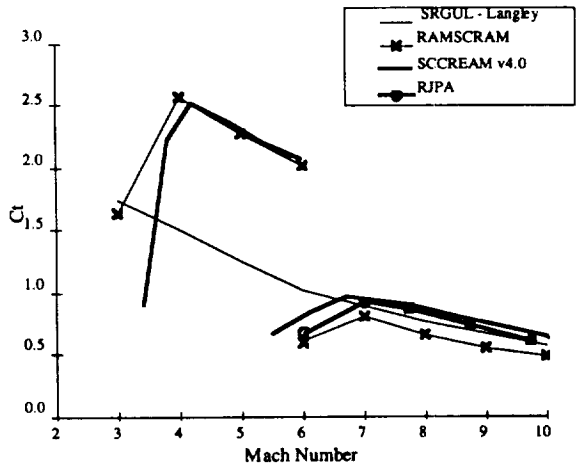

Figure 8 - C_t versus Mach Number(group 1)

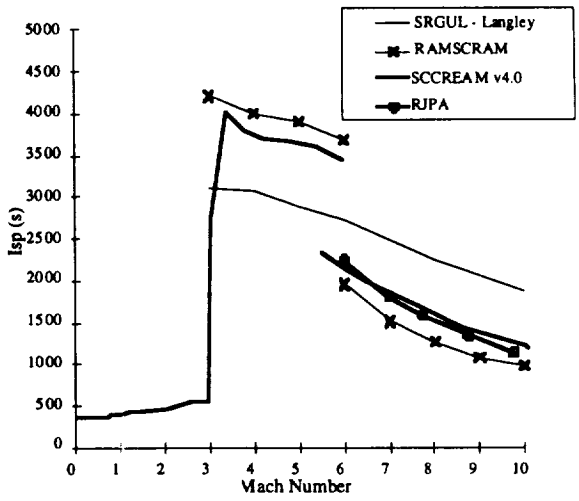

Figure 9 - I_{sp} versus Mach Number(group 1)

Figure 8 shows the thrust coefficient comparisons for the 4 codes SCCREAM, RJPA, RAMSCRAM, and SRGUL. It can be seen that SCCREAM and RAMSCRAM match very well for the ramjet portion of the trajectory. SCCREAM appears to accurately predict an equivalent drop in thrust from transitioning from subsonic to supersonic combustion. Note that an instantaneous switch from subsonic to supersonic flow is modeled here, but a real engine would likely have a much smoother transition period. In scramjet mode, RJPA and SCCREAM agree very well, as previously shown. RAMSCRAM appears to have less thrust than SCCREAM and RJPA in scramjet mode, but still displays similar trends.

The SRGUL data fits very well with all three codes at Mach numbers greater than 7. But, as Mach number decreases below Mach 7, SRGUL's thrust coefficient continues to increase while the rest are exhibiting a decrease. It is known that SCCREAM, RJPA, and RAMSCRAM have lower thrust at these Mach numbers due to throttling of the equivalence ratio. The need to throttle phi to prevent choking the flow is largely dependent on the engine geometry and inlet efficiency. It is also known that the SRGUL engine flowpath allows a phi=1 at these Mach numbers, which accounts for the increasing thrust level. Designing for the phi=1 scramjet condition can come at the expense of performance in other modes. This would not have been a consideration for the designer of a pure scramjet configuration.

Figure 9 shows the I_{sp} profiles for the 4 codes. Once again, SCCREAM and RAMSCRAM match well for ramjet mode performance. SCCREAM and RJPA match almost exactly in scramjet mode, and RAMSCRAM is displaying similar trends again. The SRGUL I_{sp} profile does not coincide with any of the codes. It should be re-iterated that this is not the same flow path design and engine configuration. The data does provide an interesting reference for comparing RBCC performance with an engine designed for only ramjet/scramjet operation.

Comparison with Historical Data

Data from the early Marquardt studies for ejector ramjet and ejector scramjet configurations has been obtained. Results from this study are commonly referred to as NAS7-377 data. This data is for a launch vehicle with an 8° half-angle wedge forebody, flying on a constant q boundary of 1500 psf.

In 1988, the Astronautics Corporation[12] performed a study for the United States Air Force. The vehicle used ejector scramjet engines and had a 10° half-angle cone. But, the data obtained and presented here are results for a 6° half-angle wedge.

Figure 10 shows the thrust coefficient profile generated by SCCREAM and compared with historical data. In the early stages of ramjet mode, the large increase in the thrust coefficient by SCCREAM can be attributed to the increasing phi in the combustor. As the flight speed increases, the maximum phi of 1 is quickly obtained. The thrust coefficient matches well with the NAS7-377 ejector ramjet predictions for the remainder of subsonic operation. SCCREAM and the trends from the Astronautics data appear to agree well in scramjet mode. Due to the differences in forebody angles, inlet efficiency, and internal geometry, it can not be expected that SCCREAM will exactly match these predictions.

Figure 11 shows the I_{sp} comparisons of SCCREAM with the historical data. It appears that agreement over the most of the trajectory is excellent. But, it does not appear that the NAS7-377 and the Astronautics data have a change in performance while transitioning from subsonic to supersonic combustion. This is curious as the recent analysis from RJPA and RAMSCRAM both display the same drop in performance being predicted here by SCCREAM. A possible explanation is that a smooth transition was modeled between ramjet and scramjet operation.

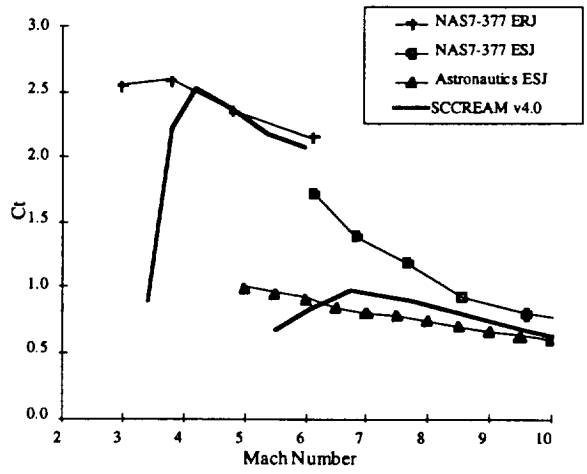

Figure 10 - C_t versus Mach Number(group 2)

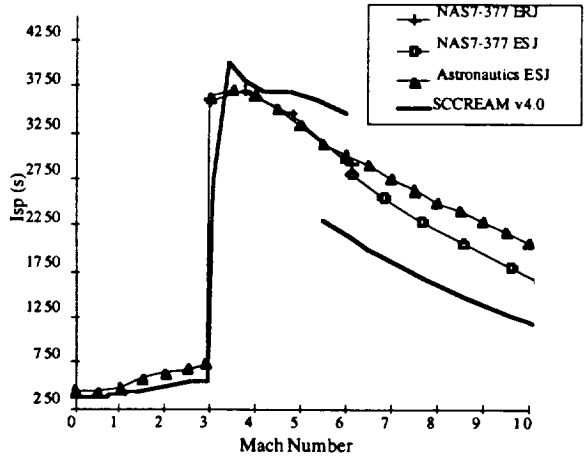

Figure 11 - I_{sp} versus Mach Number(group 2)

CONCLUSIONS

Significant improvements have been made to SCCREAM since its inception. The current version 4.0 has retained its execution speed, while at the same time improving its accuracy and capability.

Among the conclusions drawn in this paper are the following:

1. A scramjet performance model suitable for a conceptual design environment has been established. The accuracy of its results has been confirmed through direct comparison with the industry standard code, RJPA.

2. The required number of inputs for defining the rocket primary flow has been reduced from 5 to 3. This was accomplished at the same time as greatly improving the accuracy of the primary flow and increasing its modeling ability.

3. The first fuel trade study capability has been enabled by addition of a hydrogen peroxide rocket primary. This primary can be operated at 3 different initial concentrations of 85%, 90%, and 98%.

4. Valuable static pressure information has been added to the trajectory output deck. This will allow the designer to more accurately perform trades and model a vehicle's trajectory. The new data can easily be incorporated into an engine weight estimation model.

5. A web based user interface has been established. This interface readily allows remote execution, reduces the possibility of input errors, and eliminates the need for updating software by the remote user.

FUTURE WORK

SCCREAM will continue to be improved to increase modeling accuracy and capabilities without sacrificing speed, ease of use, and flexibility. Among many near-term improvements being considered are the following:

1. Addition of a combustor model that will allow for a non-constant area and account for friction and heat loss effects. This work has currently begun.

2. Allow for specifying multiple compression ramps on the forebody surface. This will be implemented for both conical and wedge configurations.

3. Creation of the additional operating mode known as 'scram-rocket'. This mode occurs near the end of scramjet operation, while transitioning to the all-rocket mode. It has the potential of maintaining adequate thrust through use of the rocket primary, while still utilizing the small amount of oxygen in the atmosphere to increase specific impulse.

4. Establish a method for determining angle of attack effects. This is a fairly simple procedure for the wedge configuration, but there does not appear to be a quick solution for conical flows at an angle of attack.
Once generated, these effects will be added to the POST deck for incorporation into the trajectory analysis.

5. Provide on-line data plotting using the web-based interface. This will allow the user to quickly assess their engine's performance.

6. Addition of a hydrocarbon primary and secondary fuel-injector analysis capability. Hydrocarbon fuels have been identified as promising candidates for RBCC missile applications.

ACKNOWLEDGMENTS

Development of SCCREAM was primarily sponsored by the NASA-Marshall Space Flight Center under grant NAG8-1302 to the Georgia Institute of Technology.

Additional support and funding for the hydrogen-peroxide work was provided by the Kaiser-Marquardt Corp.

Captain Shahnaz Punjani at Wright Patterson Air Force Base provided crucial support and was responsible for bringing the authors 'up to speed' on the RJPA code.

David Acton, a student at SSDL, was instrumental in helping establish the JavaScript code for the web-based interface.

REFERENCES

1. Escher, William J. D. and B. J. Flornes. A Study of Composite Propulsion Systems For Advanced Launch Vehicle Application. Contract NAS7-377.

The Marquardt Corporation: Van Nuys, California 1966. Vol 1-7.

2. John C. Mankins. "Lower Costs for Highly Reusable Space Vehicles". *Aerospace America*, March 1998. pg. 36-42.

3. Olds, J.R. and J.E. Bradford. "SCCREAM-Simulated Combined Cycle Rocket Engine Analysis Module". AIAA-97-2760. 1997. Conference Proceeding of the 32nd AIAA/ASME/SAE JPC in Seattle, WA.

4. Brauer, G. L., et al. "Program to Optimize Simulated Trajectories (POST)." Final report for NASA contract NAS1-18147, Martin-Marietta Corp., September 1989.

5. Shaughnessy, J. D., et. al. "Hypersonic Vehicle Simulation Model." NASA TM-102610, November 1990.

6. Gordon, S. and B. J. McBride. "Computer Program for Calculation of Complex Chemical Equilibrium Compositions and Applications", NASA Reference Publication 1311, October 1994.

7. JMP Statistical Software Package. Version 5.0, SAS Institute. Cary, NC.

8. Anderson J. D. Modern Compressible Flow, Second Edition, McGraw-Hill, Inc. New York, NY, 1990.

9. Olds, J. R. and D. J. McCormick. "Component-Level Weight Analysis for RBCC Engines", AIAA 97-3953, Defense and Space Programs Conference and Exhibit, Huntsville, AL, September 1997.

10. Pandolfini, P. "Instructions for Using Ramjet Performance Analysis (RJPA) IBM-PC Version 1.24", JHU/APL AL-92-P175. June 1992.

11. Burkardt, L. A. and L. C. Franciscus. "RAMSCRAM - A Flexible Ramjet/Scramjet Engine Simulation Program." NASA TM-102451. June, 1990.

12. Foster, R. W., W. Escher, and J. Robinson, "Air Augmented Rocket Propulsion Concepts." USAF Astronautics Laboratory Report AFAL-TR-88-004, April 1988.

SCCREAM (Simulated Combined-Cycle Rocket Engine Analysis Module): A Conceptual RBCC Engine Design Tool

Dr. John R. Olds*
John E. Bradford†
Aerospace Systems Design Laboratory
School of Aerospace Engineering
Georgia Institute of Technology, Atlanta, GA

ABSTRACT

Rocket-based combined-cycle engines are currently under consideration for use on future, reusable launch vehicles. By combining traditional rocket and airbreathing operating modes into a single engine, multi-mode RBCC engines offer a number of advantages for launch vehicle designers including higher trajectory averaged I_{sp} than pure rockets and higher installed thrust-to-weight ratios than pure airbreathers.

This paper presents a new computer tool capable of predicting RBCC engine performance (thrust and I_{sp}) over a wide range of flight conditions and engine operating modes. The tool is called SCCREAM — Simulated Combined-Cycle Rocket Engine Analysis Module. SCCREAM is an object-oriented workstation-level code written in C++. It uses quasi-1D flow analysis, component and combustion efficiencies, and an inlet pressure recovery schedule as simplifying assumptions. SCCREAM was created for the conceptual launch vehicle design environment and is capable of quickly generating large tables of engine performance data for use in trajectory optimization.

An overview of SCCREAM and the program logic is presented. Results from SCCREAM are favorably compared to historical RBCC engine performance data and to data generated by other engine design tools.

NOMENCLATURE

A_i	engine cross-sectional area at station *i* (ft^2)
C_p	constant pressure specific heat (BTU/slg-R°)
C_t	thrust coefficient (thrust/q*A_1)
ERJ	ejector ramjet
ESJ	ejector scramjet
I_{sp}	specific impulse (sec)
LH2	liquid hydrogen
LOX	liquid oxygen
P_t	total pressure
phi	combustor equivalence ratio
POST	Program to Optimize Simulated Trajectories
q	freestream dynamic pressure (lb/ft^2)
RBCC	rocket-based combined-cycle
SERJ	supercharged ejector ramjet
SESJ	supercharged ejector scramjet
SSTO	single-stage-to-orbit
γ	ratio of specific heats

RBCC BACKGROUND

Rocket-based combined-cycle engines are unique in that they combine the most desirable characteristics of airbreathing engines and rocket engines into a single, integrated engine. RBCC engines have the advantage of high average specific impulse (I_{sp}) in comparison to rockets, and high thrust-to-weight ratios in comparison to airbreathers.

The concept of combined-cycle engines has existed since the mid-60's. During this inception phase, an extensive study was conducted by the Marquardt Corporation, Lockheed-California, and the U.S. Air Force on various 'composite engine' designs, as they were formerly called [1]. This study initially analyzed 36 different variants of combined-cycle engines. At the study's conclusion, two types of RBCC engines were

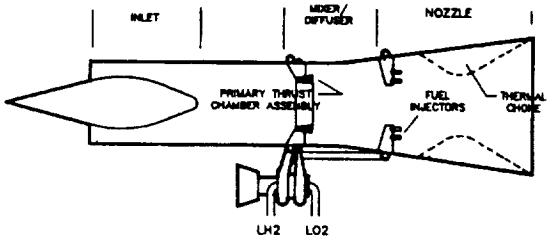

Figure 1 - Supercharged Ejector Ramjet Engine [ref. 1]

selected as the most interesting options — a near-term option and a far-term option. The decisions were made based on technological feasibility and resulting performance on a representative two-stage-to-orbit launch vehicle. The two final selections were the Supercharged Ejector Ramjet (SERJ) configuration (figure 1), and the more technically challenging Supersonic Combustion Ramjet with Liquid Air Cycle (ScramLACE) configuration. The SERJ engine configuration is composed of four operating modes: ejector, fan-ramjet, ramjet, and pure rocket. A derivative of the SERJ is the Supercharged Ejector Scramjet (SESJ). This configuration consists of five operating modes, the four from the SERJ and an additional scramjet mode.

During ascent phase, the RBCC engine initially operates in ejector mode. The ejector mode utilizes the rocket primaries (figure 2) as the main source of thrust. Entrained air from the inlet and fuel from the secondary fuel injectors is also burned in the combustor to provide additional thrust. A low-pressure

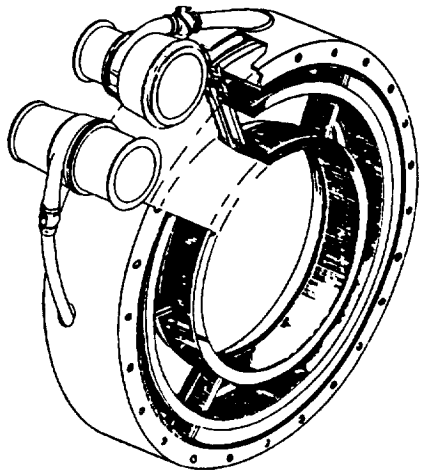

Figure 2 - Rocket Primary [ref. 2]

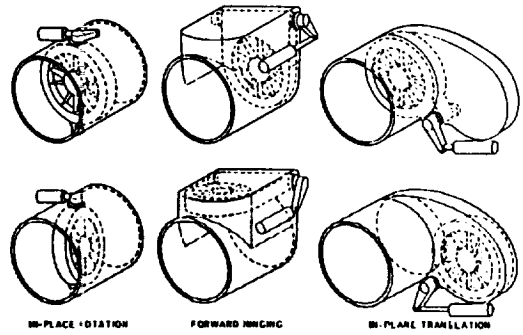

Figure 3 - Fan Storage Methods [ref. 2]

ratio fan, located between the inlet and primary, may also be used. Once significant ram pressure is achieved from the surrounding air, typically occurring around Mach 2 to 3, the rocket primaries are shut off. The fan remains functioning up to about Mach 3, constituting the fan-ramjet mode. At Mach 3, the fan is removed from the flow path or perhaps windmilled in place to as high as Mach 6. Figure 3 shows possible methods for removing the fan from the flow path should that be necessary. The engine operates in pure ramjet mode up to around Mach 6. At Mach 6, depending upon the engine type (SESJ or SERJ), the engine will transition either to scramjet mode or directly to rocket mode. If scramjet mode is available, the engine will continue operating as an airbreather with supersonic combustion up to an optimal transition Mach number. Recent conceptual vehicle designs have suggested transition to pure rocket mode might optimally occur between Mach 10 and Mach 15. While transitioning to rocket mode, the inlet face is closed and the rocket primaries are restarted. Vacuum Isp's in the range of 410-470 seconds are typical values during rocket mode.

PREVIOUS RESEARCH

Engineers in a conceptual RBCC launch vehicle design environment need to be able to assess engine performance at each point in the ascent trajectory. That is, for a given altitude, flight velocity, and engine operating mode, what thrust and I_{sp} are produced by the engine? This data is typically used in a trajectory optimization code to determine a minimum fuel flight path to orbit. Figure 4 from reference 3 gives typical RBCC engine I_{sp}'s for a representative vehicle flight profile.

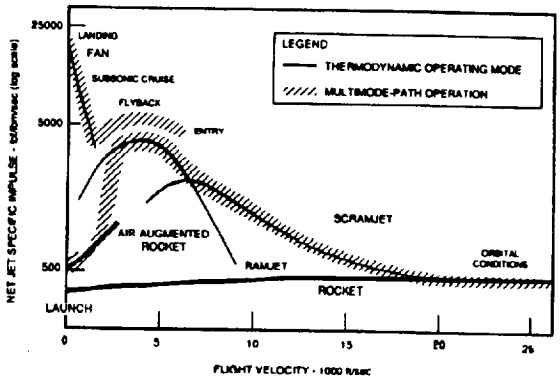

Figure 4 - Typical RBCC I_{sp} Performance [ref. 3]

Due to computing speed limitations, the required engine data is commonly generated off-line for a range of expected altitudes and flight speeds. The resultant database is formatted into a tabular form. Data is interpolated from the tables as needed by the trajectory optimization code.

The current engine analysis tool, SCCREAM, is a descendant of tools generated under earlier research efforts. Original research in 1993 resulted in a simple spreadsheet model that was capable of predicting RBCC engine performance in ejector mode only [4]. The original model could also incorporate a supercharging fan if required. The spreadsheet consisted of approximately 2,500 iterative calculation cells to perform the internal engine flow calculations. The spreadsheet generated properly formatted tabular data that could be electronically transferred to a workstation class computer and imported into a popular trajectory optimization program, POST [5].

Subsequent research extended the original spreadsheet model to include fan-ramjet and ramjet modes of operation [6]. The number of iterative spreadsheet cells increased to approximately 10,000. As in the original tool, this spreadsheet produced a properly formatted POST engine table that could be electronically transferred to a workstation for trajectory optimization. Unfortunately, recalculation of this expanded spreadsheet was slow. In addition, for certain initial guesses of flow conditions, the automatic internal spreadsheet iteration was often unstable. That is, the internal pressures, velocity, and Mach number iteration could easily diverge for certain flight conditions. To remedy the situation, a new standalone RBCC engine analysis tool was developed.

The newest tool, SCCREAM (Simulated Combined-Cycle Rocket Engine Analysis Module), is an object-oriented code written in C++. The code runs on a UNIX workstation, runs a full range of flight conditions and engine modes in under 30 seconds, has more stable internal iteration schemes, and retains the ability to output properly formatted POST engine tables. SCCREAM is not intended to be a high-fidelity propulsion tool suitable for analyzing a particular RBCC engine concept in great detail. Rather, it is a conceptual design tool capable of quickly generating a large number of reasonably accurate engine performance data points in support of early launch vehicle design studies.

SCCREAM

Overview

SCCREAM has the capability to model the performance of four types of LOX/LH2 RBCC engines. One is the configuration identified in the Marquardt study —the supercharged ejector ramjet (SERJ). The other three are the (non-supercharged) ejector ramjet (ERJ), the ejector scramjet (ESJ), and the supercharged ejector scramjet (SESJ). While SCCREAM does not model supersonic combustion directly, scramjet mode data for the latter two engine types is scaled from a previously published database of scramjet performance from NASA - Langley [7].

SCCREAM operates by solving for the fluid flow properties (velocity, temperature, pressure, mass flow rate, gamma, specific heat capacity, etc.) through the various engine stations for each of the engine operating modes. Equations for conservation of mass, momentum, and energy are used. This process is often iterative at a given engine station or between a downstream and an upstream station. The flow properties are calculated using quasi-1D flow equations. Engine cross-sectional area is the only geometry variable along the stream direction. Component inefficiencies are used to simulate losses of total pressure in the mixer and nozzle, and reduced enthalpy in both the rocket primary and main

combustor. The inlet is simulated by a simple total pressure recovery schedule. Thrust and I_{sp} are determined using a control volume analysis of the entering and exiting fluid momentum and the static pressures at the inlet and exit planes.

Most internal areas in SCCREAM are determined based on ratios to the inlet/cowl cross-sectional area. Default area ratios are supplied, so typically a user enters only the inlet area. The size of the rocket primary unit is based on a user-entered propellant mass flow rate for the rocket primary. These two independent variables can be varied to produce an engine with a desired sea-level static thrust and secondary-to-primary mass flow ratio. In practice, however, the inlet area is often limited by overall vehicle geometry or shock-on-lip conditions. Optionally, the user can enter a desired sea-level static thrust and inlet area, and SCCREAM will iterate to determine the primary mass flow rate required.

In order to generate a POST engine table, a candidate engine's performance is evaluated over a range of altitudes and Mach numbers. These Mach number and altitude ranges can be set by the user. For example, a ramjet's operational Mach numbers might be set from 2 to 6, with altitude ranges from 30,000 feet to 150,000 feet. Overlapping Mach numbers and altitudes between various operating modes allows POST to select optimum engine mode transition points if desired. Default Mach number and velocity ranges are provided for each mode.

Performance in pure rocket mode is determined using flow equations for a high expansion ratio rocket engine operating in a vacuum. A user-enterable nozzle

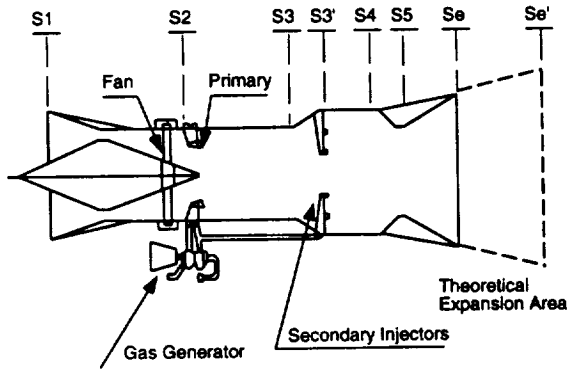

Figure 5 - SCCREAM Station Locations

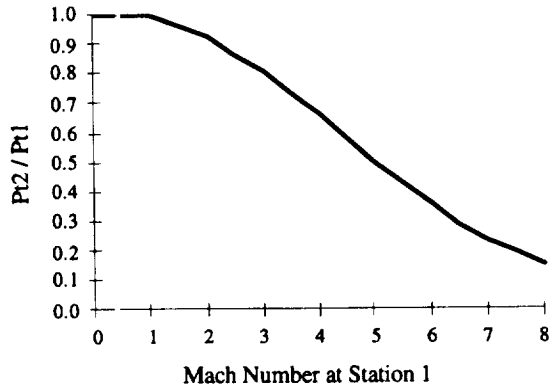

Figure 6 - MIL-E-5007D Inlet Pressure Recovery

efficiency is used to account for losses associated with the expansion of the primary exhaust through the engine and then onto the aftbody.

Station Calculations

Figure 5 shows the station numbers and reference locations for a generic RBCC engine used by SCCREAM. Station 1 is the inlet plane of the engine. Freestream flow conditions at station 'infinity' are modified by a single shock wave to simulate the precompression effect of a vehicle forebody on the engine. The forebody shape (wedge or cone) and the forebody angle are entered by the user. Therefore the flow conditions at station 1 are typically not the same as the freestream flight conditions.

From station 1 to station 2, the total pressure recovery through the inlet is determined using a standard Mil-Spec recovery schedule for an inlet terminating with a normal shock (figure 6). Pressure recovery is defined as the total or stagnation pressure at station 2 divided by the total pressure at station 1. If a supercharging fan is present and operating, the total pressure at station 2 is subsequently adjusted by the fan pressure ratio. Typical single-stage fan pressure ratios are 1.3 to 1.5. Total enthalpy from station 1 to station 2 is constant. The mixer is assumed to be of constant cross sectional area, but the flow area at station 2 is reduced by the total exit area of the rocket primaries. That is,

$$A_2 = A_3 - A_p \qquad (1)$$

where A_p is a function of the size of the rocket primaries. A_2 is therefore a 'pinch point' in the engine inlet due to the blockage caused by the rocket primary.

In ejector mode, the secondary mass flow (i.e. the mass flow rate of air through the inlet) is determined by the minimum inlet area or 'inlet throat' area. The flow is assumed to be choked at this point. By default, the inlet throat area is assumed to be 25% of the inlet area in ejector mode. Should the combination of rocket exhaust from the primaries and secondary air flow through the inlet exceed that amount which can be passed through the mixer exit (A_3) for a given flight condition, SCCREAM automatically reduces the inlet throat area and thus the secondary airflow through the engine until the flow is just choked at station 3.

In fan-ramjet and ramjet modes, the default inlet throat area is assumed to be equal to A_2. That is, the inlet is opened up until the minimum inlet area occurs at the pinch point around the rocket primaries. In this case, the secondary airflow through the engine is either the mass flow rate that can be passed through station 2 or the maximum mass flow rate captured by a wide open inlet area — whichever is less. At flight Mach numbers up to 3 or 4, the secondary mass flow tends to be limited by the pinch point at A_2 (note that the inlet area A_1 must also be reduced in this case). At higher Mach numbers, the secondary mass flow is generally limited by the maximum inlet area and is more typical of standard ramjet analysis.

Knowing total pressure, total enthalpy, secondary mass flow, and area, the solution for the Mach number at station 2 is iterative. For a guessed Mach number, the flow velocity at station 2 can be calculated in two ways — one using the temperature and Mach number (i.e. the definition of Mach number) and the other using pressure, temperature and mass flow rate (i.e. conservation of mass). SCCREAM uses a bisection routine to find the Mach number that drives the difference between the two calculated velocities to zero. For ejector, fan-ram, and ramjet modes, the subsonic solution for Mach number is always selected.

Between stations 2 and 3, the primary rocket exhaust (if present) is mixed with the secondary air from the inlet. SCCREAM assumes that the rocket primaries operate stoichiometrically (LH2/LOX = 1/8 by weight) and that no combustion occurs in the mixer. This is known as the diffusion-then-afterburning cycle. Again, the equations for conservation of mass, momentum, and energy are used to iteratively solve for the static pressure, temperature, and velocity at station 3 using the Mach number as an iteration variable. New primary + secondary flow specific heat (C_p), ratio of specific heats (γ), and molecular weight are also calculated at station 3 during the iteration process. Mass averaging techniques are used for C_p and molecular weight. The primary rocket mass flow rate (set by the user), the exhaust velocity, enthalpy, and pressure, the primary exit area, and the secondary flow conditions at station 2 are all knowns in the station 3 iteration process. As previously mentioned, if the total mass flow rate in ejector mode is too large to be passed through station 3, the inlet throat area is reduced until the flow is just choked at station 3. The total pressure calculated at station 3 after the solution has converged is multiplied by a mixer efficiency to account for viscous losses, etc.

The flow undergoes a simple isentropic expansion from station 3 to station 3' — just before the secondary fuel injectors. The combustor is assumed to be constant area. Therefore,

$$A_{3'} = A_4 \qquad (2)$$

The combustor area is input by the user as a ratio to the mixer area (A_4/A_3). The mixer ratio is specified as a ratio to the inlet area (A_1/A_3). Default area ratio values are provided.

The combustor operates at a user-defined maximum equivalence ratio, phi. Phi is the actual fuel-to-air ratio divided by the stoichiometric fuel-to-air ratio. A phi of 1 indicates stoichiometric combustor operation. For a given phi, SCCREAM uses the conservation equations for heat and mass addition in a 1-D flow to determine the exit conditions from the combustor (station 4). As with other stations, these equations require an iterative solution. The combustion of hydrogen fuel with atmospheric oxygen is modeled as a heat release based on the fuel flow rate and the heat of reaction. An efficiency is included on the heat of reaction. Combustion is assumed to be complete and one way. O_2, H_2, H_2O, and N_2 are the only valid combustion species. A phi = 1 therefore results in

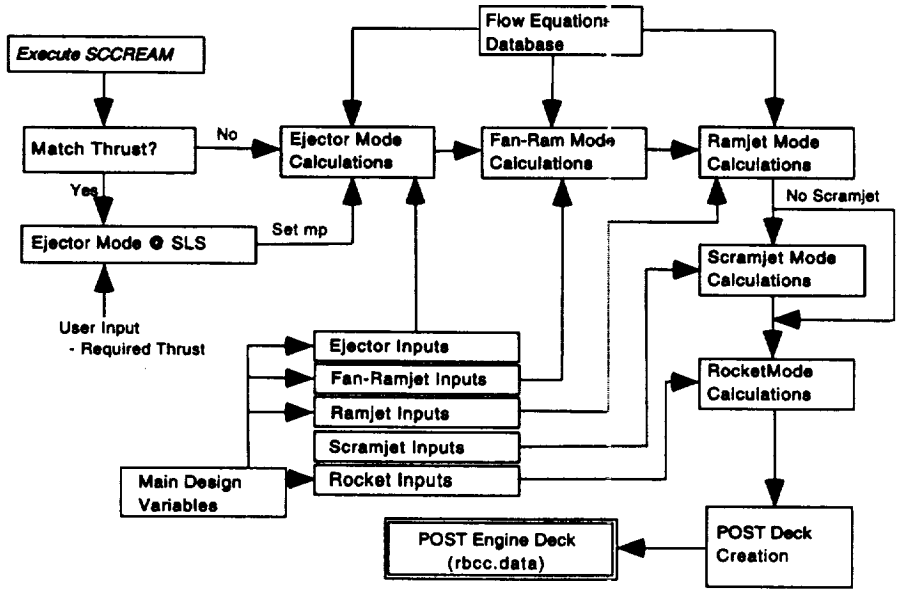

Figure 7 - SCCREAM Execution and Data Flow

only H_2O and N_2 products of combustion. A new γ, C_p, and molecular weight are also calculated at station 4.

If the user-input maximum phi results in a mass flow rate that cannot be passed through the combustor exit, SCCREAM automatically reduces phi at that flight condition until the flow is just choked at station 4. This typically occurs at the lower Mach numbers in fan-ramjet and ramjet modes.

The total pressure entering the nozzle (just past station 4) is reduced by a nozzle efficiency to account for viscous losses in the nozzle. Otherwise, the chemistry of the nozzle is assumed to be frozen at the composition exiting the combustor. The nozzle is a simple converging-diverging nozzle that expands the flow to supersonic speeds. At lower altitudes, the nozzle expands the flow to atmospheric pressure (ideal expansion). At higher altitudes, nozzle expansion is limited by a maximum exit area and the flow is often underexpanded. SCCREAM allows a user to model the effect of vehicle aftbody expansion by including a 'maximum theoretical expansion area' that increases with altitude. The rate at which the theoretical exit area increases and it's maximum value are user inputs. The exit pressure, exit velocity, and exit mass flow rate are used in a control volume equation along with the inlet conditions to determine the overall engine thrust, thrust coefficient (C_t), and I_{sp}. Thrust coefficient in the airbreathing modes is defined as,

$$C_t = \frac{\text{Thrust}}{q * A_1} \qquad (3)$$

where A_1 is a fixed constant (the inlet area). C_t is a common way to non-dimensionalize engine thrust to enable parametric scaling by inlet size and flight path.

Program Execution

Figure 7 is a flowchart that describes the general execution logic of SCCREAM. The flow diagram begins with the 'Execute SCCREAM' block and proceeds through each operational mode of the engine, with a few contingencies depending upon the engine configuration selected. Worth noting is the 'flow equations database' block. This block represents a C++ class object that contains all the necessary equations to determine temperatures, pressures, Mach numbers, etc. at each station inside the engine. The equations in this shared database are used in determining performance in the ejector fan-ramjet, and ramjet modes. The use of C++ and the class construct eliminates the need for excessive variable passing, as all variables are contained in a common area accessible by each other. This feature makes SCCREAM easy to read, debug, and modify.

Note that the flowchart also includes a block labeled 'scramjet'. While SCCREAM does not analyze supersonic combustion directly, a previously published scramjet performance database [7] generated at NASA - Langley has been included in SCCREAM for creating engine performance tables for scramjet-capable SESJ and ESJ RBCC engines. This existing data consists of a table of scramjet I_{sp} and C_t vs. Mach number. It is linearly scaled to provide a smooth transition from SCCREAM's Mach 5 ramjet data at each altitude. That is, for scramjet engines, SCCREAM is used to generate ramjet values for C_t and I_{sp} up to Mach 5 for various altitudes. Then the NASA scramjet data is scaled up or down and appended to the SCCREAM data *at each altitude* so that no discontinuity occurs in C_t or I_{sp}, but the trends in the NASA data are maintained.

SCCREAM Input and Output Files

SCCREAM operates either as a standalone executable code or as a contributing analysis in a larger design process. User input data is read from several files. Each engine mode has its own input file which contains that particular mode's requested Mach number and altitude ranges. A common input file for the main design variables (figure 8) is used by all modes except for scramjet. Included in this file are the primary flow rate, engine geometry, and station efficiencies. After each engine mode has been analyzed, a properly formatted POST engine file (figure 9) and additional data analysis files are created. SCCREAM runs very quickly. 100 different flight conditions and operating modes can be analyzed in about 30 seconds on a Silicon Graphics Indigo^2 workstation.

```
Primary_Flow_Rate      216.0 LBM/S
Number_Throttles       1
Throttle_Setting1      1.0
Forebody_Shape         CONE
Fan_Po_Ratio           1.0
Area_Inlet             30.0 ft2
Equivalence_Ratio      1.0

eta_Mixer              0.98
eta_Combustor          0.95
eta_Nozzle             0.98
```

Figure 8 - Sample Common Input File

```
I$tblmlt genv6m=577.8,
tvc1m=5,tvc2m=1,tvc3m=1,
 $
0,
      0, 80351.4
   0.25, 78268.2,
   0.50, 81398.3,

      6, 2611.57,
 $end
I$tab table=4hae2l,0,150 $
I$tab table=4hae3l,0,88.1674 $
```

Figure 9 - Sample Output (POST Engine File)

RESULTS

Reference Vehicle

To compare the RBCC engine data generated by SCCREAM to data available from other sources, a test case vehicle was adopted. Figure 10 shows a packaging view of the Hyperion launch vehicle. Hyperion is an advanced single-stage-to-orbit (SSTO) launch vehicle currently being investigated by students in the Aerospace Systems Design Laboratory at Georgia Tech. The vehicle is fully reusable and takes off and lands horizontally. It uses five LOX/LH2 ejector scramjet (ESJ) RBCC engines for primary propulsion. Small rocket engines are provided on the top of the aftbody to provide trim on ascent. The forebody has a conical lower surface with a 10° cone half angle and a shallow elliptical upper surface.

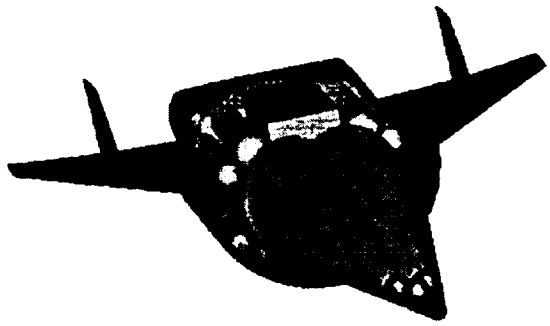

Figure 10 - Hyperion SSTO Launch Vehicle

Hyperion is capable of powered landing and self-ferry using four small hydrocarbon-fueled ducted fans mounted under the wings. These engines are protected by a retractable inlet cover during ascent and entry.

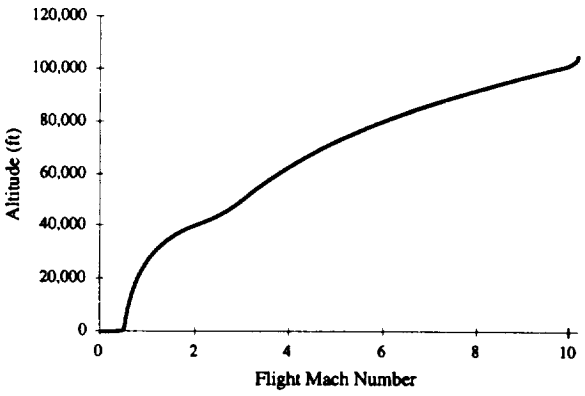

Figure 11 - Hyperion Ascent Trajectory

Hyperion is designed to deliver 10,000 lb to the International Space Station (220 nmi. x 220 nmi. x 51.6°) from Kennedy Space Center. It is unpiloted and could be operational by the year 2010. In ramjet and scramjet modes, the vehicle flies a constant dynamic pressure boundary trajectory of 1,500 psf (figure 11). Transition from scramjet mode to pure rocket mode occurs at Mach 10.

Table 1 summarizes the per engine ESJ engine characteristics for each of the five RBCC engines on the Hyperion. Note that the combination of required sea-level static thrust and fixed inlet area resulted in an ejector mode primary mass flow rate of 216 lbm/s. A pure rocket mode vacuum I_{sp} of 462 sec. was assumed.

Table - 1 Hyperion (Reference) ESJ Engine Data

inlet area, A_1	27 ft^2
'pinch point' area, A_2	8.24 ft^2
mixer area, A_3	11.25 ft^2
combustor area, A_4	22.5 ft^2
maximum exit area	95 ft^2
required sea level thrust	92,650 lb
nominal maximum phi	1.0

SCCREAM was run to generate engine performance data sets in ejector mode (from Mach 0 to Mach 3) and ramjet mode (from Mach 2 to Mach 6) over a range of altitudes for the reference engine. A second data set for a maximum phi = 0.6 was also generated. NASA - Langley scramjet data was scaled

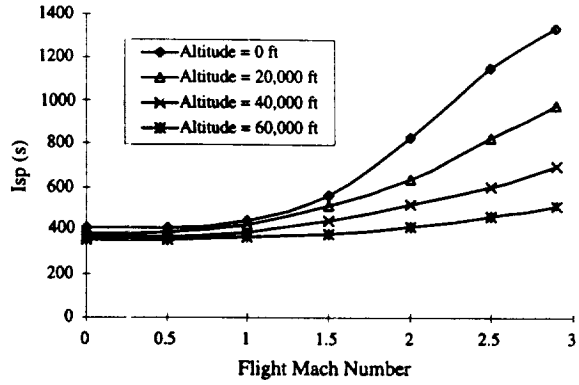

Figure 12 - Ejector Mode I_{sp} Results

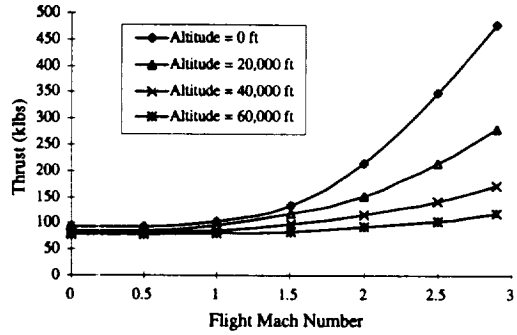

Figure 13 - Ejector Mode Thrust Results

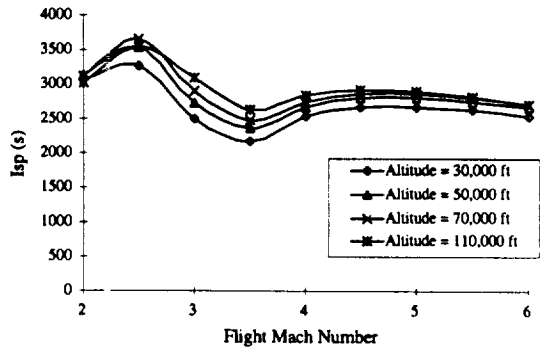

Figure 14 - Ramjet Mode I_{sp} Results

and appended to the ramjet data between Mach 5 and Mach 10 as previously described.

Figures 12 and 13 show a sample of the data set generated for ejector mode. Note the expected improvement in ejector I_{sp} and thrust as the vehicle accelerates (increases secondary flow rate). However, this augmentation effect is reduced at higher altitudes.

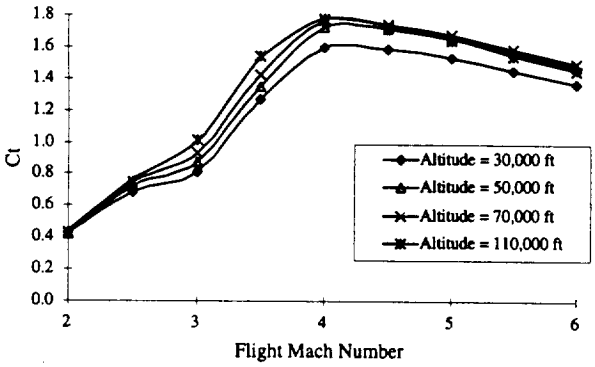

Figure 15 - Ramjet Mode C_t Results

SCCREAM generated data for ramjet mode I_{sp} and thrust coefficient are shown in figures 14 and 15. Note the unusual behavior in I_{sp} around Mach 3. As expected, the I_{sp} rises between Mach 2 and Mach 2.5 as thrust increases due to increased total pressure and secondary mass flow rate through the engine. However at around Mach 2.5, the I_{sp} unexpectedly begins to decline. A more detailed investigation of the results indicated that this decline is a result of secondary mass flow being limited by the area at station 2 — the inlet pinch point. As flight Mach number rises, the total pressure losses through the inlet increase, but in this case, the increase in secondary mass flow rate through the engine is slow to offset the losses. This effect is also evident in figure 15 as a smaller increase in C_t between Mach 2.5 and 3.

Between Mach 3 and 4, the limitation on engine secondary mass flow rate switches to become limited by the inlet area (like a more traditional ramjet), but the combustor would choke at the user-input phi = 1.0. SCCREAM has automatically throttled phi in this range. The result is a temporary increase in I_{sp} around Mach 4. I_{sp} and C_t behavior beyond Mach 4.5 is more typical of a ramjet with a phi = 1 and secondary mass flow rate limited by inlet area. Note that the effect of increased thrust coefficient with increasing altitude is primarily due to the increasing theoretical (aftbody) exit area as the vehicle ascends.

Using the phi = 1 SCCREAM data set, thrust and I_{sp} were calculated along a reference trajectory for Hyperion. Engine performance was determined at each altitude. Typical engine station flow values at two points along the reference trajectory are shown in table 2. It is important to note that a SCCREAM *data set* is not associated with a particular flight path, but is a range of thrust and I_{sp} vs. Mach number and altitude. Flying an optimum trajectory though the data set results in a specific history of I_{sp} and C_t (or thrust) vs. Mach number.

Table 2 - Sample SCCREAM Station Results

Ejector Mode for Reference Hyperion SSTO

Flight M=0.5 Phi=1.0	S_1	S_2	S_4	S_9
Area (ft^2)	27.0	8.24	22.5	17.3
Local Mach Number	0.50	0.57	-	1.51
Velocity (fps)	558.1	636.5	-	5290.1
Total Pressure (lb/in^2)	17.7	17.7	50.8	50.8
Total Temperature (R°)	544.6	544.6	5544.7	5544.7

Ramjet Mode for Reference Hyperion SSTO

Flight M=3.5 Phi=1.0	S_1	S_2	S_4	S_9
Area (ft^2)	27.0	8.24	22.5	44.3
Local Mach Number	3.02	0.63	0.90	2.08
Velocity (fps)	3278	1083	2488	4870
Total Pressure (lb/in^2)	100.4	78.2	45.3	45.3
Total Temperature (R°)	1345	1345	3446	3446

Comparison with Other Engine Performance Data

To validate the thrust, C_t, and I_{sp} values generated by SCCREAM, the results have been compared to engine data from other sources. The early Marquardt study [1] (referred to as NAS7-377 on the following figures) contains extensive RBCC engine performance data including ERJ ramjet and ESJ scramjet mode thrust and I_{sp} for a vehicle flying along a 1500 psf dynamic pressure boundary. The NAS7-377 data used in this paper is for an 8° half-angle wedge. The ERJ thrust data was converted to C_t using an 82 ft^2 inlet area and q = 1500 psf. The ESJ data used a 100 ft^2 inlet area.

A study of RBCC engines performed in 1988 by the Astronautics Corporation for the U.S. Air Force [3] contains C_t data for a scramjet and complete I_{sp} data for a ESJ engine over a 1500 psf trajectory. In the reference, C_t data is tabulated directly and does not have to be calculated from a known thrust. Although the vehicle baselined in that study was a 10° half-angle cone, the available tabulated I_{sp} data in the reference is for a 6° half-angle wedge.

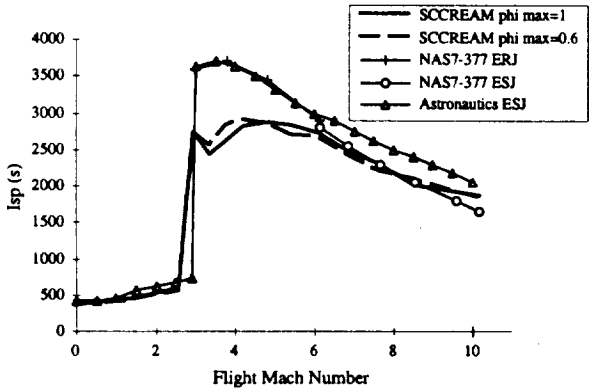

Figure 16 - I_{sp} Comparison Data (group 1)

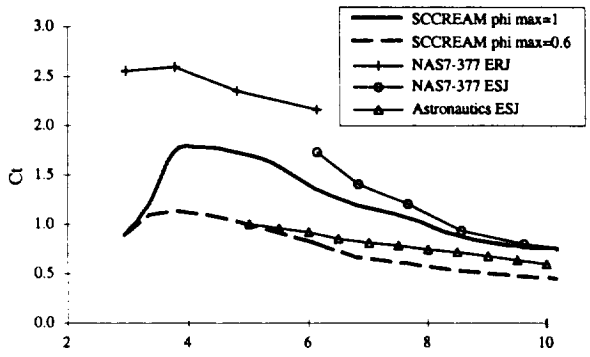

Figure 17 - C_t Comparison Data (group 1)

The effect of forebody precompression on an RBCC engine is not insignificant. Larger forebody angles tend to generate more thrust, but have a slightly lower I_{sp}. In addition, internal geometry areas and assumptions will certainly cause differences between data sets. However, the data from NAS7-377 and the Astronautics study are thought to provide a reasonably good comparison for SCCREAM appled to the Hyperion trajectory.

Figure 16 shows the engine I_{sp} for the two SCCREAM cases, the NAS7-377 ERJ and ESJ data, and the Astronautics study data for an ESJ. Figure 17 shows comparison data for C_t in ramjet and scramjet modes. C_t provides a better comparison in airbreathing modes than overall thrust due to the differences in reference vehicle size among the data sets.

Comparison of I_{sp} in figure 15 indicates good agreement in ejector mode and scramjet modes. However, SCCREAM yields a slightly lower I_{sp} in ramjet mode than the comparison data. It is thought that this effect is caused by the small A_2 in the Hyperion engine and it's effect on limiting secondary mass flow rate at those Mach numbers. However, work is continuing to verify this conclusion. The SCCREAM thrust coefficient data in figure 17 is nicely bounded by the two comparison sets. Compared to the I_{sp} results, the larger differences among the C_t data sets are probably due to different internal engine geometries and forebody precompression assumptions as previously discussed.

Comparison with Other Engine Analysis Codes

A comparison also was made to evaluate SCCREAM against other engine performance codes. SRGUL is the engine performance tool used to generate the NASA - Langley ramjet and scramjet performance data in reference 7. SRGUL is a higher fidelity code than SCCREAM, but is more time consuming to set up and run. It uses oblique shock solutions in the inlet, a marching solution for reacting flow through the combustor, and a method of characteristics solution for the nozzle. Viscous effects due to boundary layer growth are handled throughout. To achieve this extra detail, each engine flight condition requires significant setup and validation time. SRGUL is typically used in a *preliminary* design effort where the vehicle, engine geometry, and the flight profile are better established rather than in the *conceptual* environment for which SCCREAM was developed.

Note that the SRGUL data from reference 7 is also the data internally scaled by SCCREAM to predict scramjet performance above Mach 5. However, the SRGUL data presented in the following charts is the raw data (unscaled) from reference 7 for both ramjet and scramjet modes. The SRGUL data was generated for a 5° half angle cone. However, it is not for an RBCC engine. That is, the engine is a straight dual-mode ramjet/scramjet. There are no rocket primaries in the flow and therefore no pinch point in the inlet.

RAMSCRAM [8] is a ramjet and scramjet analysis tool developed by the NASA - Lewis Research Center. It is also capable of modeling ejector mode. RAMSCRAM is similar to SCCREAM, in that it was created for use in the conceptual design environment. It uses a pressure recovery through the inlet (or a kinetic energy efficiency) and quasi -1D flow

throughout. The combustion model in RAMSCRAM is more detailed than that used in SCCREAM, and accounts for equilibrium chemistry. That is, the composition of the flow leaving the combustor is a function of chemical equilibrium determined from pressure and temperature. Recall that SCCREAM assumes the reaction is complete and that only major constituents are produced in the combustor. The combustor area in RAMSCRAM can be constant or increasing.

RAMSCRAM does not automatically adjust phi or secondary mass flow rate if there is a choking problem in the engine (the user must correct the error manually), but it does have a feature to vary station area as needed to pass the mass flow (called engine design mode). The code can run a number of flight conditions at once, but the output is not formatted as a POST engine input table and must be post-processed. Typically, RAMSCRAM is run only for points along a predetermined flight path, rather than creating a broad data set over a range of Mach numbers and altitudes. RAMSCRAM is written in FORTRAN.

RAMSCRAM was used (by the authors) to model the reference Hyperion engine geometry and to predict engine thrust and I_{sp} at several points along the reference 1500 psf flight path. In ramjet mode, RAMSCRAM used the same inlet pressure recovery as that used by SCCREAM (figure 6). In scramjet mode, RAMSCRAM used a 98.5% inlet kinetic energy efficiency. The engine mixer area, pinch point area, and combustor areas according to table 1 were kept constant in RAMSCRAM. Inlet throat area and combustor phi were adjusted according to the same logic used by SCCREAM as necessary to prevent choking. Precompression effects for a 10° cone and aftbody expansion benefits were also included.

Figures 18 and 19 compare the SCCREAM results to SRGUL and RAMSCRAM for the Hyperion trajectory. The SRGUL data is for phi = 1. The RAMSCRAM data is for a maximum phi = 1. When running RAMSCRAM, the secondary mass flow rate (pinch point) and phi (combustor) both had to be reduced to prevent choking in ramjet mode at Mach 3. The phi also had to be reduced to prevent combustor choking in scramjet mode at Mach 6.

With the exception of the dip in the SCCREAM data around Mach 3, the SRGUL data and the SCCREAM data compare favorably in I_{sp}. Recall that SCCREAM and RAMSCRAM model a pinch point area due to the rocket primary and the SRGUL data does not. The RAMSCRAM I_{sp} data bounds the other two sets but at a somewhat higher than expected margin of error. However, the I_{sp} trends for all three codes appear to be similar. Note the sharp transition from subsonic to supersonic combustion operation predicted by RAMSCRAM. A smooth transition between modes was not modeled, rather the entire internal flow was either subsonic or supersonic.

SCCREAM and SRGUL C_t results compare well. As expected, the SCCREAM phi = 1 results are slightly higher than the SRGUL data due to the benefits of extra forebody compression (a cone half angle of 10° vs. 5° for SRGUL). The effects of limited secondary mass flow at the pinch point and a throttled phi to prevent choking in the constant area combustor

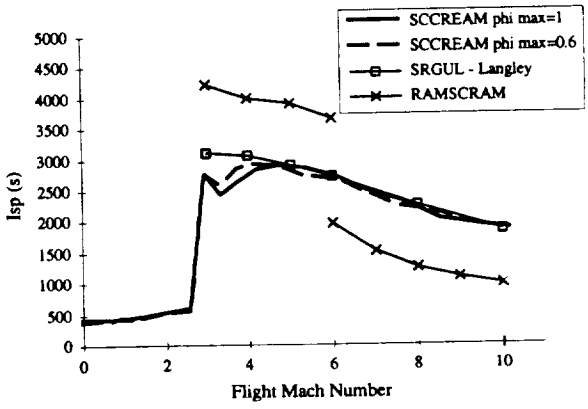

Figure 18 - I_{sp} Comparison Data (group 2)

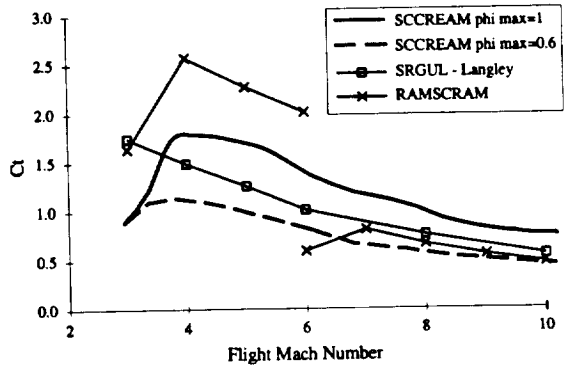

Figure 19 - C_t Comparison Data (group 2)

are clearly evident in the downturns in C_t for SCCREAM and RAMSCRAM at Mach 3 and for RAMSCRAM's supersonic flow result at Mach 6. Recall that there is no pinch point in the SRGUL data and there is no downturn of C_t at Mach 2.

The higher thrust coefficient predicted by RAMSCRAM in ramjet mode is almost certainly causing the higher I_{sp} also seen in figure 18. Work is continuing to identify the cause of this discrepancy, but it is likely due to differences in the combustor model between SCCREAM and RAMSCRAM.

CONCLUSIONS

An analysis tool for predicting RBCC engine performance has been developed and is well suited for use in the conceptual launch vehicle design environment. SCCREAM uses a quasi-1D engine analysis method to predict engine I_{sp} and thrust over a wide range of flight conditions. The code outputs a properly formatted engine table for use in an industry standard trajectory optimization code, POST. Among the conclusions drawn in this paper are the following:

1. Written in C++ and running operating on a UNIX workstation, SCCREAM is a significant improvement over it's spreadsheet-based predecessors in terms of speed, stability, and flexibility.

2. SCCREAM was easily integrated into the conceptual design process for a reference RBCC SSTO launch vehicle. SCCREAM generated engine performance tables were used to identify an optimum flight path trajectory.

3. For the reference engine geometry and flight profile tested, the results from SCCREAM compare favorably with previously published RBCC engine performance data as well as data produced by other engine analysis tools.

FUTURE WORK

SCCREAM will continue to be improved to increase it's accuracy and capabilities without sacrificing speed, ease of use, and flexibility. Among the near-term improvements being considered are the following:

1. The ability to analyze scramjet mode performance directly within SCCREAM. While the basic flow equations are in place, improvements to the combustion model, the inlet model, and modification of the iteration flow property iteration schemes will be required. This will eliminate the dependence on NASA scramjet data.

2. An improved method of calculating specific heat capacity, C_p, for the flow at various stations. The current very limited table look-up mechanism will be replaced with a more detailed table or curve fit.

3. An improved inlet pressure recovery model. A new pressure recovery model will be created that includes information about the actual inlet geometry in the calculation of pressure recovery.

4. Demonstrate that SCCREAM can be included in an automated launch vehicle design framework or computing architecture. From the beginning, SCCREAM was created to be a design-oriented code. It can operate as a standalone code, but can also be included as a subroutine or contributing analysis in a larger multidisciplinary design optimization framework. This capability will allow the system-level designer to optimize the entire vehicle (propulsion, trajectory, configuration, material, etc.) for an overall objective function (e.g. return on investment).

ACKNOWLEDGMENTS

Development of SCCREAM was primarily sponsored by the NASA - Marshall Space Flight Center under grant NAG8-1302 to the Georgia Institute of Technology.

The authors would like to thank members of the Georgia Tech Hyperion design team for providing reference concept data — John Bradford, David McCormick, David Way, and Mike Lee. Patrick McGinnis was instrumental in setting up the RAMSCRAM runs for comparison and Chris Snyder of NASA - Lewis provided valuable RAMSCRAM support. In addition, we acknowledge Greg Saks for

his work in developing earlier models that have lead to the current SCCREAM tool.

REFERENCES

1. Escher, William J. D. and B. J. Flornes. A Study of Composite Propulsion Systems For Advanced Launch Vehicle Application. Contract NAS7-377. The Marquardt Corporation: Van Nuys, California 1966. Vol 1-7.

2. William J. D. Escher, ed. The Synerjet Engine: Airbreathing/Rocket Combined-Cycle Propulsion for Tomorrow's Space Transports, SAE PT-54, Society of Automotive Engineers, Warrendale, PA, 1997.

3. Foster, R. W., W. Escher, and J. Robinson, "Air Augmented Rocket Propulsion Concepts." USAF Astronautics Laboratory Report AFAL-TR-88-004, April 1988.

4. Olds, J. R. "Multidisciplinary Design Techniques Applied to Conceptual Aerospace Vehicle Design." Ph.D. Dissertation. North Carolina State University, Raleigh, NC, 1993.

5. Brauer, G. L., et al. "Program to Optimize Simulated Trajectories (POST)." Final report for NASA contract NAS1-18147, Martin-Marietta Corp., September 1989.

6. Olds, J. R. and G. Saks. "A Conceptual Design Tool for RBCC Engine Performance Analysis." *Published in the proceedings of the 1997 Space Technology and Applications International Forum (STAIF-97)*, American Institute of Physics and the University of New Mexico, Albuquerque, NM, January 26-30, 1997.

7. Shaughnessy, J. D., et. al. "Hypersonic Vehicle Simulation Model." NASA TM-102610, November 1990.

8. Burkardt, L. A. and L. C. Franciscus. "RAMSCRAM - A Flexible Ramjet/Scramjet Engine Simulation Program." NASA TM-102451. June, 1990.

NAG8-1302 Report Attachments

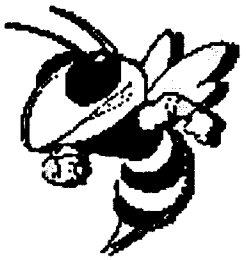

- SCCREAM Development
  - SCCREAM summary slides (Bradford, 1998 AIAA JPC)
  - 1998 and 1997 technical papers (Bradford/Olds)

- *Hyperion* Vehicle
  - Current *Hyperion* status slides (SSDL team/Bradford, 1/99)
  - RBCC vehicle "Honest Assessment" slides (Olds, 2/98 RBCC Workshop)
  - RBCC vehicle "Better Direction" slides (Olds, 1998 NASA summer stay)
  - 1997 *Hyperion* trade studies (Bradford, 1997 summer internship)

- 1998 Bantam-X Support
  - 1998 LOX/LH2 *Stargazer* overview slides (SSDL team/Ledsinger, 1/99)
  - *Stargazer* staging Mach number trade study (Ledsinger, 1998 summer internship)
  - 1998 *Bantam Argus* overview slides (SSDL team/Way, 6/98)

- 1998 Mars Exploration Support
  - Mars Mission trajectory evaluation slides (Poston, 1998 summer internship)

Hyperion Vision Vehicle

John E. Bradford

Dr. John Olds, Ashraf Charania,

Laura Ledsinger, David McCormick,

Kirk Sorensen

Georgia Tech Aerospace Engineering

Space Systems Design Laboratory

Outline

- Vehicle Concept & Technologies Description
- Baseline Performance Results
- Baseline Cost Results
- Mach Number Trade Performance Results
- Mach Number Trade Cost Results

Baseline Hyperion Concept

Hyperion Mission Overview

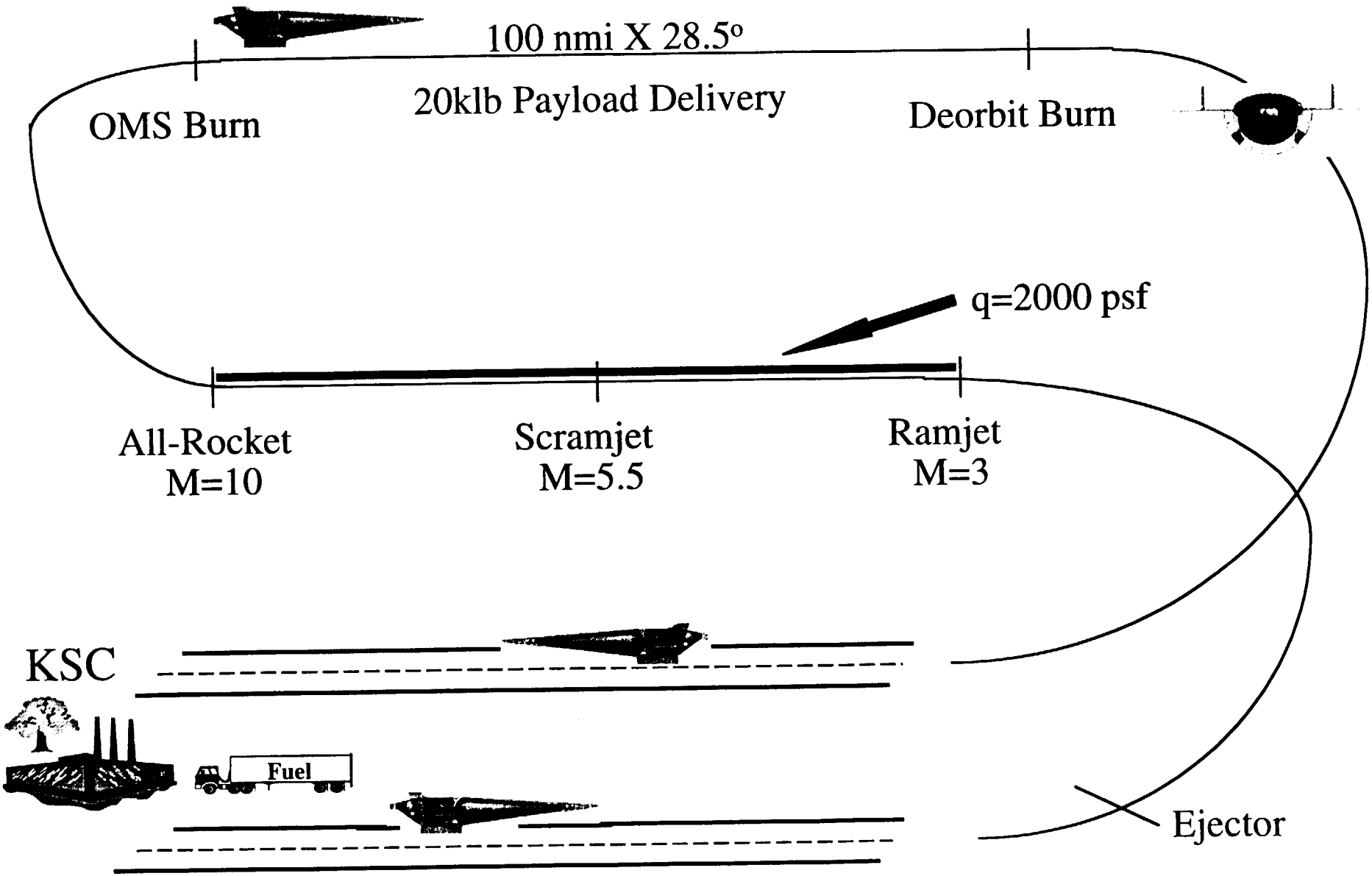

Hyperion Ramjet Ascent

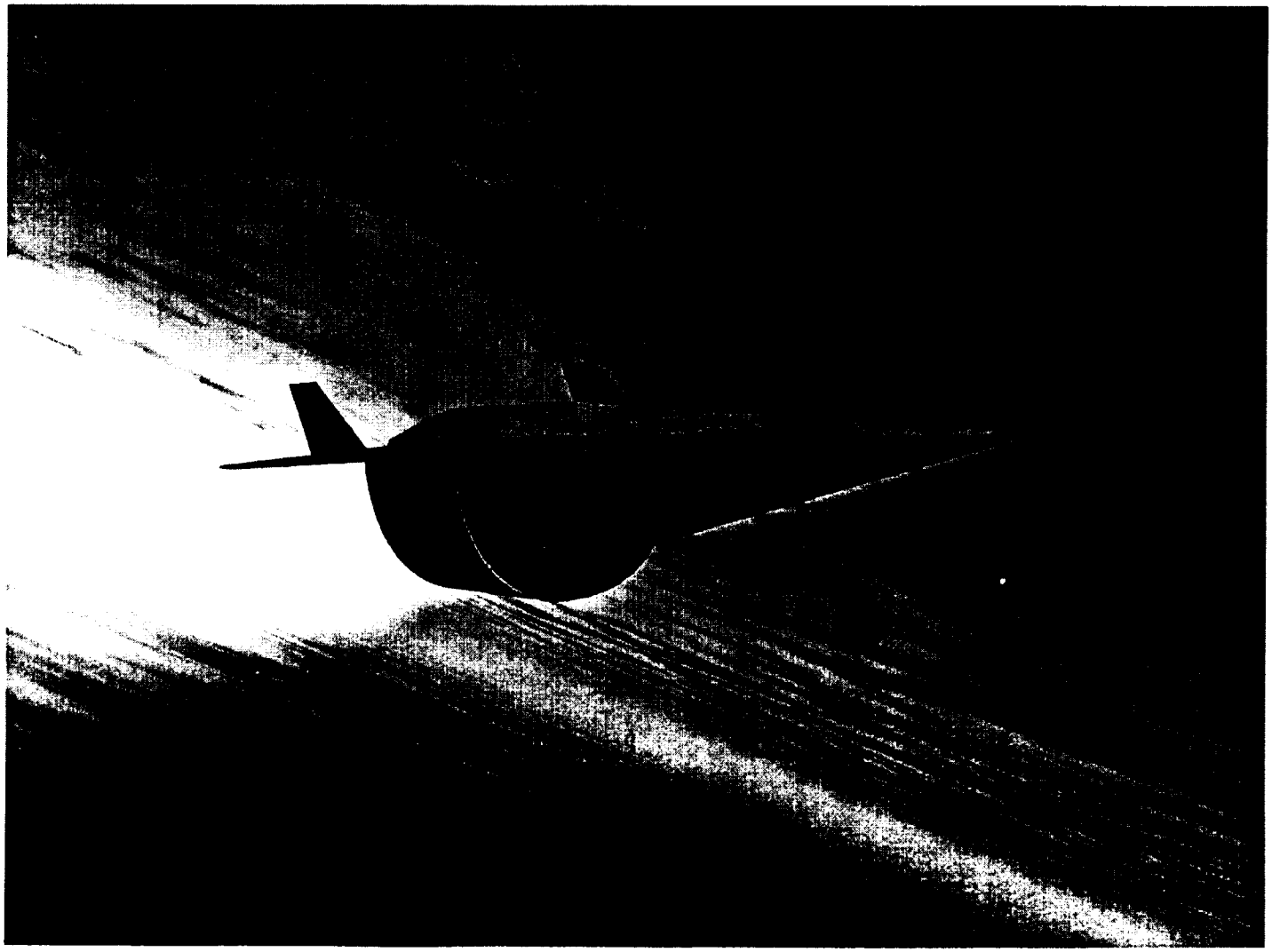

jeb/7.97/4

Hyperion Scramjet Ascent

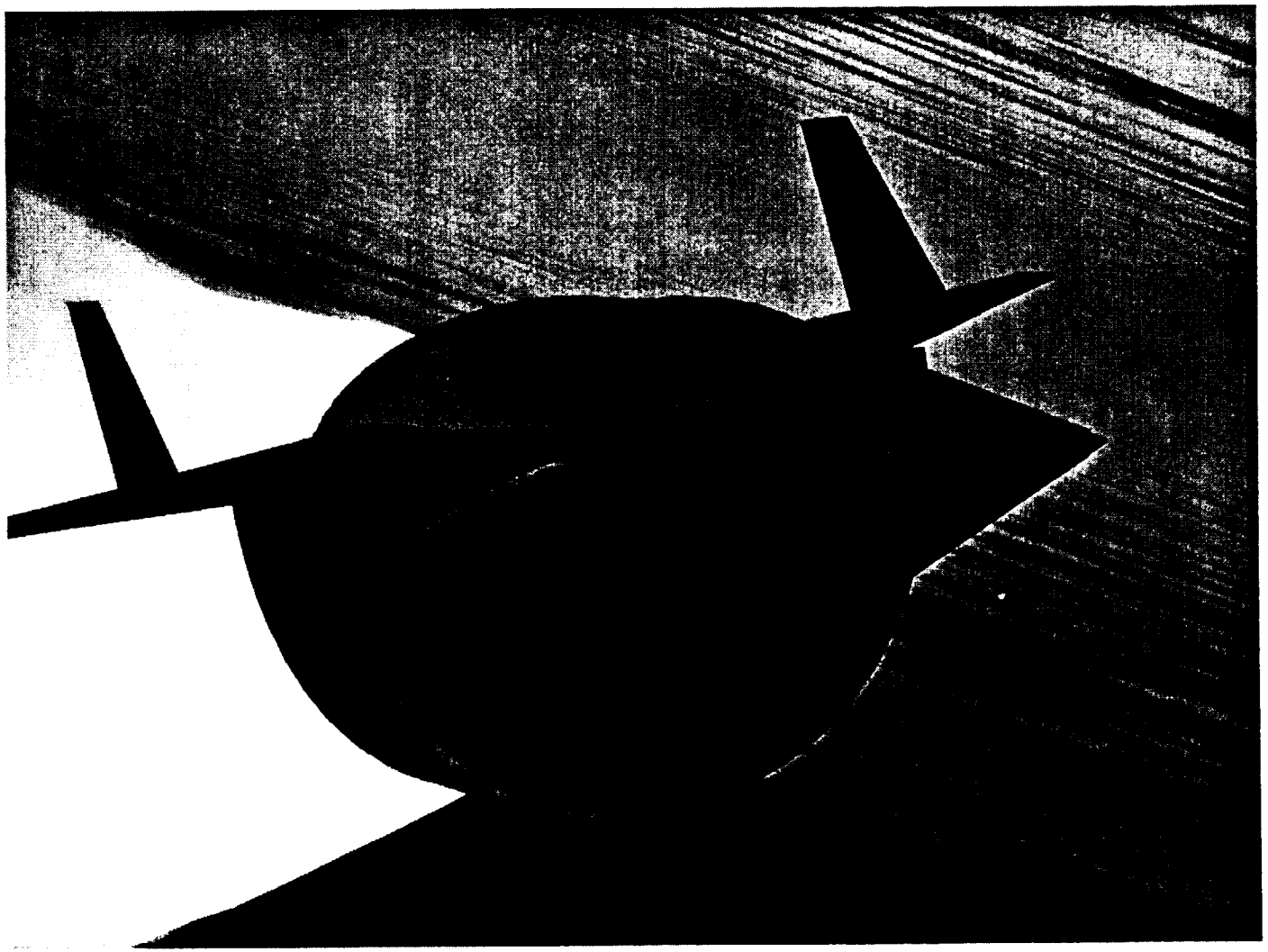

Hyperion Orbit Operations

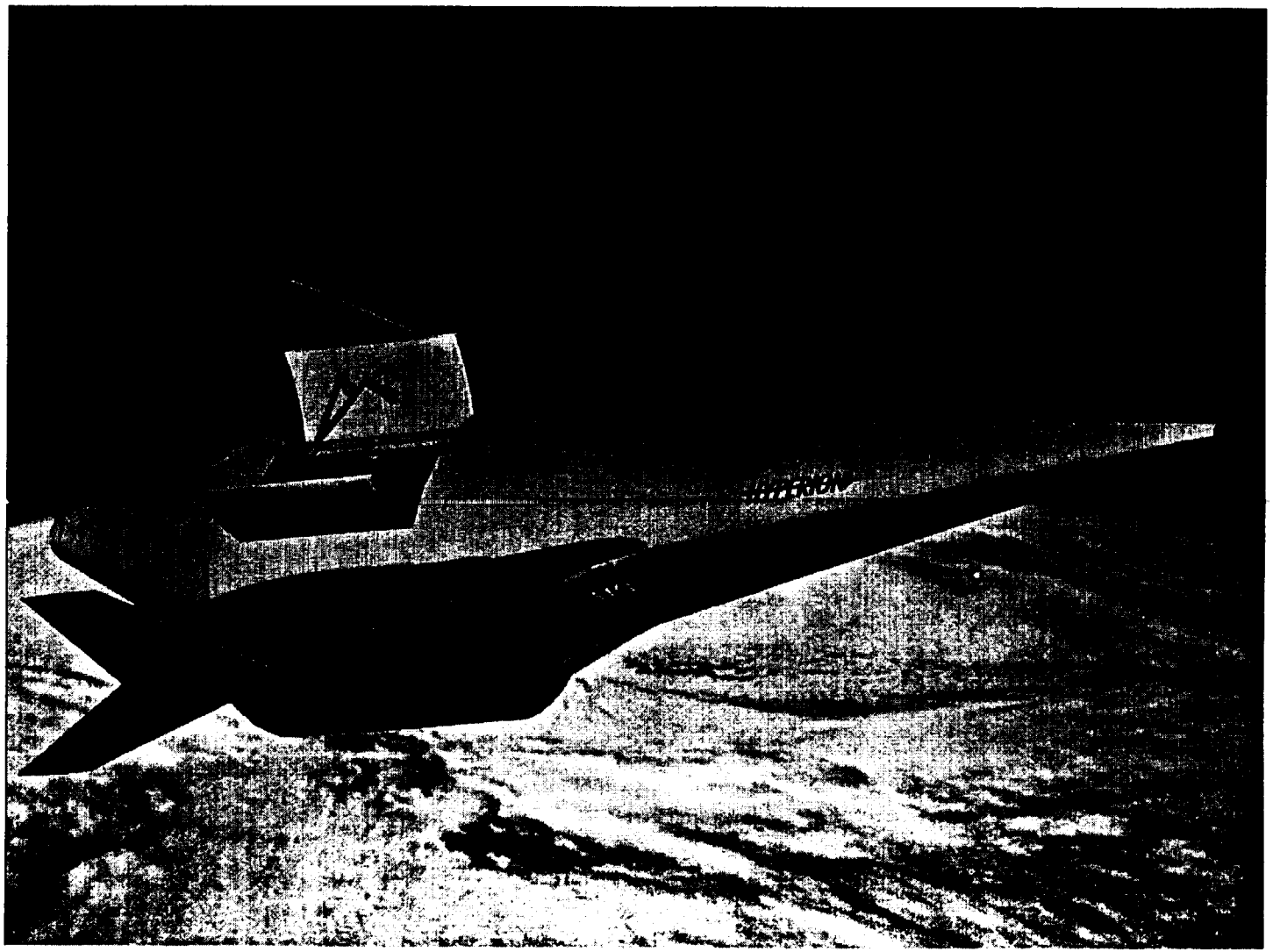

Hyperion Flyback

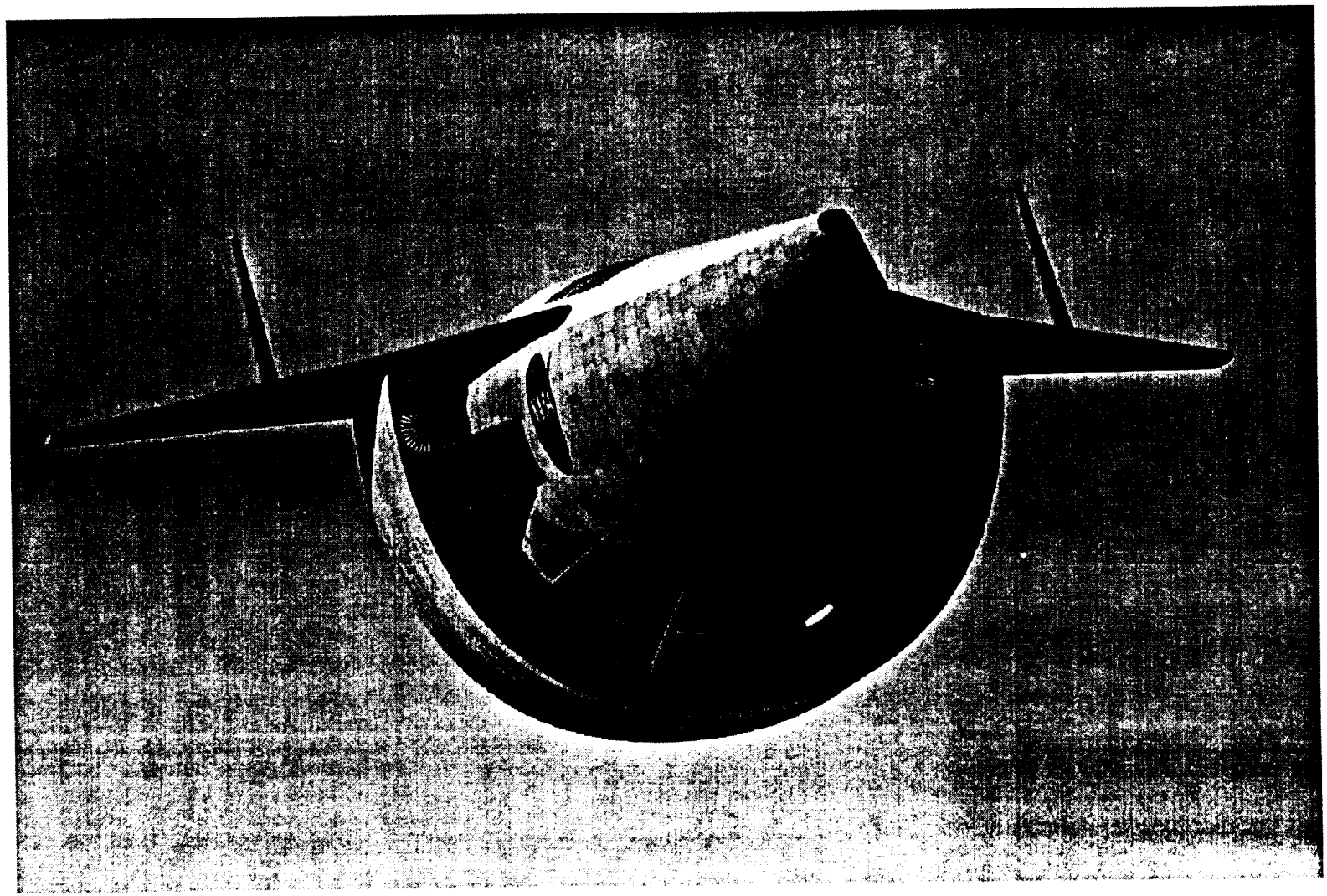

CAD/Packaging Model

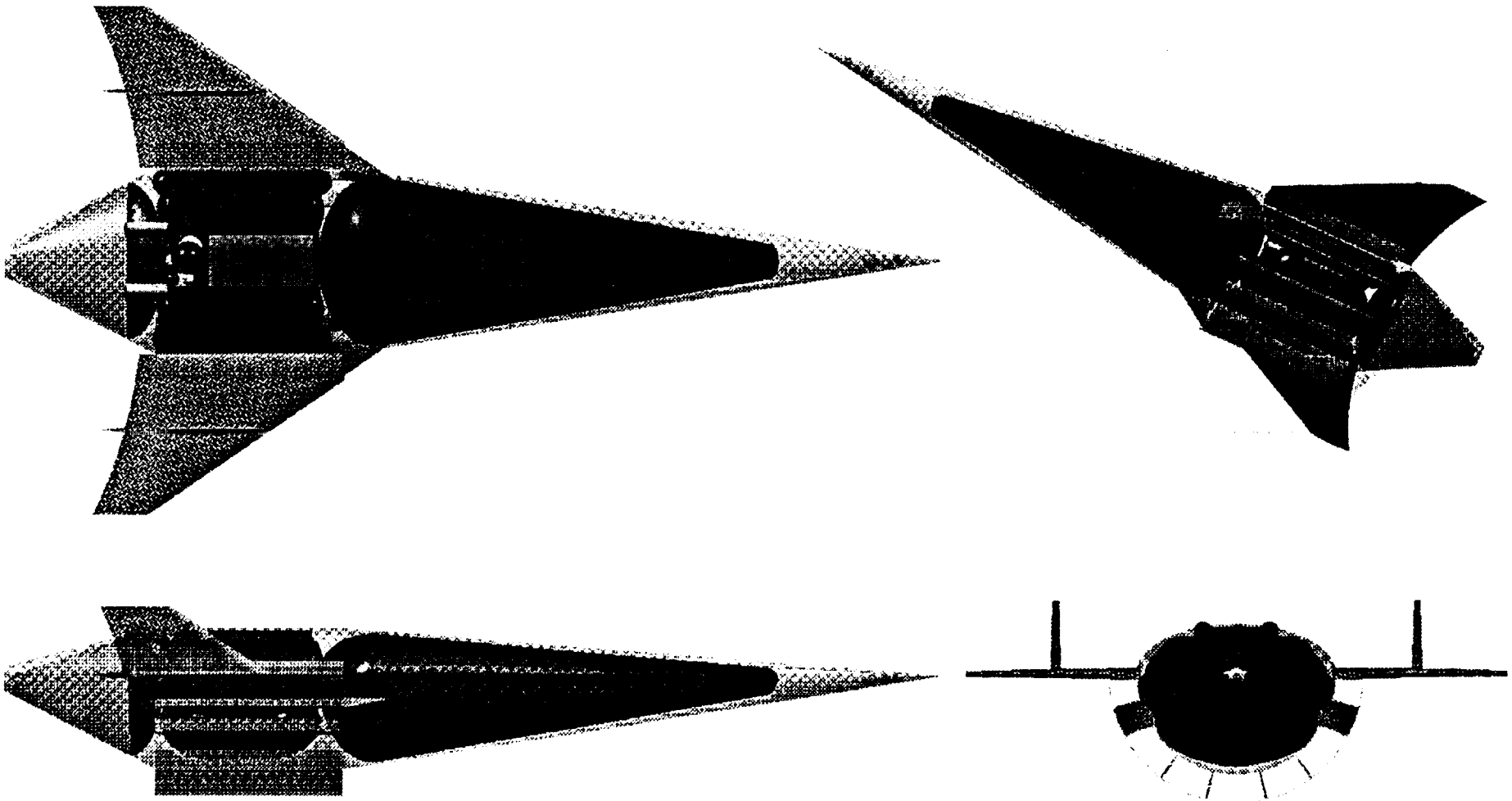

jeb/7.97/8

Baseline Hyperion Concept

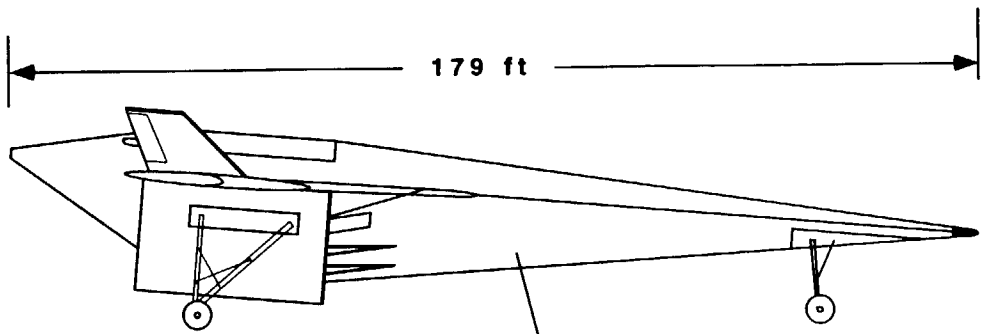

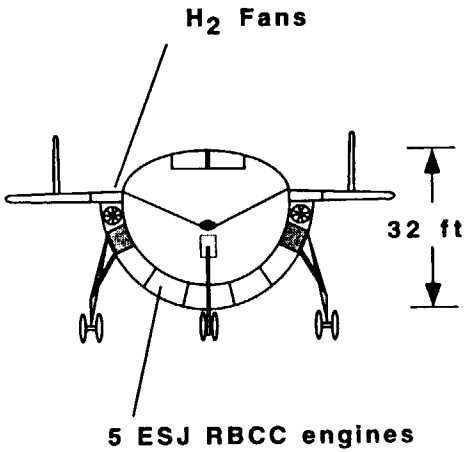

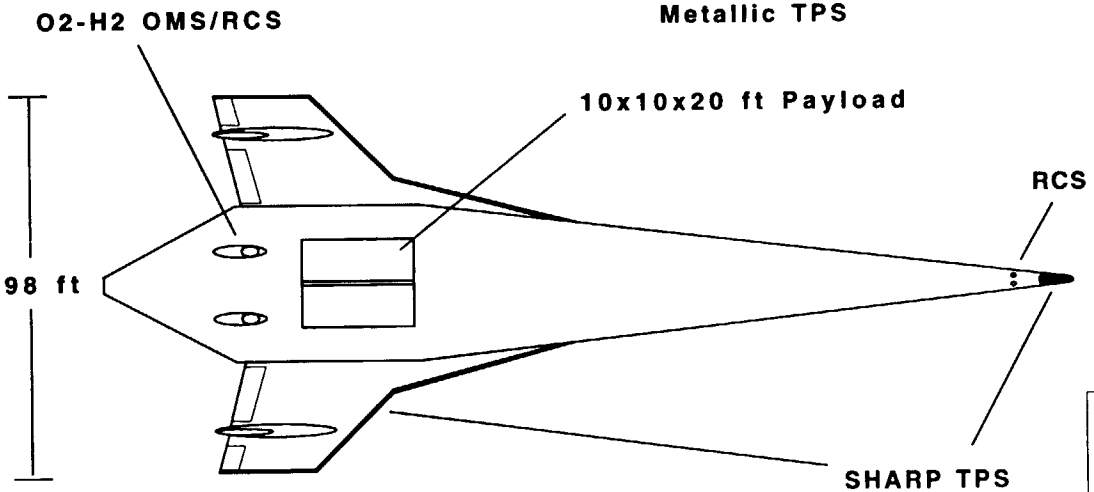

Vehicle Characteristics:	
Gross Weight:	800,700 lbs.
Propellant Weight:	645,250 lbs.
Payload Weight(LEO):	20,000 lbs.
Inert Weight:	155,450 lbs.
Mass Ratio:	5.151
Mixture Ratio:	3.08

jeb/7.97/9

Baseline Hyperion Concept

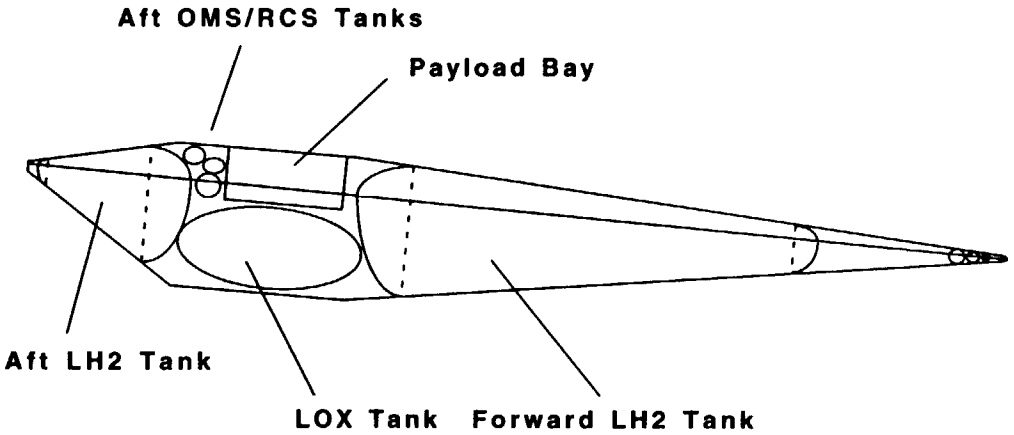

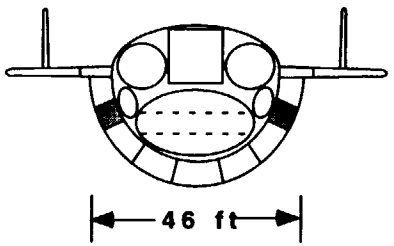

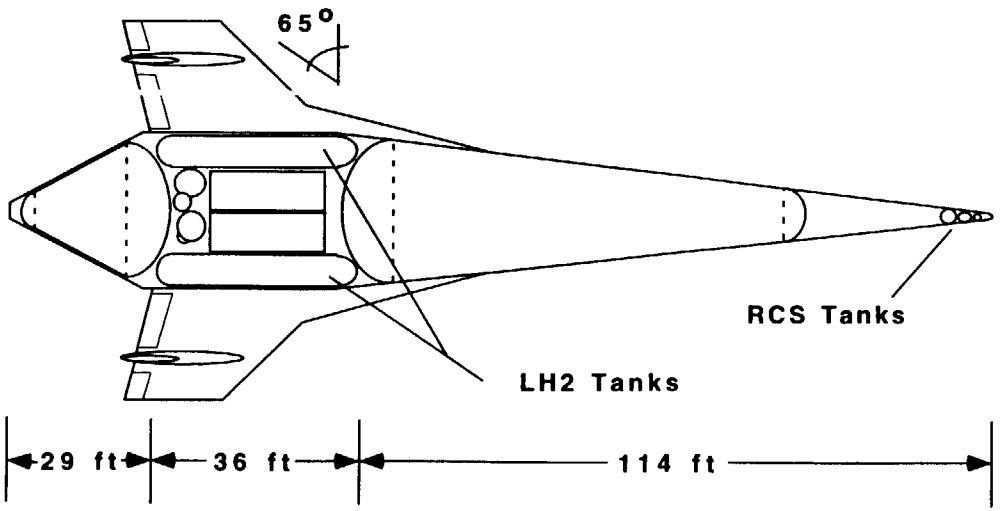

Vehicle Characteristics:	
Gross Weight:	800,700 lbs.
Propellant Weight:	645,250 lbs.
Payload Weight(LEO):	20,000 lbs.
Inert Weight:	155,450 lbs.
Mass Ratio:	5.151
Mixture Ratio:	3.08

jeb/7.97/10

Hyperion Highlights

- Five ESJ RBCC Main Propulsion
  - » ejector, ramjet, scramjet, and rocket mode
  - » Two H_2 Powered Fans
  - » Provide 5 minutes of loiter capability
  - » Self-ferry between sites
- Lightweight Materials and Subsytems
  - » integral graphite/PEEK tanks (w/metal liners)
  - » Ti-Al wings with Ti-Al/Si-C carry-through structure
  - » SHARP TPS on nose, engine cowl, and wing leading edges
  - » high power density fuel cells, EMA's, adv. avionics

Design Analysis Tools

- Performance — POST
- Aerodynamics — APAS
- Propulsion — SCCREAM
- Vehicle Weights — MER's in MS Excel Spreadsheet
- Engine Weight — WATES
- Solid Modeling — IDEAS
- Cost — CABAM

Design Analysis Assumptions

- Photographically scaled vehicle
  - » eliminated feedback to aerodynamics and packaging when resizing
- Curve fit packaging efficiency
- Maximum wing load limit of 1.75*GLOW

Baseline Hyperion

- Target Orbit: 100 nmi circular x 28.5 deg
  - » MECO at 50 X 100 nmi
  - » OMS burn to 100 nmi circular
- Payload: 20,000 lbs LEO (~11,000 lbs ISS from KSC)
- Maximum airbreathing Mach number: 10
- 9° Conical forebody angle
- Dynamic Pressure: 2000 psf
- Dry Weight Margin: 15%
- Vehice takeoff T/W: 0.6
- Installed RBCC T/W (SLS): 28.8
- Rocket Mode Isp : 455 sec.

Baseline Hyperion Weights

Name	Weight (lbs)
Wing and Tail Group	19,200
Body Group (incls. tanks)	28,150
Thermal Protection	7,600
Main Propulsion	20,750
OMS/RCS Propulsion	2,500
Subsystems and Other Dry Weights	28,950
Dry Weight Margin (15%)	16,100
Dry Weight	123,250
Payload	20,000
Other Inert Weights (residuals, etc.)	12,200
Insertion Weight	155,450
Ascent Propellants	645,250
Gross Lift-off Weight	800,700

jeb/7.97/15

Dry & Gross Weight Breakdown

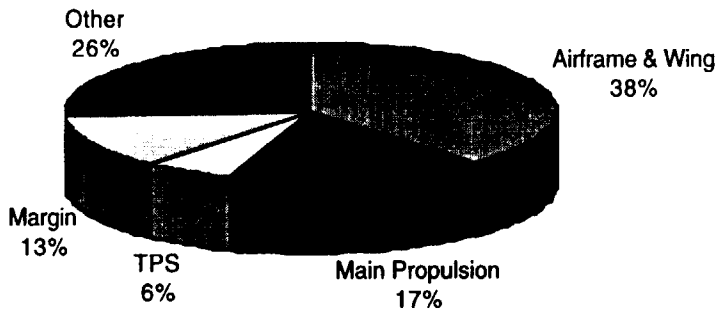

Dry Weight = 123,250 lbs

Gross Weight = 800,700 lbs

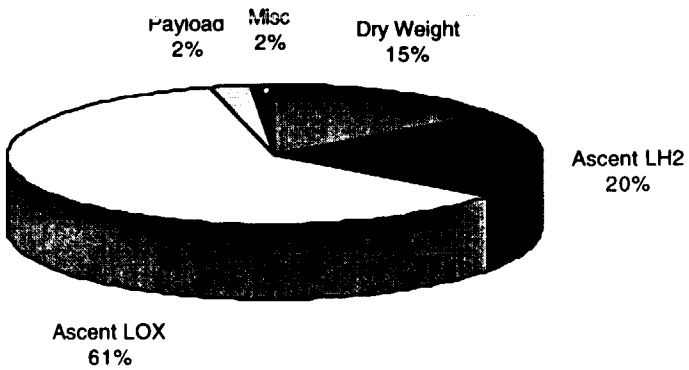

Ascent ΔV Breakdown

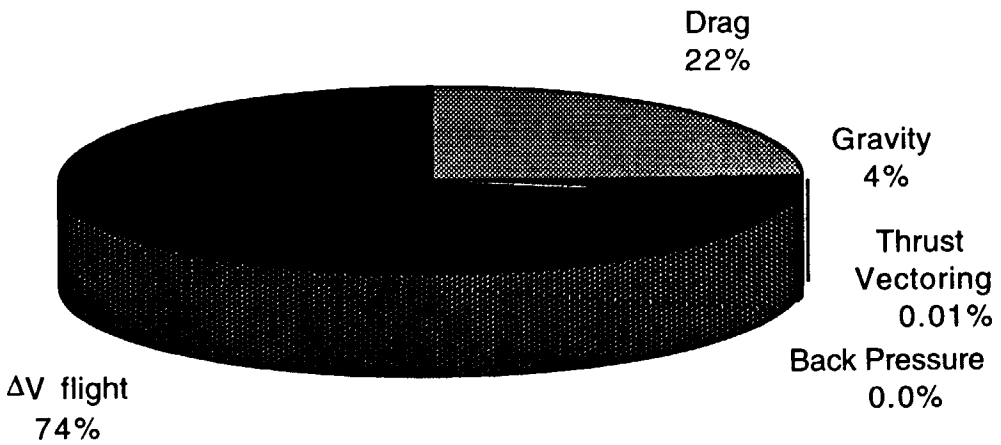

Total Losses = 8,610 fps
ΔV Ideal = 33,105 fps
Isp* = 471 sec
Isp bar = 661 sec

jeb/7.97/17

Mach Number vs. Time

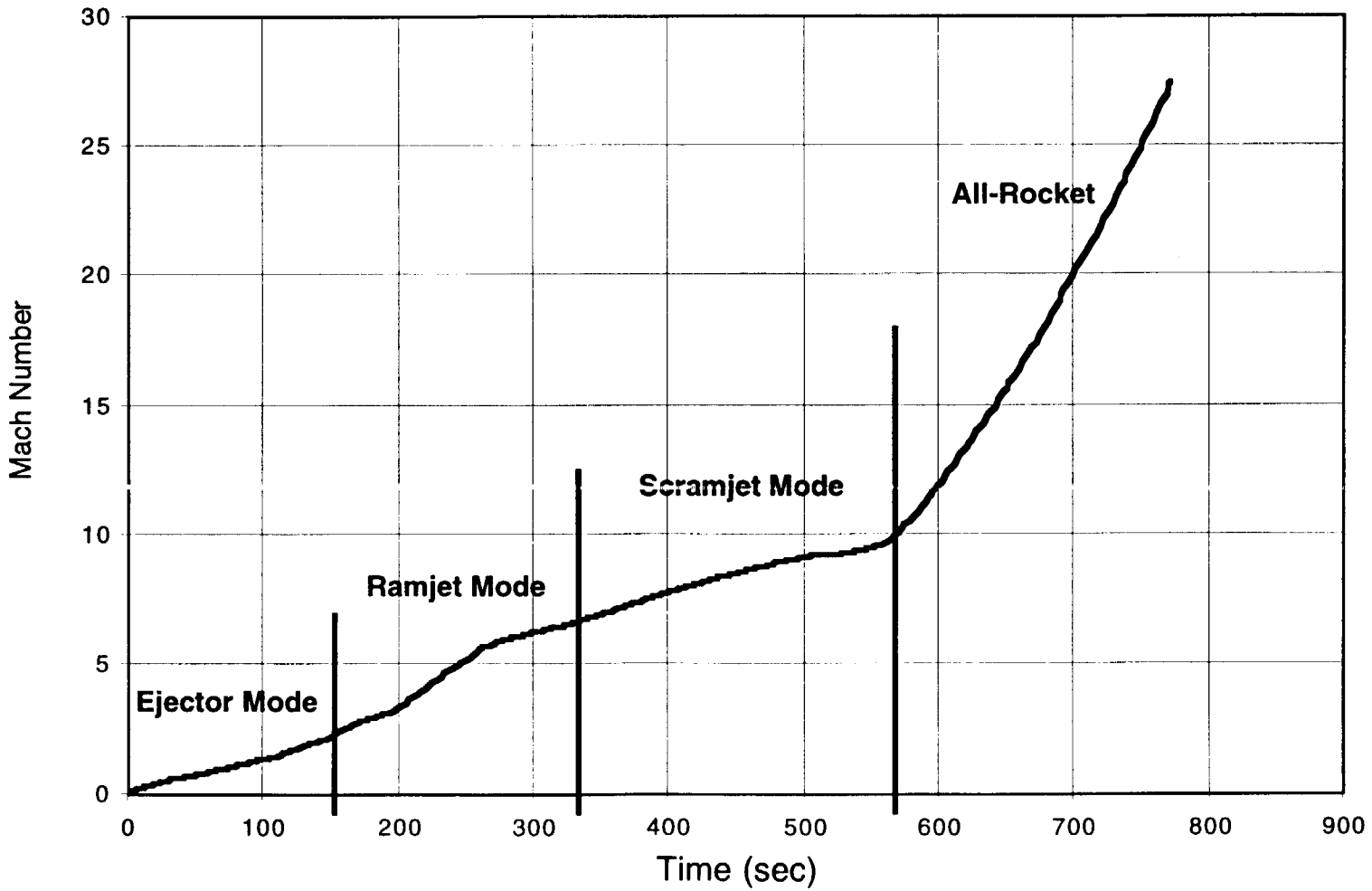

jeb/7.97/18

Thrust Coefficient vs. Time

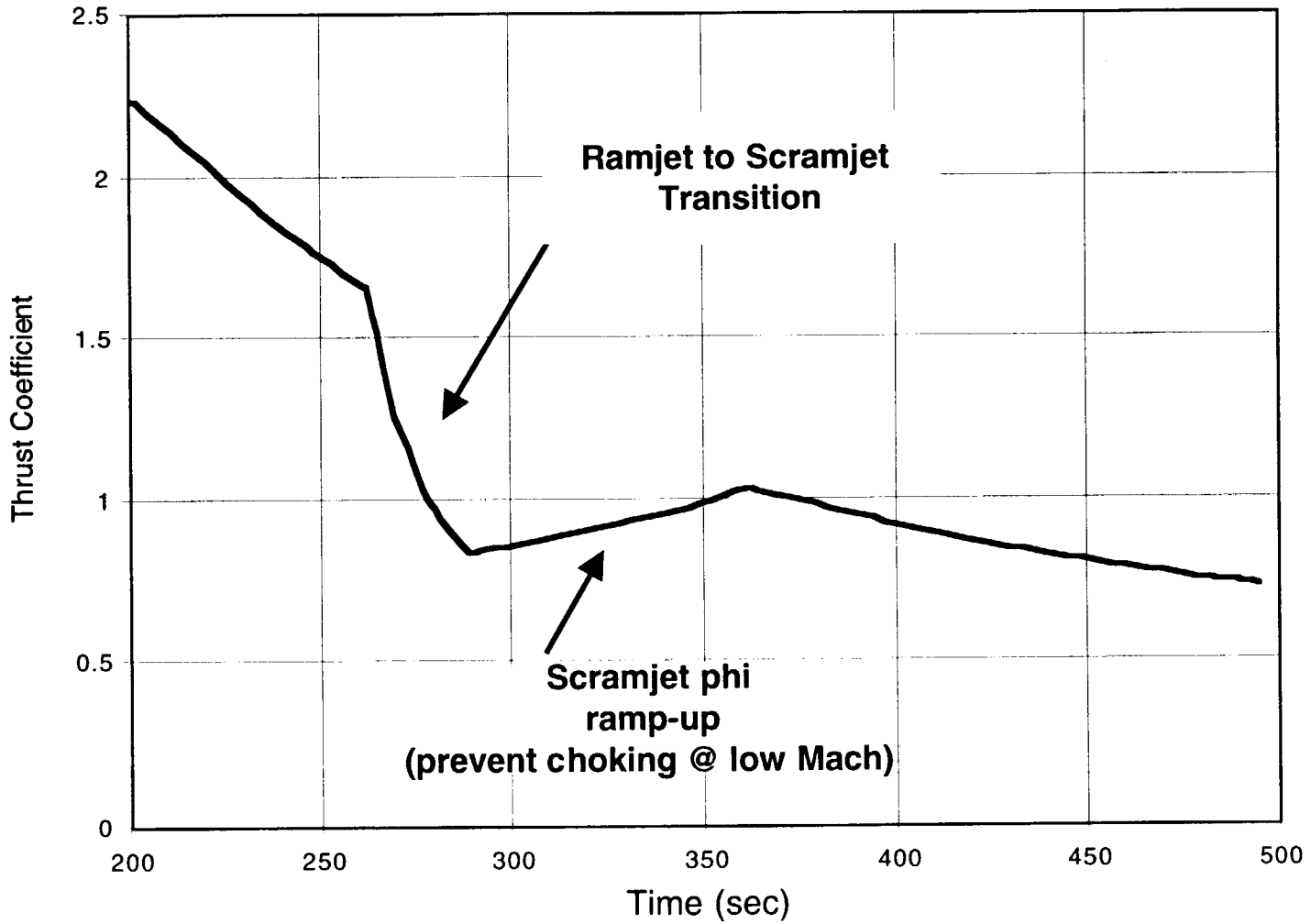

Net Isp vs. Time

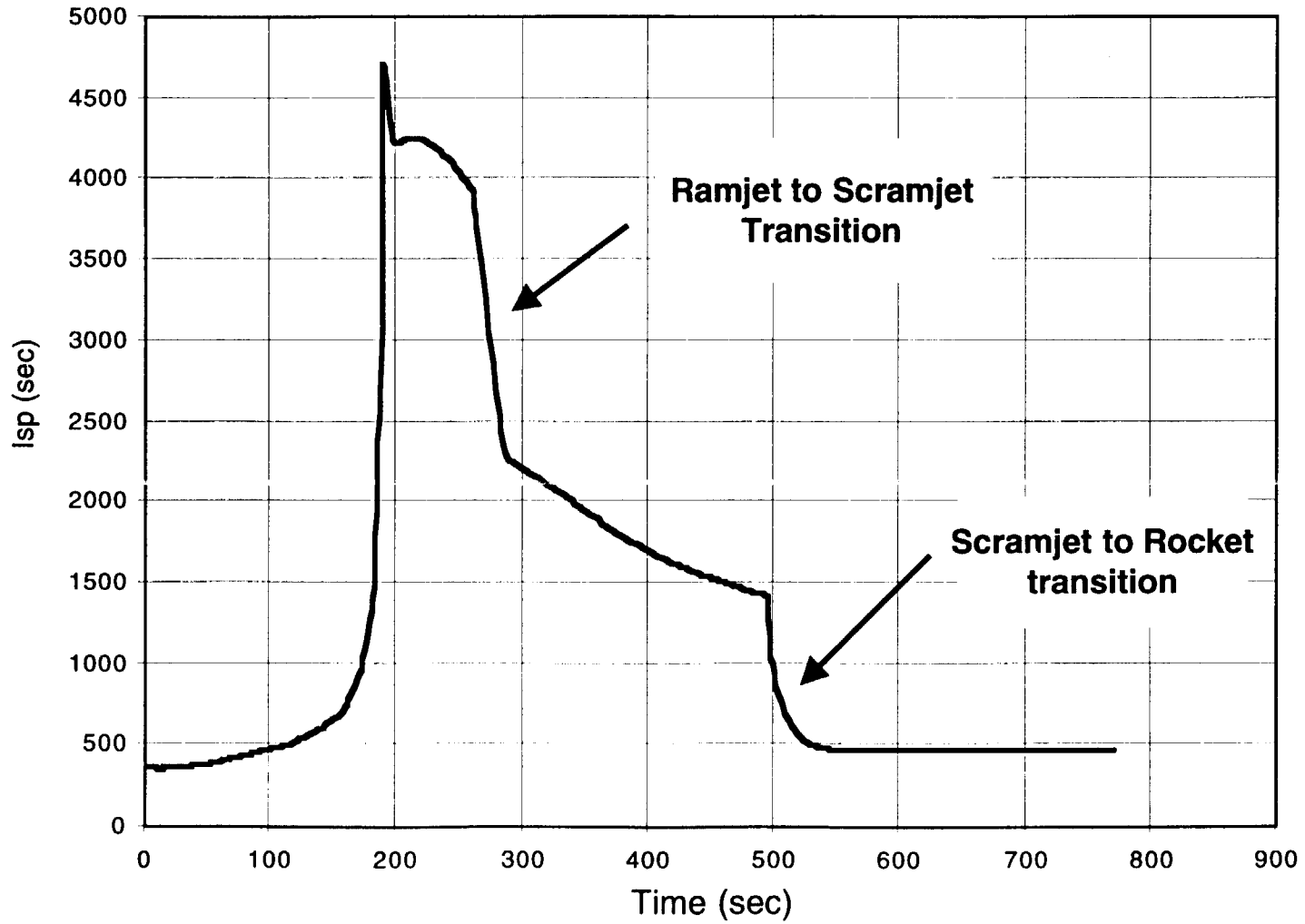

jeb/7.97/20

Dynamic Pressure vs. Time

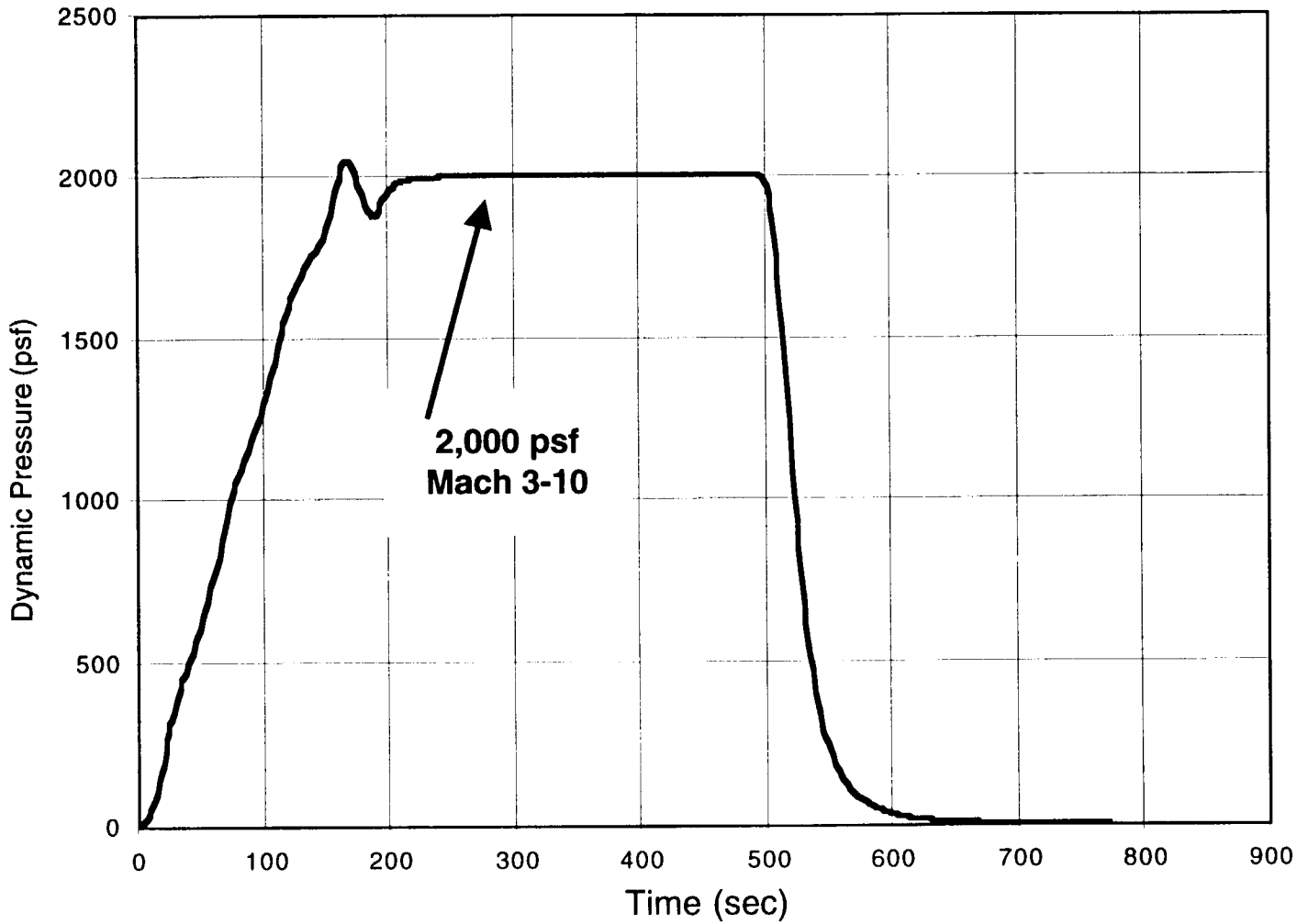

jeb/7.97/21

Baseline Hyperion Cost Analysis

Hyperion Cost Assumptions

- Program Years
  - » Initial operational capability in 2010(full by year 2012)
  - » Program termination in 2027
- Market Includes modified CSTS Cargo & Passengers only
  - » All traffic assumed to be delivered to 220 nmi. x 51.6° (worst case)
  - » No nuclear waste disposal, separate gov't and commercial markets
- Gov't Cost Contributions
  - » Airframe (DDT&E only): 20%
  - » Propulsion (DDT&E only): 100%
  - » Facilities (DDT&E and Construction): 100%
  - » Gov't pays ~10% premium on its missions for first 7 years
- All cost figures in 1998 dollars unless otherwise noted

Hyperion Cost Results

- Optimum launch prices and market sizes for max IRR
  - » Commercial Cargo: $800/lb (1000 klb/yr)
  - » Government Cargo: $1,845/lb (250 klb/yr)
  - » Comm. Passenger: $0.62M/passenger (46 "tourists" per year)
  - » Gov't Passenger: $8.27M/passenger (39 astronauts per year)
- Maximum (optimized) concept IRR = 8.14%
- Non-Gov't Life Cycle Cost = $20.035 B (Gov't cost contrib.=$1.803 B)
  - » Non-Gov't LCC/flight = $8.105 M
  - » Pre-Tax (Gross) Program Revenue = $27.99 B
  - » Break Even Year = 2012 (2nd quarter)
  - » Max Debt = $8.263 B (then-year $) in 2011

Hyperion Operations

- 450 Required Ground Personnel (assumed)
  - » 1 set of ground facilities (single launch site)
- Only 3 Hyperion Airframes & 30 ESJ Engines Required for Program
- Launch Rates
  - » 133 payload flights per year steady state (106 comm., 27 govt.)
  - » 15 passenger flights per year (8 comm., 7 govt., @6 pass. per flight)
  - » 2,472 total flights
- Recurring Cost (LRU's, Propellant, Labor, Insurance)
  - » Total Program Recurring Cost = $5.005 B
  - » Avg. Recurring Cost/Flight = $2.024 M
  - » Avg. Recurring Cost/lb of Payload = $214.5 /lb to ISS ($119 /lb due east)

Hyperion LCC Breakdown

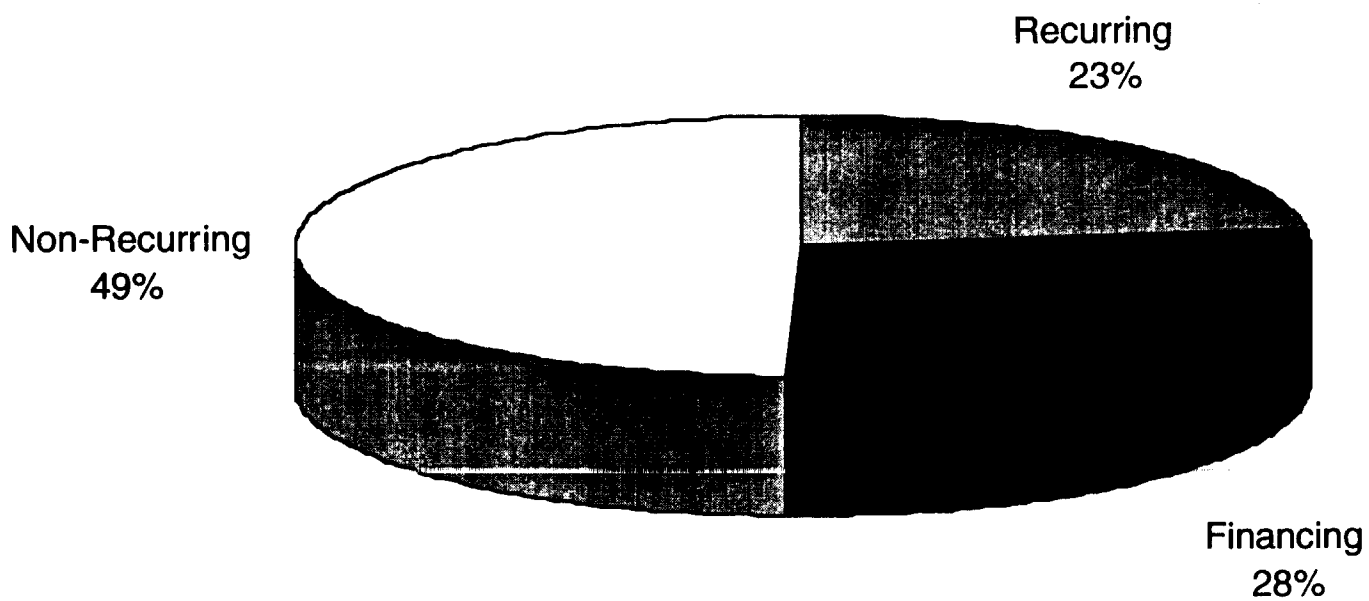

Total Life Cycle Cost* = $21.837 B

*Prior to government contributions

jeb/7.97/26

Hyperion Non-Recurring Costs

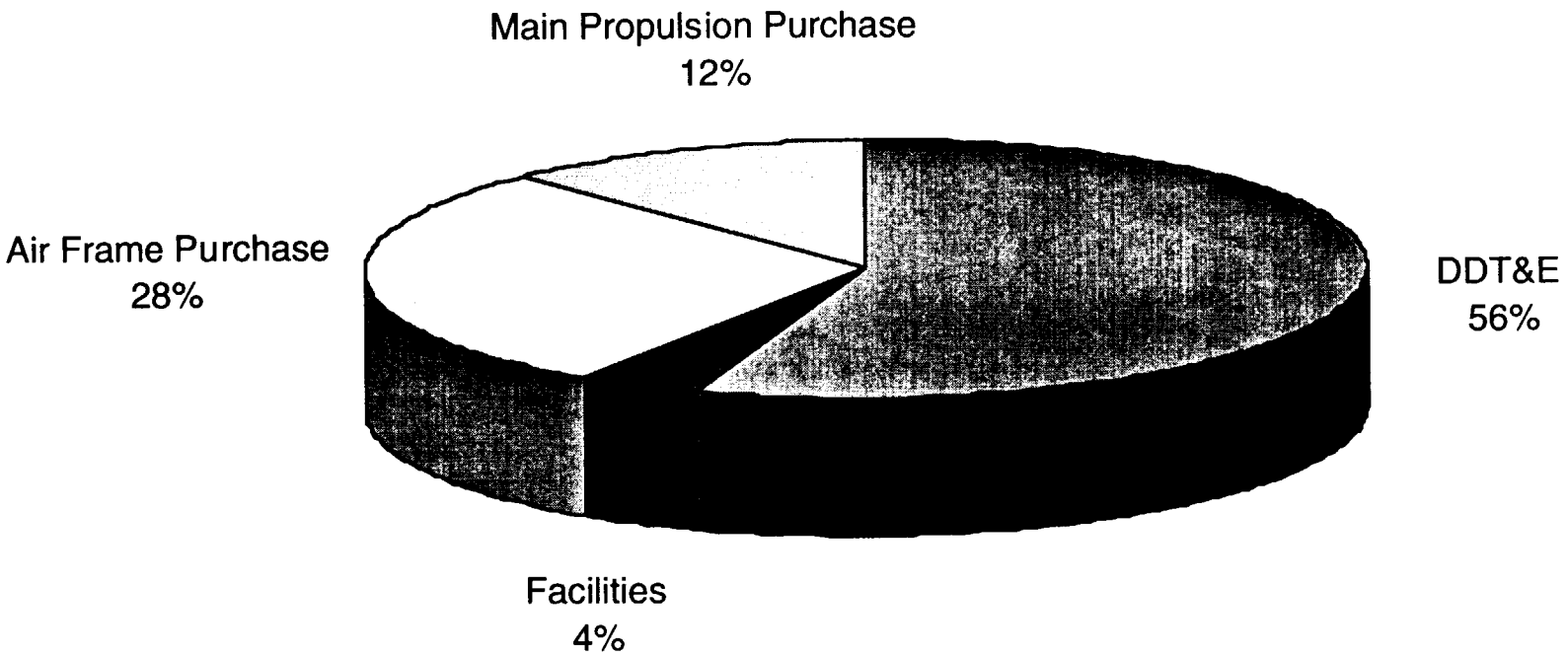

Total Non-Recurring Cost* = $10.77 B

*Prior to government contributions

jeb/7.97/27

Hyperion Recurring Costs

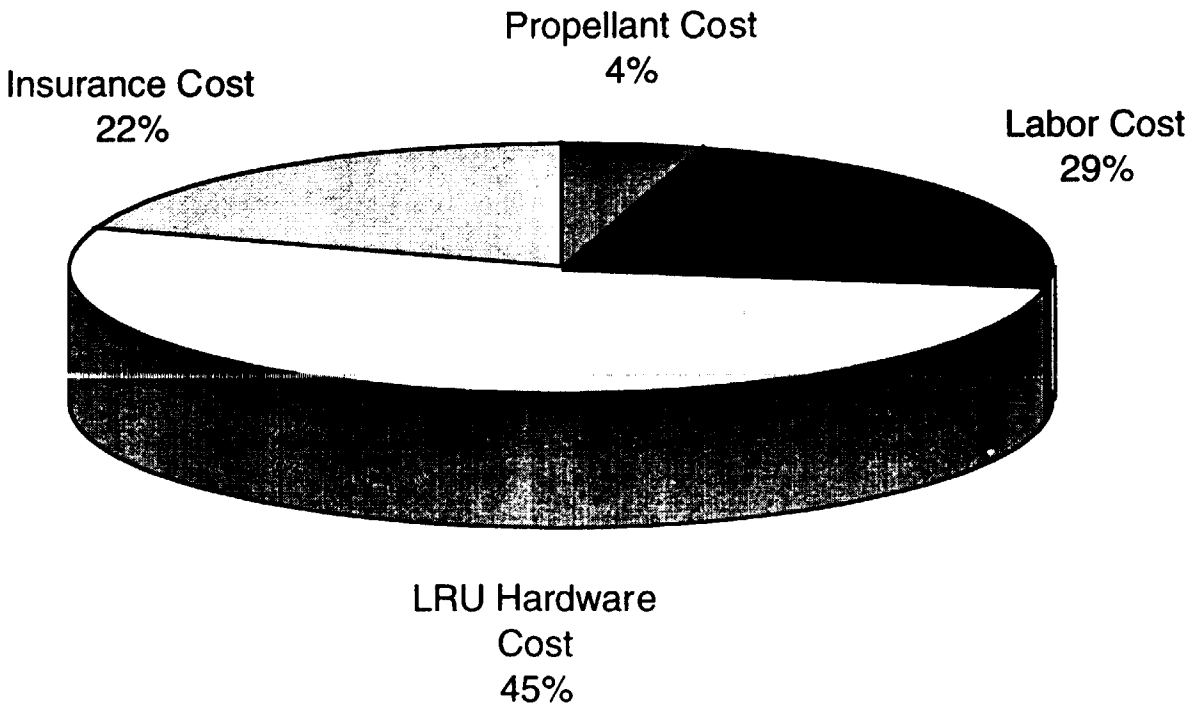

Avg. Recurring Cost/Flight = $2.024 M

Trade Study Performance Analysis

Transition Mach Number Trade

- baseline vehicle Mach 10
- examined Mach 9 and Mach 11 transition in scramjet modes
- inlet height adjusted for shock-on-lip condition at maximum Mach number
- changes in installed engine thrust-to-weight ratios accounted for

Vehicle Gross Weight Results

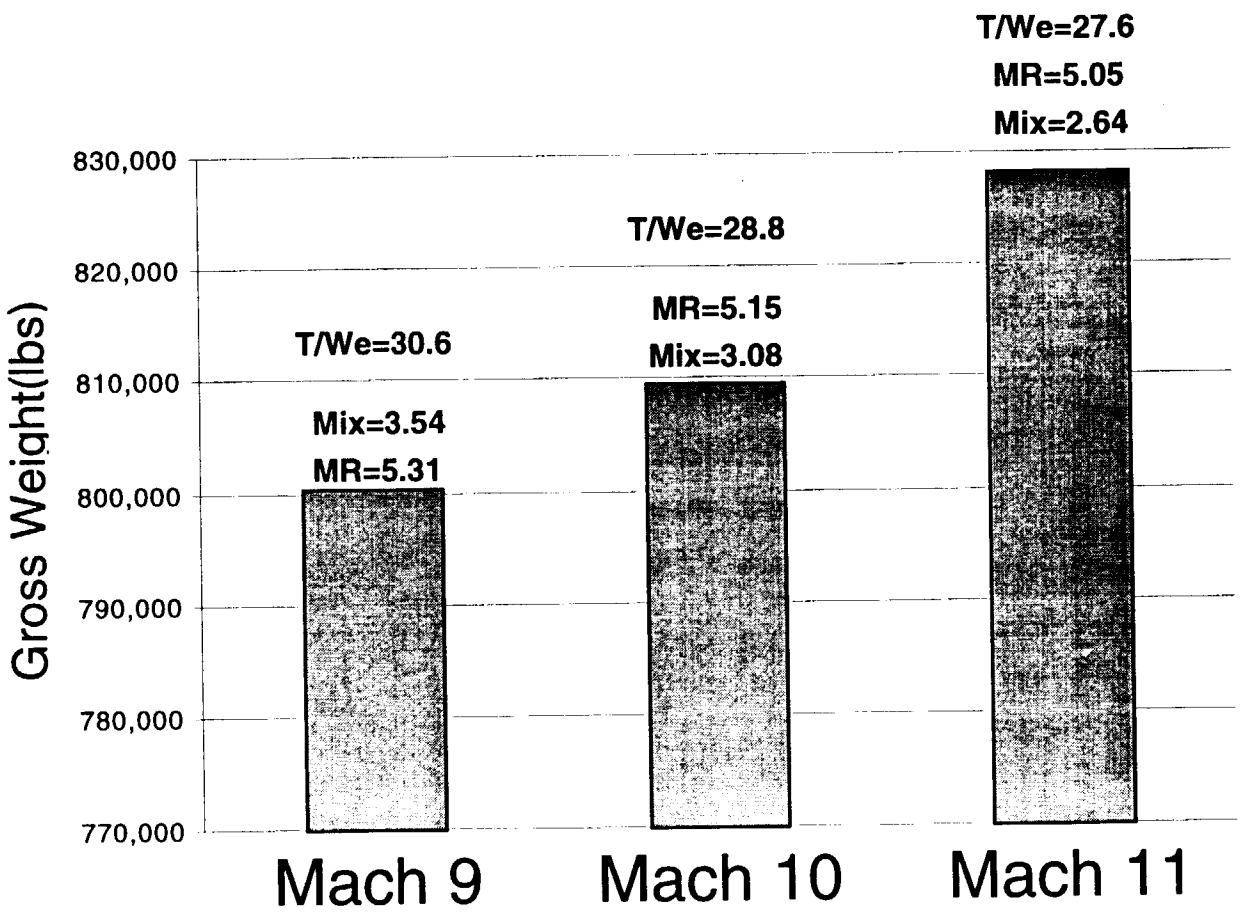

dynamic pressure and takeoff T/W are the same for all cases

Vehicle Dry Weight Results

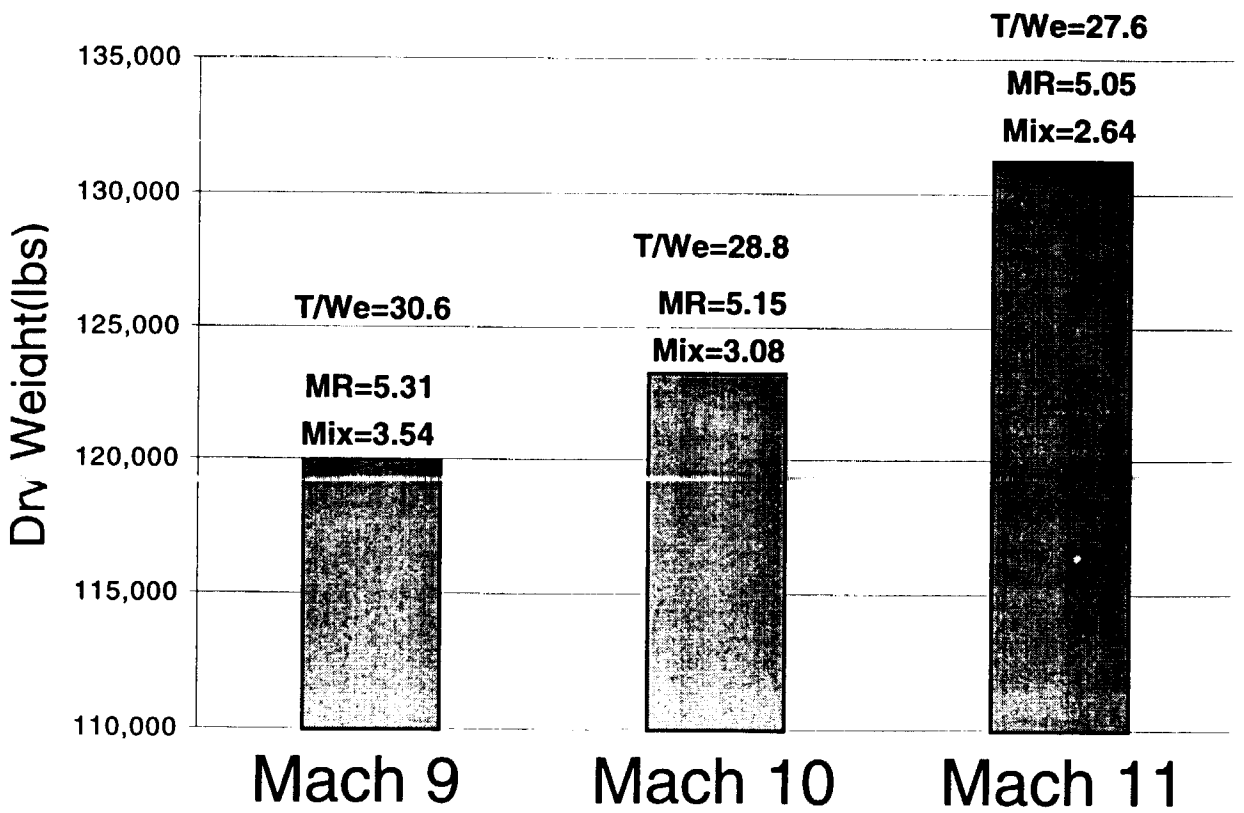

dynamic pressure and takeoff T/W are the same for all cases

jeb/7.97/30

Trade Study Cost Analysis

Trade Study Cost Assumptions

- engine complexity factors adjusted for higher and lower transitioning Mach numbers
- launch prices optimized for maximum IRR for each new configuration
- same dept-to-equity ratio assumed for each configuration

Trade Study Costs Results

	Transition Mach Number		
	9	10	11
IRR	8.77%	8.14%	7.76%
DDT&E	$5.665 B	$5.993 B	$6.207 B
Non-Gov't LCC	$18.7 B	$20.0 B	$21.1 B
Max. Debt	$7.74 B	$8.26 B	$8.61 B
Avg. Recurring Cost/Flt.	$1.96 M	$2.02 M	$2.11 M

Mach 9 transition has best IRR and lowest DDT&E.

Trade Study Status

- further examination of design space in Mach 9 transition region is required
  - » Mach 8 transition study
  - » reset baseline to lower transition Mach number?

<u>To be performed</u>:

- cone angle trade study
  - » examine 6° and 12° cone angle (current baseline is 9°)
- constant dynamic pressure (q) boundary study
  - » 1500 and 1750 psf trades (current baseline is 2000 psf)
  - » incorporate more detailed TPS analysis

Baseline Hyperion Summary

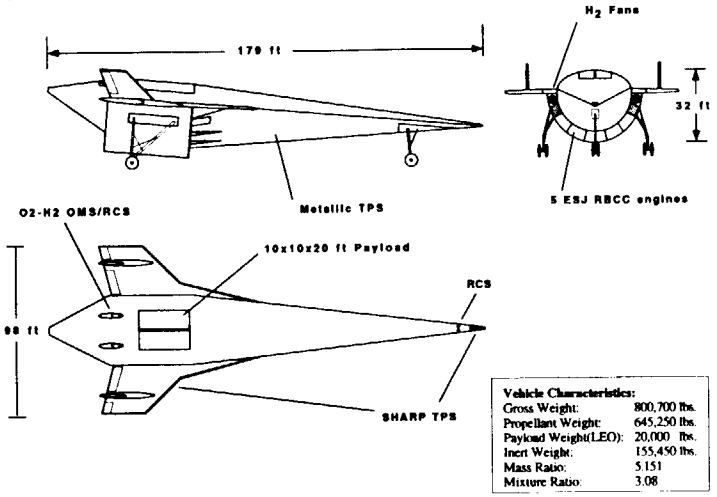

Vehicle:

payload = 20 klb to 100 nmi orbit @ 28.5°
dry weight = 155.5 klb
gross weight = 800.7 klb

Propulsion:

5 Ejector Scramjet (ESJ) RBCC engines
Isp @ sea level static = 360 sec. (LOX/LH2)
I* = 471 sec. (for baseline trajectory)
thrust@sea level static = 96.1 klb/ea. (vehicle T/W=0.6)
engine installed T/We = 28.8

Vehicle Technologies:

Mach 10 capable ejector scramjet engines
integral graphite/PEEK tanks (w/liners)
titanium-aluminide/Si-C hot structure (wings, etc.)
SHARP/Metallic/TABI TPS
cryogenic O2/H2 OMS/RCS
BITE/BIT in key components
electro-mechanical surface actuators

Trajectory/Operational Modes:

ejector mode to Mach 2.5
ramjet mode to Mach 5.5 (const.q = 2000 psf)
scramjet mode to Mach 10
built-in RBCC rocket mode to orbit (Isp = 455 s vac)
horizontal landing
5 minute loiter capability with H2 fans

Notes and Issues:

- fully autonomous (no pilots), up to 6 passengers can ride in module in cargo bay
- metallic TPS on windward fuselage, simplifies installation & maintenance
- ESJ RBCC engine builds on historical development; eliminates fan hardware and storage problems

The Case for RBCC Propulsion: An Honest Assessment

Dr. John R. Olds
School of Aerospace Engineering
Georgia Institute of Technology

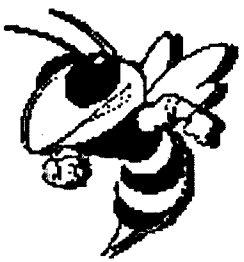

phone: 404-894-6289
email: john.olds@ae.gatech.edu
web: http://redstone.ae.gatech.edu/~olds

The Current Case for RBCC

RBCC proponents have for years advocated a detailed ground test program, a subsequent flight test, and eventual development of a full scale launch vehicle.

Why then, have we failed to produce a robust budget authority and consensus among NASA/AF decision makers and Congress?

We have not produced a well founded "case for RBCC"

The I* Argument

RBCC Vision Vehicles have nearly twice the trajectory averaged Isp (I) of an all-rocket vehicle for the same ETO mission - thus a lower propellant mass fraction. RBCC wins, right?*

No. The reusable launch vehicle design space is closer to a cube and is dependent on 3 major contributors — I, engine T/W, and propellant bulk density (total prop. wgt./total tank vol.). RBCC wins on I*, but the all-rocket vehicle wins the other two variables.*

I* is not a sufficient metric by itself to justify RBCC

A Better Performance Metric

A better performance metric for reusable ETO vehicles is:

not gross weight →

$$\frac{W_{payload}}{W_{dry} + W_{payload}}$$

(higher values are preferred)

How does RBCC compare to all-rocket on this performance metric?

RBCC = ~.17 .20

All-rocket = ~.19 - .23

>

for a representative, due east LEO launch, SSTO, non-launch assist, 2010 technologies

For the same space launch mission, payload, and <u>technology assumptions</u>, RBCC is usually slightly heavier than all-rocket

Even Better, A Cost Metric

But we should really be focused on a cost-oriented metric, not a performance metric anyway, right? Like the following,

- Recurring cost $ per lb. of payload or per flight
- Total cost per lb. per payload of per flight
  - amortized hardware, DDT&E, finance, labor, fuel, etc.
- Total LCC to deliver a given ETO mission model

How does RBCC compare on these cost metrics?

With equivalent ops cost reductions for the all-rocket (current assumptions are very uncertain), RBCC may have a slight ops cost advantage, but a slight DDT&E and hardware cost disadvantage.

RBCC cost advantages have not and may not be proven

The Ops Cost Argument

Some have shown an advantage in RBCC ops cost, and LCC is dominated by ops. "It's the ops cost stupid," right?

No. A properly discounted cash flow analysis shows that early non-recurring costs (DDT&E, hardware procurement) are more important than ops cost to achieving a desired return on investment. Out year dollars tend to diminish in importance.

Slightly heavier and more complex RBCC hardware leads to higher non-recurring costs (early $) and lower IRR's than all-rocket. Any ops cost advantages are lost when discounted.

Other False Arguments

1. **"A lower propellant mass fraction means higher margin."**

   In fact, margin is independent of propellant mass fraction. A vehicle is always sized so that the PMF, structural fraction and payload fraction add to 1.0, so there is no "unused excess to be used for margin." RBCC structural fraction is required to be higher than an all-rocket case due to larger TPS, engine, tanks per lb. of gross weight. Payload fraction is also higher (due to lower gross). Margin items -- dry weight margin (typ. 15%), structural load factors, tank burst pressures, etc. are all identical to the all-rocket case.

2. **"Low RBCC recurring costs ($100/lb!) save NASA money."**

   Recurring costs and eventual market price are not the same. Adding profit, debt service, and amortization of DDT&E and hardware procurement will yield a market price an order of magnitude higher than the recurring cost. NASA and satellite customers will pay market price, not the recurring cost.

So Why RBCC?

RBCC Vision Vehicles have challenged all-rockets in an area in which all-rockets are very well suited, namely ETO cargo delivery (25 lb to space station orbit, flight rates < 50 year)

RBCC should highlight areas in which it has clear advantages:

- enabling new markets (PTP)
- offset launch (multi-inclin.)
- self-ferry
- powered landing
- easier horizontal take-off
- flexible basing options*
- CONUS global reach*
- standoff launch * (dual use)
- favorable abort options
- small payload delivery

To build a strong case, advocates should focus on RBCC's clear advantages, not <u>solely</u> on traditional rocket missions

Aside on Non-Recurring Costs

For large, Titan-class (25klb to ISS) reusable vehicles, DDT&E and procurement costs dominate. The resultant vehicles are physically large. Is this the best payload size to achieve high IRR?

No. Smaller vehicles cost less to develop, test, and build. They start making money sooner and fly more often to achieve operations efficiencies. Atlas-class (10 klb to ISS) vehicles make more economic sense and achieve higher rates of return

RBCC Vision Vehicles should be designed to deliver smaller payloads than 25 klb to ISS. 10 klb is better.

Conclusions

For the 25klb to Space Station SSTO mission (reference for current Vision Vehicles and previous Access to Space studies)

1. RBCC vehicle dry weight is near or higher than all-rocket
2. Ops cost advantages for RBCC are uncertain
3. Higher RBCC DDT&E and hardware procurement are significant IRR disadvantages in discounted cash flow analysis
4. RBCC can do this mission, but doesn't show clear advantage over all-rocket
5. But, RBCC has clear unexploited advantages in mission flexibility

A new Vision Vehicle reference is needed to building a strong "case for RBCC"

Recommendations

First, coordinate NASA and Air Force activities and jointly fund combined Vision Vehicle assessment activities

Second, change and expand the Vision Vehicle definition to include a broader range of concepts and ideas. Perhaps the following 3,

1. A point-to-point, trans-Pacific fast package delivery concept
2. A 20klb to LEO operable space access SSTO with powered landing, self-ferry, offset launch, and horizontal processing
3. A military application vehicle for pop-up payload delivery and/or CONUS-based global reach with 5klb payload

These changes will build a stronger "case for RBCC" because they will show and exploit clear advantages

Future RBCC Vehicles: Charting a Better Direction

Dr. John R. Olds
School of Aerospace Engineering
Georgia Institute of Technology

phone: 404-894-6289
email: john.olds@ae.gatech.edu
web: http://redstone.ae.gatech.edu/~olds

The Future of Space Launch

NASA is committed to an all-rocket SSTO whose primary mission is to deliver and return cargo (25klb) from the International Space Station. At launch prices from $25M - $35M /flight, these RLV's should also compete well for commercial LEO payloads >15klb and GTO/GEO payloads >5klb (with an upper stage).

At the same time, several small companies are attempting to enter the low-end LEO market (<8 klb) with reusable vehicles priced from $10M - $15M/flight. One or more will likely succeed.

Is there a place for airbreathing in future space launch?

What about Human Spaceflight?

Supporting ISS will require rotating 6-8 crew members to and from the space station every few months. How should this be accomplished?

1. International launch agreement? (Soyuz, Hermes?)
2. Bi-directional US Crew Return Vehicle? (ACRV + ELV)
3. STS upgrades and continued long term support?

None of these options make good political or financial sense for the United States

Why Not Just Use the RLV?

For better economic return, we should make the next generation SSTO rocket vehicle capable of serving crew and cargo missions. Lockheed Martin's RLV should just be configured to transport passengers to ISS, right?

No. Current Lockheed Martin plans do not include financing ISS crew rotation modules. Low cost cargo missions are it's primary goal. Adding a passenger capability means extra expense and design requirements that may compromise the RLV's success for cargo.

Airbreathing makes the best sense for an ISS crew vehicle

RBCC Advantages for Crew

1. Safety
   - multiple abort modes throughout ascent and decent (high average Isp, range)
   - on-board pilots increase confidence and probability of safe return
   - powered flyback and optional powered landing capability

2. Horizontal Takeoff and Landing
   - large offset launch can provide ISS crew service to and from all partner countries
   - flexible basing options due to simpler launch infrastructure (no pad)
   - HTHL configuration increases passenger appeal (aircraft-like)

3. Intangibles
   - can involve second major airframer and engine supplier in large program
   - dedicated crew-rated mission avoids conflicts inherent with crew+cargo mission

Anything Else?

Ok, so airbreathing makes good sense for a new, dedicated vehicle for getting humans to and from the space station. Is there anything else? Any other sweet spots for RBCC?

Who's working on space tourism, LEO sat servicing, satellite and debris return, and military requirements?

The RBCC community should be.

NASA's Launch Missions

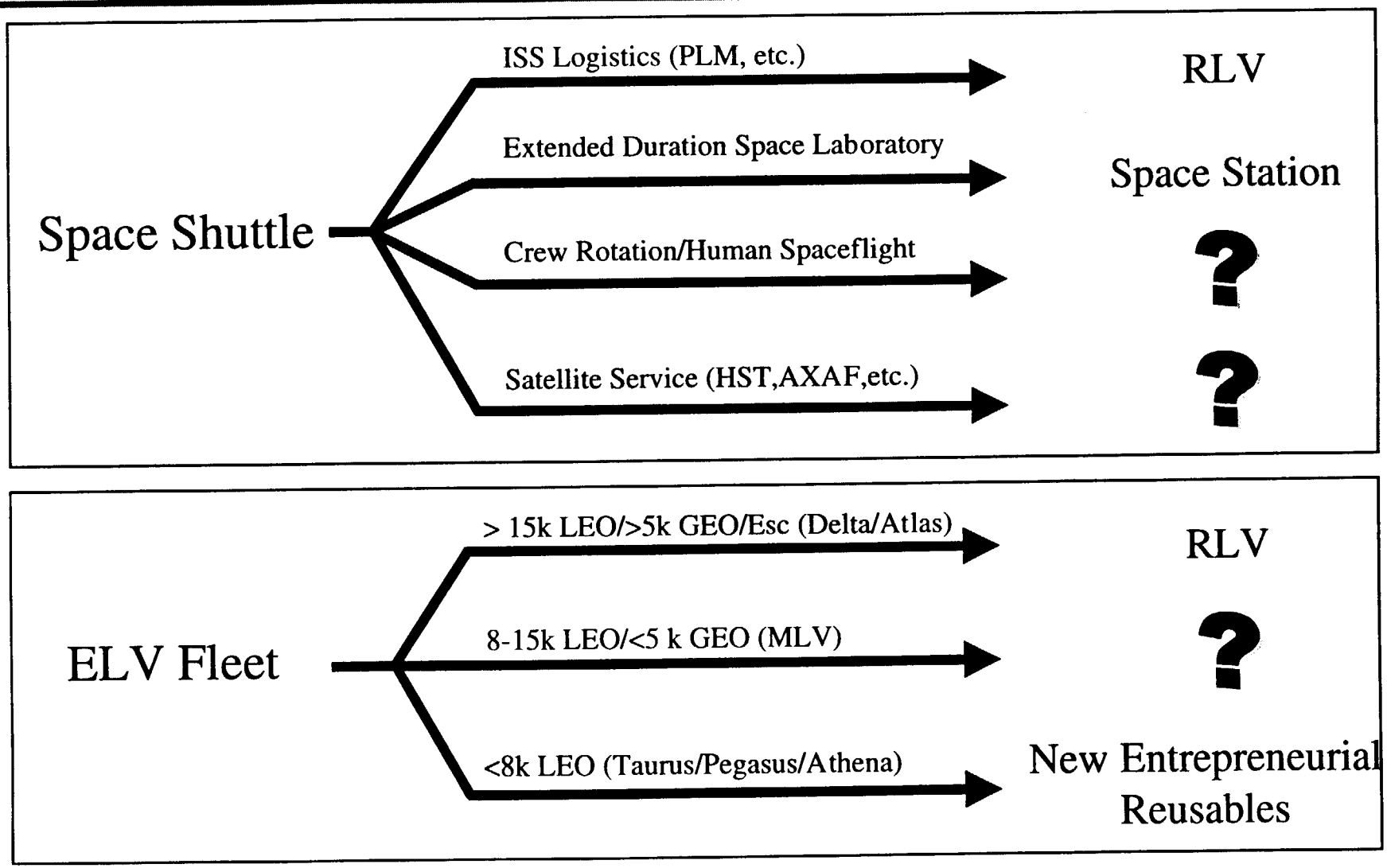

Commercial & Military Missions

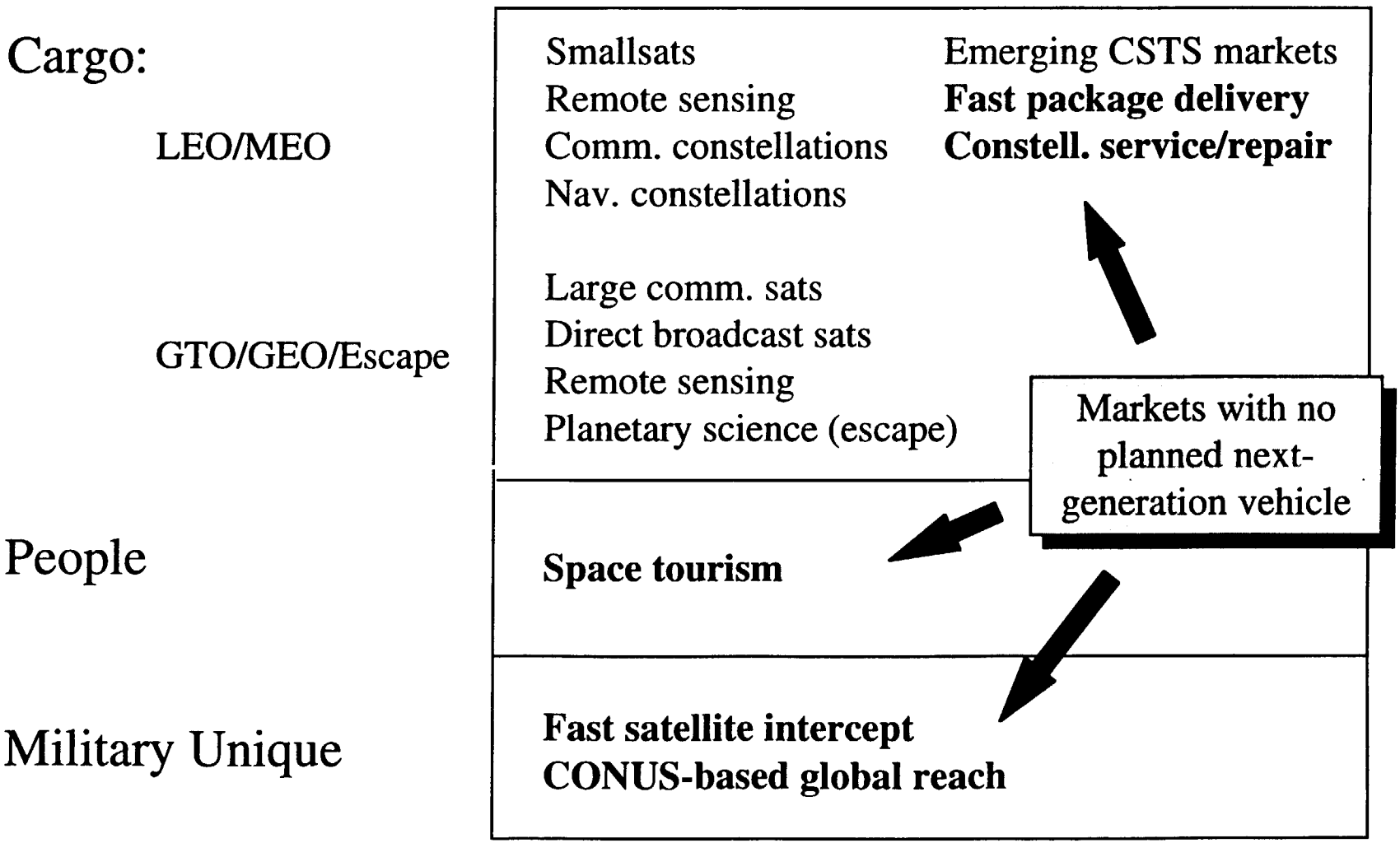

High Altitude Sat Service

In the next 10 years, over 500 small satellites will be launched into high LEO orbits (over 300 nmi) for paging, messaging, voice communications, remote sensing, and navigation. These satellites will be launched into a variety of orbital inclinations from various launch sites. In addition, NASA's large observatories will continue to need servicing (HST, AXAF, Compton, etc.). How will these satellites be serviced or recovered?

An autonomous RBCC vehicle equipped with telerobotic arms and a large on-orbit ΔV capability could take advantage of its all-azimuth launch capability to reach these orbits from a single base.

Fast Package Delivery

What about fast-package delivery? Couldn't FedEx and UPS use an RBCC vehicle to cut trans-Atlantic and trans-Pacific flight times?

Preliminary indications are that this market is not yet mature. Revenues per flight will probably not exceed $100k/flight in the near term at rates less than one round-trip per day. A requirement to operate directly between high volume city pair airports (NY-London, LA-Tokyo) places additional constraints on RBCC design. Rocket-mode propulsion isn't required. TBCC seems a better choice than RBCC here.

8k - 15k LEO Cargo Delivery

This segment of the market seems underserved by new RLV's. It's too small for VentureStar to compete economically and too large and expensive for small entrepreneurial firms to capture. Shouldn't NASA try to develop an RBCC entry into this market?

It's doubtful. This market is being served by ELV's, just not RLV's. For a simple cargo delivery mission, RBCC is not a clear choice over a second smaller all-rocket vehicle. If RBCC propulsion technology is developed for other missions, this market might later be revisited.

Military Unique Missions

The Air Force has defined a requirement for a military spaceplane to perform all-azimuth fast intercept missions and global force projection/reconnaissance missions (SOV). A second configuration can use pop-up trajectories for TSTO operation (SOV/SMV). Is there a role for RBCC here?

Yes, definitely. The large offset launch (ascent plane changes), flexible basing, self ferry, hypersonic cruise, and all-azimuth launch capability of an RBCC vehicle make it an excellent choice for a military spaceplane.

The RBCC Sweet Spots

1. A safe, flexible ISS crew rotation vehicle with a derivative space tourism path.

2. A high altitude, small LEO satellite service, recovery, and satellite (and debris) deorbit vehicle.

3. A global range, CONUS-based military asset with fast satellite intercept capability to all inclinations.

Recommendations

1. Develop a new set of Vision Vehicle designs that exploit RBCC
   - abandon the single Access to Space reference mission (25klb cargo to ISS)
   - avoid the "us" vs. "them" confrontation with all-rocket SSTO
   - define several new DRM's that complement and augment NASA policy
   - allow vehicle designers to build a portfolio of attractive vehicles for these DRM's
   - use these vehicle designs to build a common case for RBCC ground and flight test

2. Develop a generic engine technology that supports all paths
   - Mach 10-12 LOX/LH2 ejector scramjet seems common with multiple paths
   - encourage engine company teams and consortia (avoid premature competition)
   - supercharging option should also be investigated for landing flexibility

These changes will build a stronger "case for RBCC"

Appendix

Sample Design Reference Missions

DRM 1 - Crew Rotation

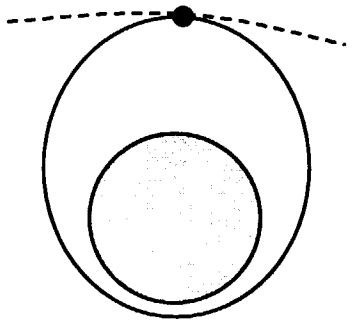

Mission Statement

Deliver 6-8 passengers to ISS at 220 nmi. circ. by 51.6°. Return to 6-8 passengers to earth. Similar configuration for space tourism market.

DRM 1 Requirements

- 2 pilots required (in addition to passengers)
- Dock at ISS for up to 5 days (cold gas RCS required)
- Depart from and return to ISS partner country spaceport/airport as required (multi-bases)
- 10 minutes of powered landing/subsonic maneuvering for flexible approach ops
- Provide global self-ferry capability after landing (base to base)
- Do not exceed STS entry and landing loads
- Provide safe, intact abort for engine out throughout mission (recovery reliability >.9999)
- Mission price on the order of $5M - $10M (including all costs, profit, debt)

DRM 2 - LEO/MEO Sat Service

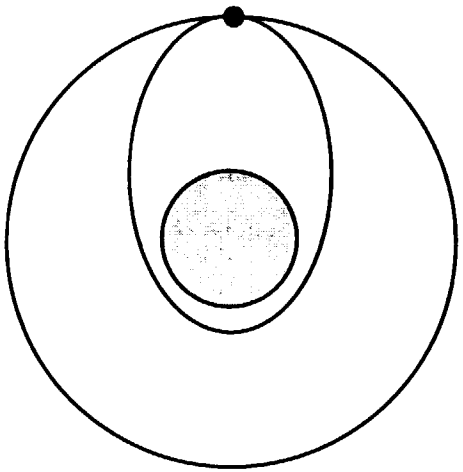

Mission Statement

Deliver 3000 lb payload to 500 nmi circ. orbit, rendezvous with satellite/telescope, repair or recover, and return to earth.

DRM 2 Requirements

- Completely autonomous (no pilots or crew on board)
- Remain on station up to 5 days
- Service all inclinations up to 105° from single east coast launch/landing site (KSC)
- Provide telerobotic/RMS system for satellite capture and remote servicing
- Provide deorbit/landing capability for recovered satellites and stray debris up to 10klb
- Mission price on the order of $5M - $10M (including all costs, profit, debt)

DRM 3 - Global Military Asset

Mission Statement

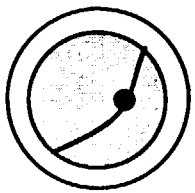

Serve multi-role military spaceplane mission including satellite launch, global reach, and fast satellite intercept

DRM 3 Requirements

- 2 pilots required (no other crew)
- Deliver 5000 lb payload to antipodal point and return to CONUS base
- Deliver 2000 lb payload to 150 nmi circ. polar orbit and return to CONUS base
- Intercept LEO satellite in any inclination within 2 hours of launch from CONUS base
- 12 hour maximum ground processing turnaround time (4 hours in surge condition)
- Horizontal takeoff and landing for ground infrastructure compatibility
- 1000 flight airframe (500 flights for engines), 250 flights between major maintenance

Performance and Cost Impact of Launch Assist on a Conceptual RBCC SSTO Vehicle

John Bradford
NASA Academy
Summer 1997

With Contributions:
Dr. John R Olds, Hosung Lee, David McCormick, David Way
Georgia Tech Aerospace Systems Design Lab

Baseline Vehicle

- Georgia Tech "Hyperion" Vision Vehicle
- horizontal takeoff, horizontal landing
- 2nd generation RLV
- operation ~ 2015+
- unpiloted; can support up to 6 passengers in cargo bay

Hyperion

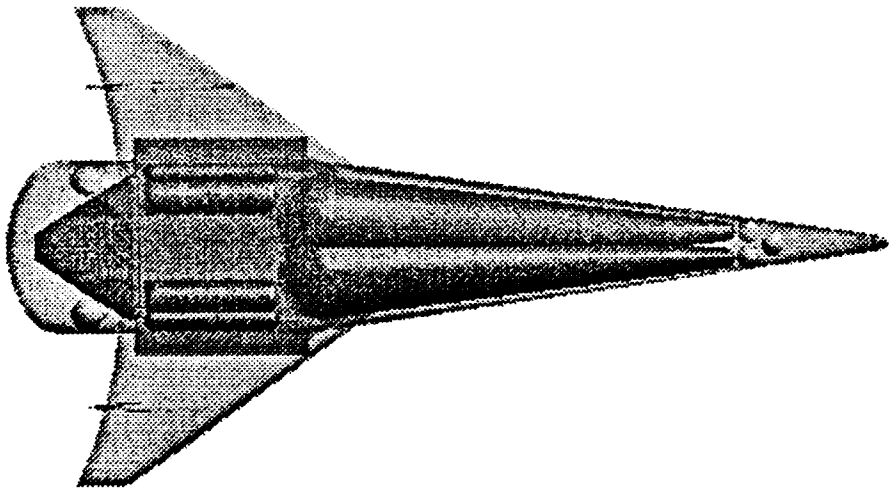

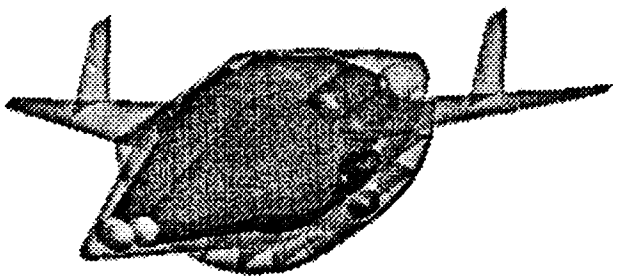

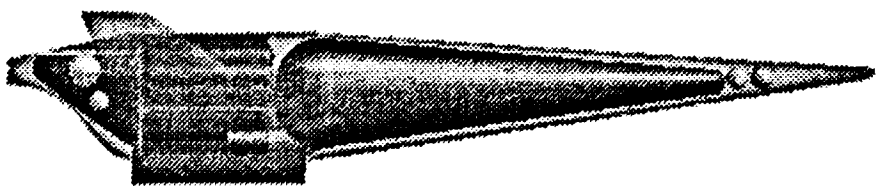

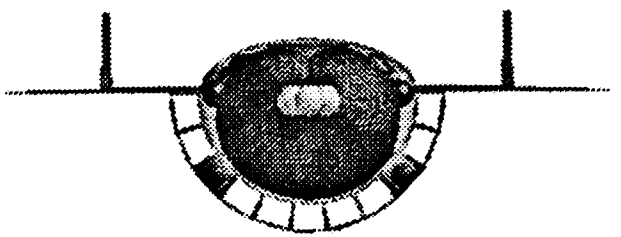

Vehicle Features

- 5 LOX/LH2 ejector scramjet (ESJ) rocket based combined-cycle engines (T/We=28)
- non-integral, filament wound (with liners) graphite epoxy tanks
- 4 JP powered fans for 5 minute loiter and fly around capability
- SHARP TPS on nose, wing leading edges
- titanium aluminide / silicon-carbide hot structure wings

Design Structure Matrix

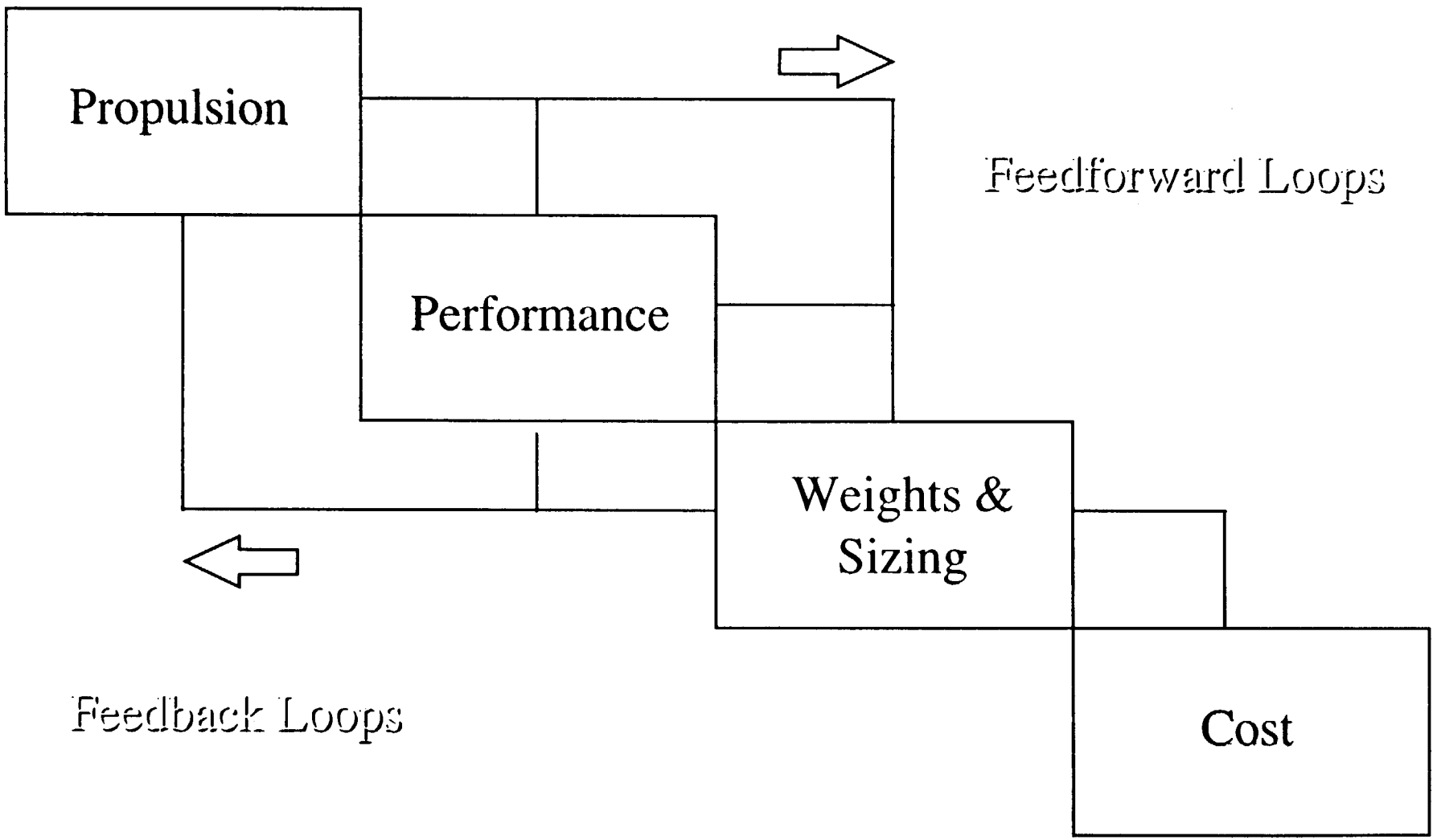

Performance Analysis

- Design tool : Program to Optimize
  Simulated Trajectories (POST)
- Input Variables: GLOW, Sref, Wnorm,
  thrust, specific impulse
- Output Variables: mass ratio, mixture ratio,
  maximum wing normal force

Baseline Trajectory Profile

- horizontal takeoff at 400 kts, T/W=0.6
- initially in ejector or AAR mode
- switch to ramjet mode at Mach 3
- fly constant dynamic pressure from Mach 3 to Mach 10 at 2000 psf
- scramjet operation at Mach 6
- transition to all-rocket mode at Mach 10
- insert into 50 by 100 nmi orbit at 28.5°
- OMS burn to 100 nmi circular at 28.5°

Propulsion Analysis

- Design tool : Simulated Combined Cycle Rocket Engine Analysis Module (SCCREAM)

- Input Variables: inlet capture area, required thrust, number engines, equivalence ratio
- Output Variables: POST engine performance deck (Ct, Isp)

What is RBCC Propulsion?

- Rocket based combined cycle engines combine two propulsion systems into a single, integrated unit
- Have higher Isp than pure rocket engines, combined with higher T/W ratios than all airbreathing engines

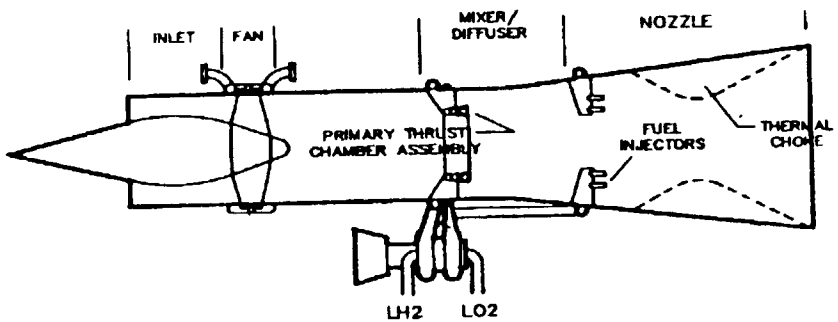

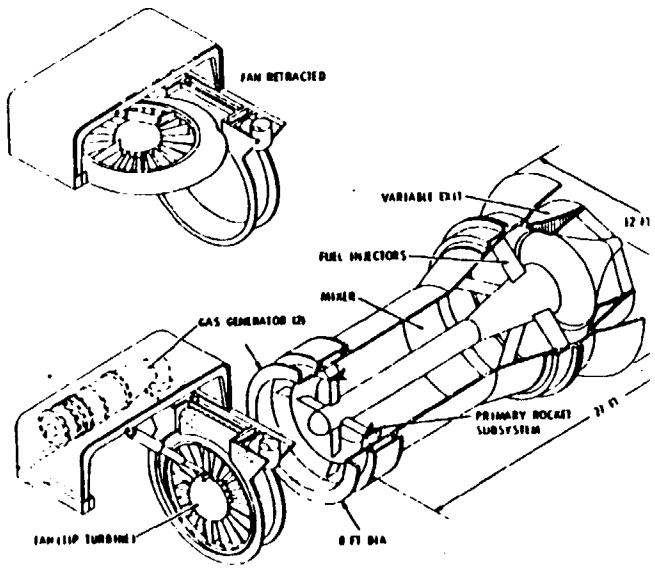

Weights and Sizing

- Design Tool: Excel spreadsheet with mass estimating relationships (MER)
- MER's are equations that use volumes, surface areas, load ratios to estimate component weight
- Input Variables: mass ratio, mixture ratio, wing normal force
- Output Variables: GLOW, wing normal force, wing reference area, inlet area size, required thrust

Baseline Configuration Weights

Name	Weight (lbs)
Wing and Tail Group	21,450
Body Group (incls. tanks)	32,450
Thermal Protection	6,750
Main Propulsion	21,900
OMS/RCS Propulsion	2,700
Subsystems and Other Dry Weights	29,175
Dry Weight Margin (15%)	17,175
Dry Weight	**131,600**
Payload	20,000
Other Inert Weights (residuals, etc.)	12,475
Insertion Weight	164,075
Ascent Propellants	660,450
Gross Lift-off Weight	824,525

Cost Analysis

- Design Tool: Cost and Business Analysis Module (CABAM)

- Inputs Variables: vehicle weights, engine type, launch price, payload and mission capability, etc...
- Output Variables: IRR, recurring and non-recurring costs
- Developed by: Hosung Lee

Trade Studies

- Baseline:
  - Payload = 20,000 lbs to LEO
  - No Launch Assist
  - Dry Weight Margins: 15%, 25%
- Maglev Configurations
  - Payload = 20,000 lbs
  - Track Velocity: 600, 800 fps
  - Dry Weight Margins: 15%, 25%

Typical Track Configuration

- Acceleration Limit: 1 g
- Length: Acceleration 1.9 miles
  Abort 0.95 miles @ 2g's
- Levitation System: Superconducting Magnets
- Sled Propulsion: Inductive Thrust Coils
- Power System: Utility Grid
- Energy Storage: Capacitors

Levitation Schematic

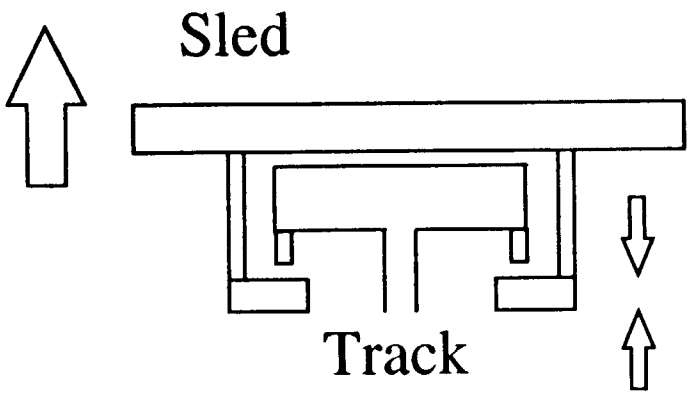

Attracting Magnets

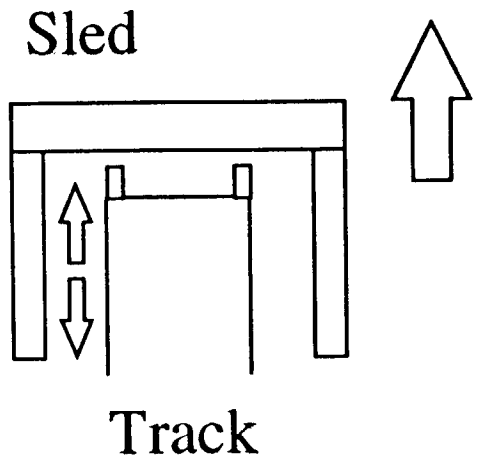

Repelling Magnets

Ascent Velocity Breakdown

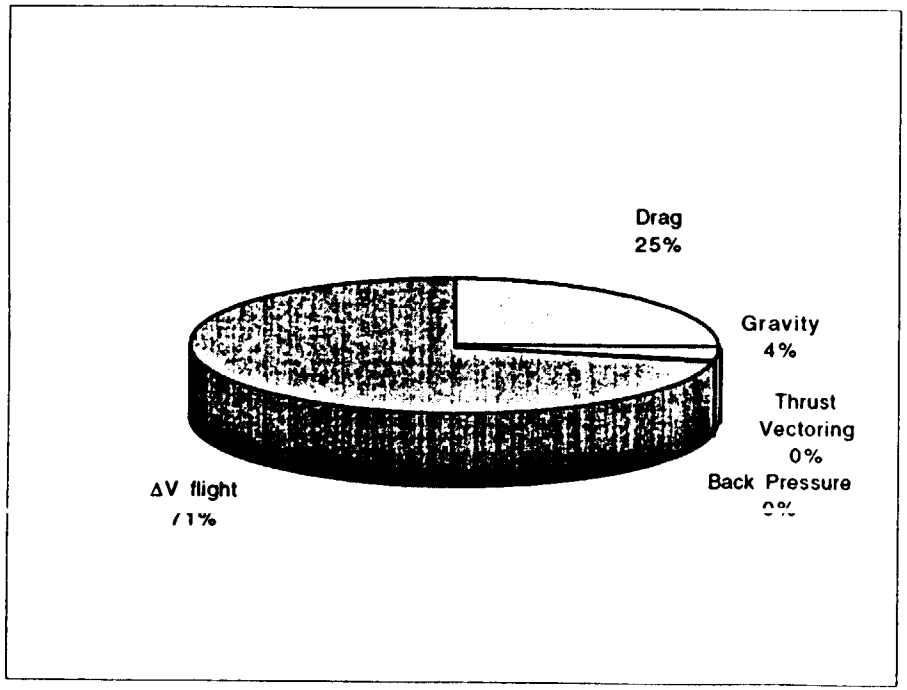

Baseline Case

Length = 181.2 feet
Mass Ratio = 5.03
Mixture Ratio = 2.95

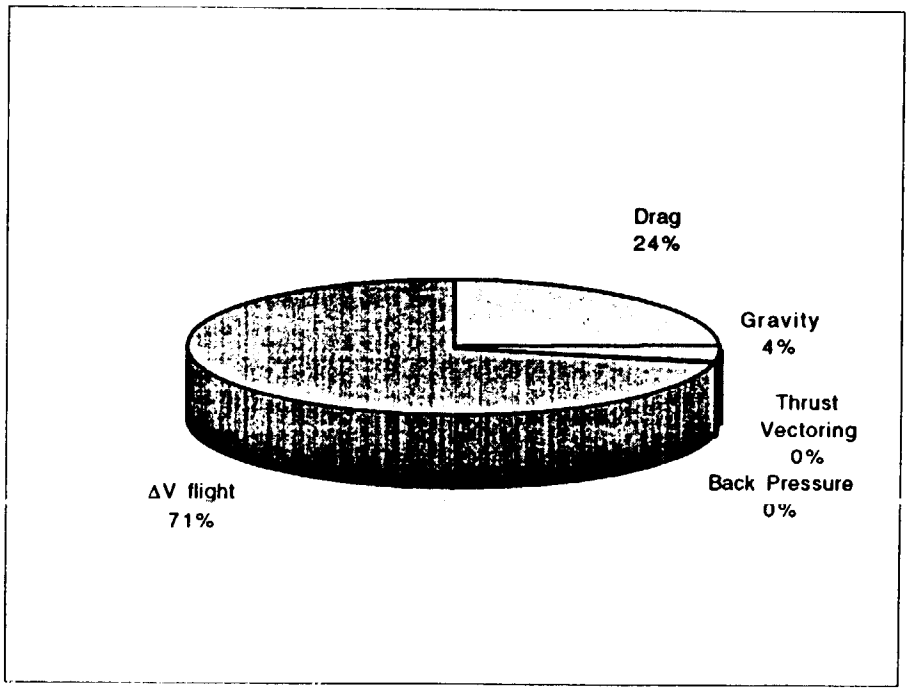

Maglev Case (V=800)

Length = 157.7 feet
Mass Ratio = 4.57
Mixture Ratio = 2.79

Performance Results

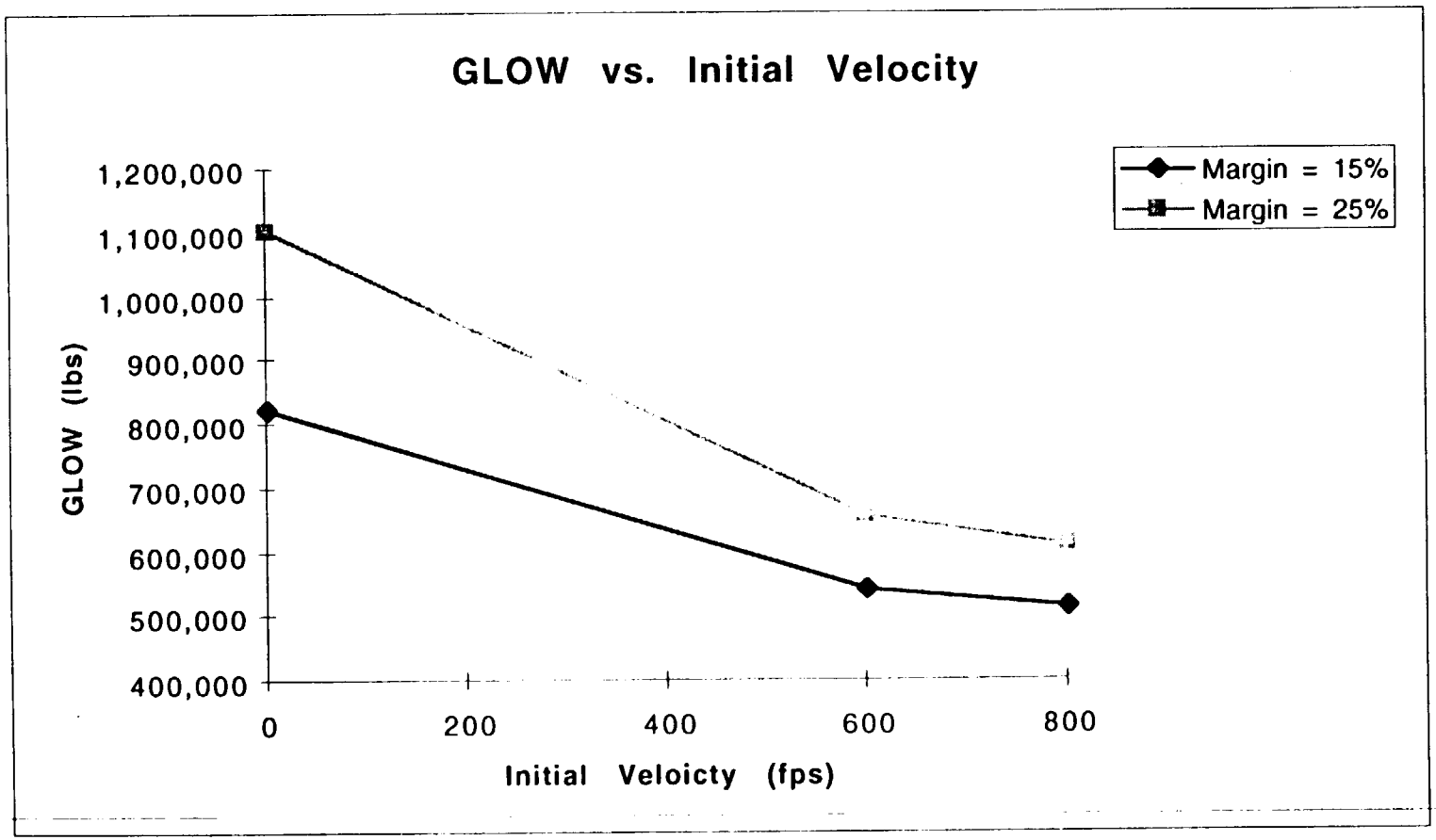

Performance Results

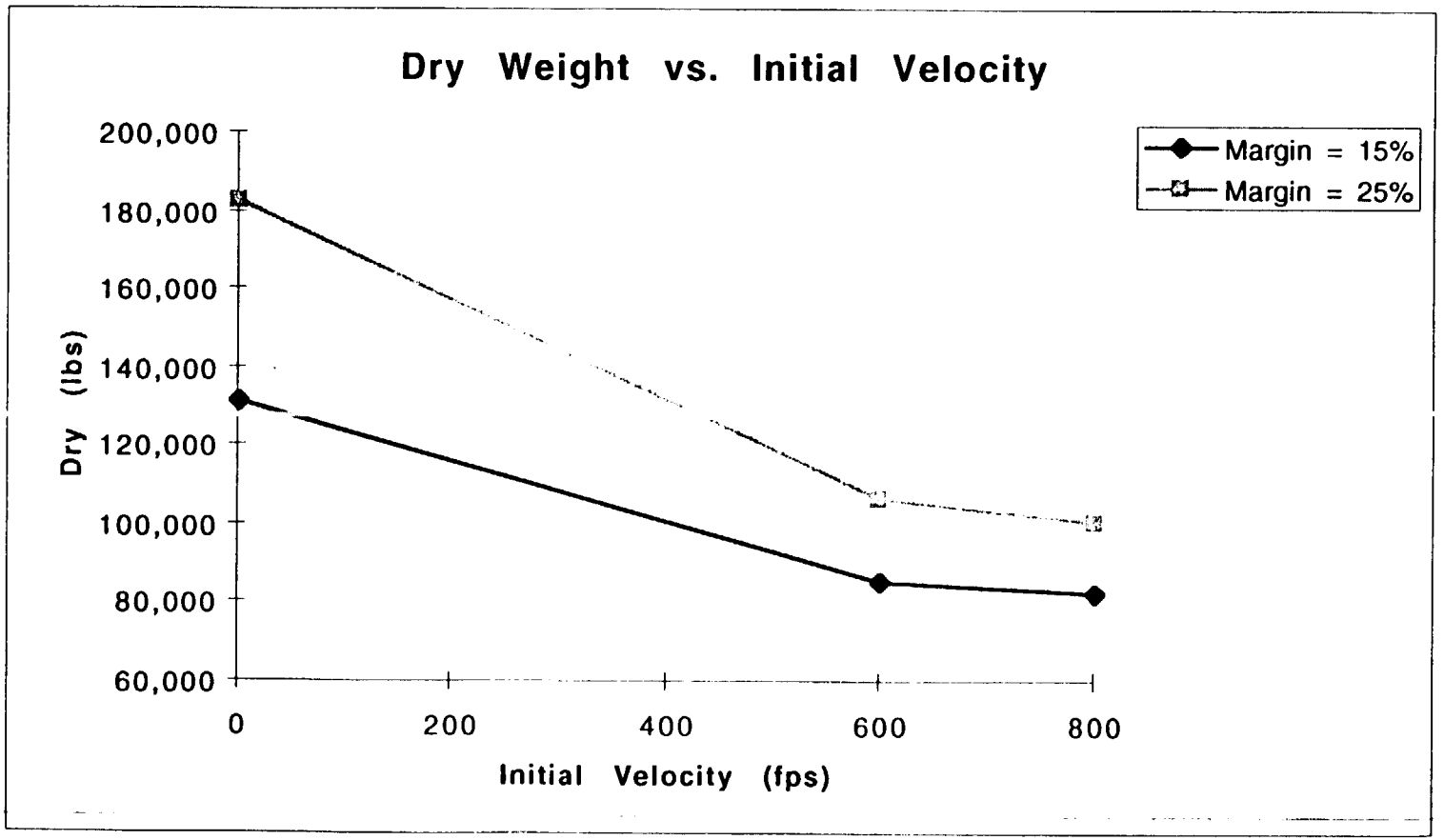

Cost Results

- Still to be determined
- analysis will result in the maglev system having a higher IRR, due to the assumption that the government will provide the facilities
- the maglev system will have higher recurring costs due to track maintenance

Special thanks too...

- Whit Brantley
- Bill Pannel
- Emory Lynn
- George Kearns
- rest of MSFC PD group

NAG8-1302 Report Attachments

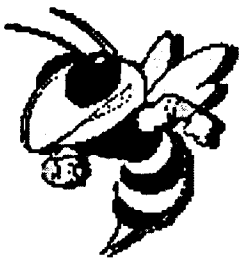

- SCCREAM Development
  - SCCREAM summary slides (Bradford, 1998 AIAA JPC)
  - 1998 and 1997 technical papers (Bradford/Olds)
- *Hyperion* Vehicle
  - Current *Hyperion* status slides (SSDL team/Bradford, 1/99)
  - RBCC vehicle "Honest Assessment" slides (Olds, 2/98 RBCC Workshop)
  - RBCC vehicle "Better Direction" slides (Olds, 1998 NASA summer stay)
  - 1997 *Hyperion* trade studies (Bradford, 1997 summer internship)
- 1998 Bantam-X Support
  - 1998 LOX/LH2 *Stargazer* overview slides (SSDL team/Ledsinger, 1/99)
  - *Stargazer* staging Mach number trade study (Ledsinger, 1998 summer internship)
  - 1998 *Bantam Argus* overview slides (SSDL team/Way, 6/98)
- 1998 Mars Exploration Support
  - Mars Mission trajectory evaluation slides (Poston, 1998 summer internship)

Stargazer: A Bantam-X Concept Vehicle

TSTO with Reusable RBCC Booster & Expendable Pump-fed Fastrac-powered Upper Stage

Dr. John Olds, Laura Ledsinger, John Bradford, Ashraf Charania, Chris Cowart, Rebecca Cutri-Kohart, Dave McCormick, Kirk Sorensen, Dave Way

Space Systems Design Lab

School of Aerospace Engineering
Georgia Institute of Technology
Atlanta, GA

Preliminary Results, Rev.C, 1/26/99

Bantam-X Program Requirements

Mission

- 300 lb. payload
  - university explorer class
- 200 nmi. circular LEO orbit

Programmatics

- 24 flights/yr.
- Recur. cost goal <$1.5M/flt.

Partial reusability and simplified base operations may be the key to meeting Bantam cost goals

Stargazer Configuration

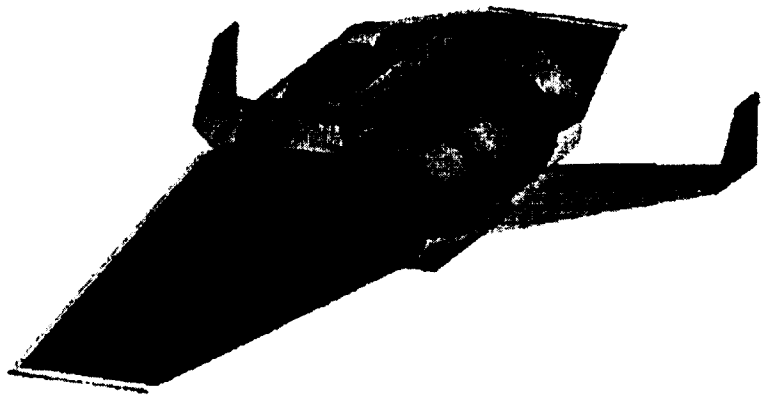

Isometric View

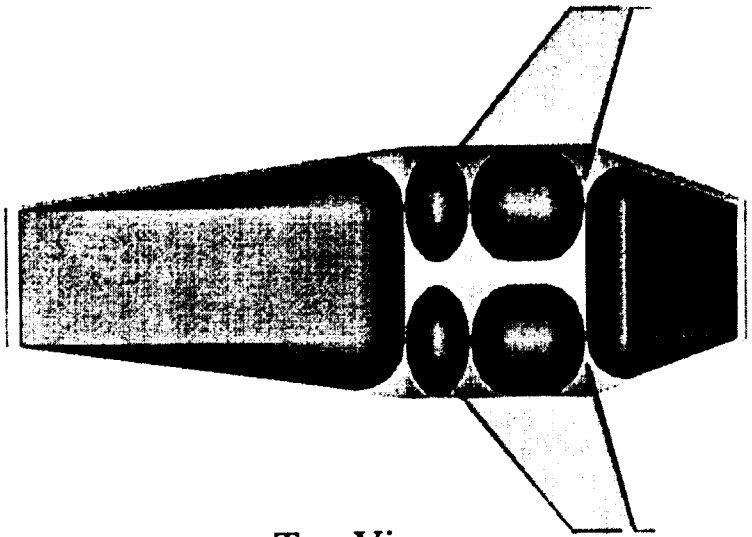

Top View

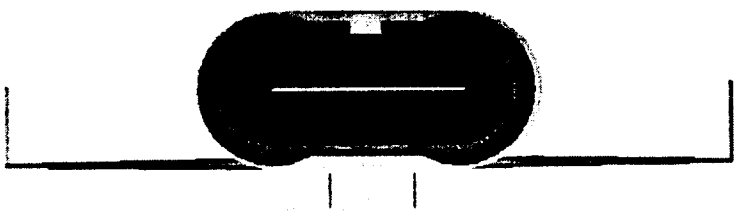

Front View

- TSTO configuration
- Horizontal takeoff & landing
- Reusable booster, expendable upper stage
- Autonomous flight (no crew)
- 300 lb to 200 nmi. circ. x 28.5°

Stargazer Concept Highlights

Key Technical Features

- Reusable Aerodynamic Booster
  - HTHL configuration
  - auto-flyback to launch site
  - advanced materials & TPS used
- Ejector Scramjet RBCC Engines
  - LOX/LH2 booster propellants
  - peak A/B at Mach 10
- Expendable Upper Stage (pop-up)
  - Low $ pump-fed upper stage
  - Fastrac-derived LOX/RP engine

Key Programmatic Features

- Highly Reusable RBCC Booster
  - very little maintenance required
  - long life components
  - Skunkworks-style flying prototype
- 'Bantam Corp.' Operations
  - launch/landing from KSC
  - two new buildings constructed
  - only 40 ground personnel req'd
  - low recurring costs/flt.

Stargazer Booster 3-View

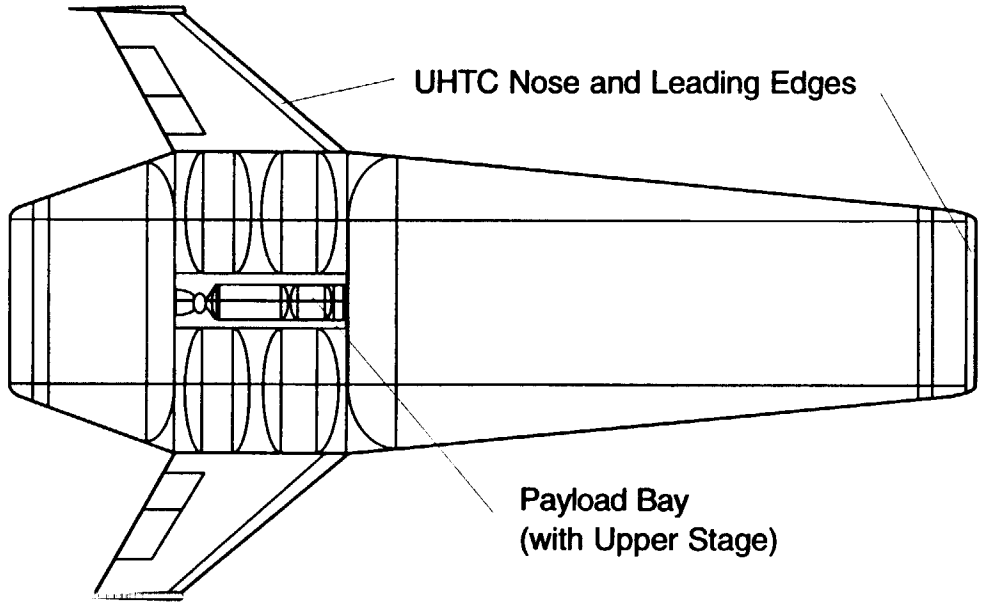

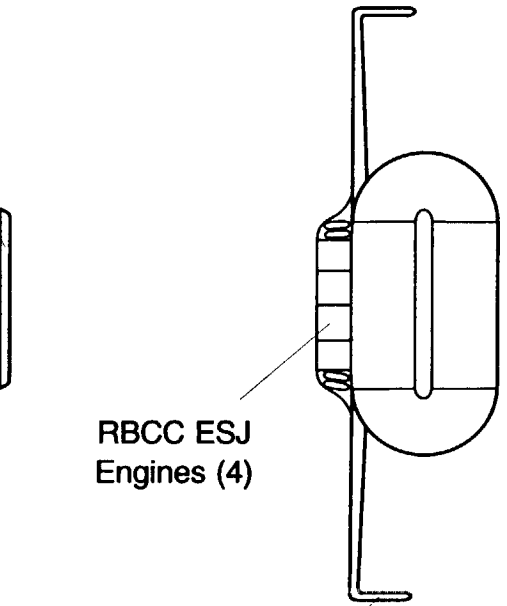

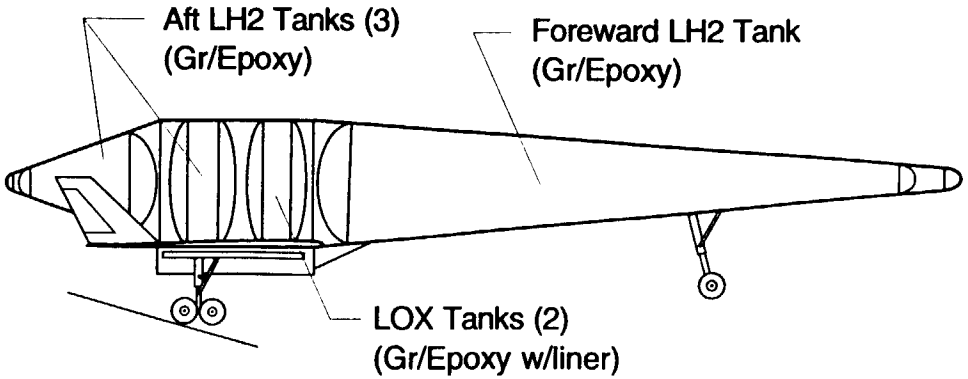

GLOW:	58,750 lb.
Dry Wt:	18,000 lb.
Payload:	300 lb.
Length:	75 ft.
Wingspan:	40 ft.
Mass Ratio:	2.113 (booster)

Stargazer Flight Profile

- Fully reusable LOX/LH2 booster
- Autonomous flight (no crew)
- Powered flyback (ramjet mode)
- Expendable LOX/RP upper stage

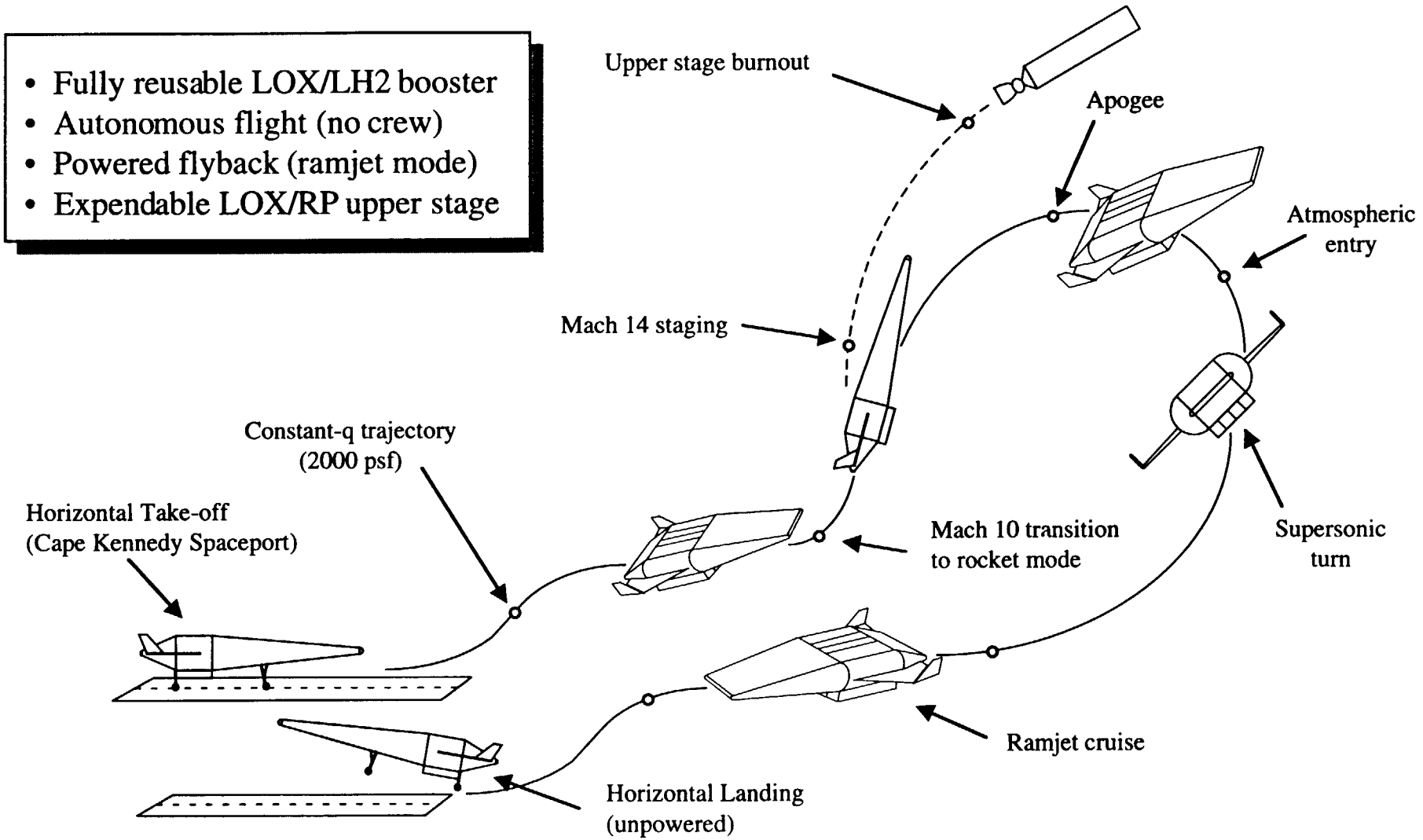

Stargazer Weight Statement

1.0	Wing Group	1,550
2.0	Tail Group	250
3.0	Body Group	4,650
4.0	Thermal Protection	1,800
5.0	Landing/Takeoff Gear	1,500
6.0	Propulsion	2,350
7.0	RCS Propulsion	200
8.0	OMS Propulsion	0
9.0	Primary Power	50
10.0	Electrical Conversion & Dist.	2,000
11.0	Hydraulic Systems	0
12.0	Surface Control Actuation	150
13.0	Avionics	400
14.0	Environmental Control	750
15.0	Personnel Equipment	0
16.0	Dry Weight Margin	2,350
	Dry Weight	**18,000**
17.0	Crew and Gear	0
18.0	Payload Provisions	0
19.0	Cargo (up and down)	0
20.0	Residual Propellants	50
21.0	OMS/RCS Reserve Propellants	0
	Landed Weight	**18,050**
22.0	Entry/Flyback Propellants	7,500
	Entry Weight	**25,550**
23.0	RCS/OMS Propellants (on-orbit)	0
24.0	Cargo Discharged	1,700
25.0	Ascent Reserve and Unusable Propellants	300
26.0	Inflight Losses and Vents	250
	Insertion Weight	**27,800**
27.0	Ascent Propellants	30,950
	Gross Liftoff Weight	**58,750**
28.0	Startup Losses	250
	Maximum Pre-launch Weight	59,000

Dry Weight Breakdown

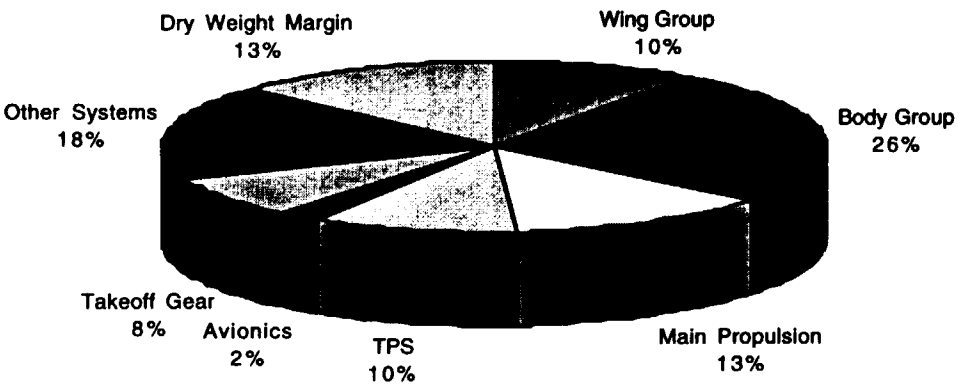

Gross Weight Breakdown

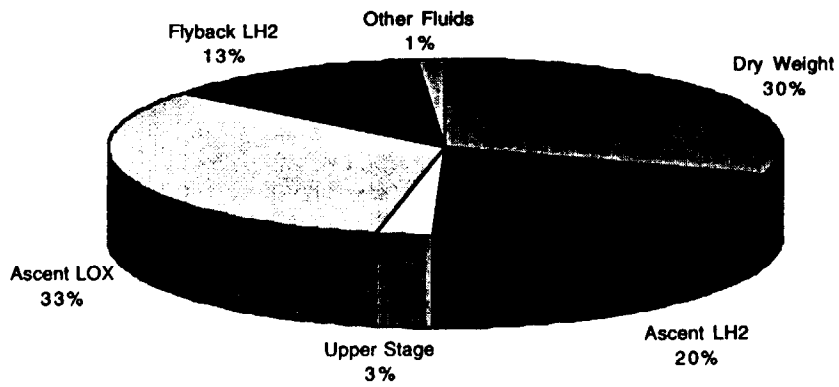

ESJ RBCC Booster Engines

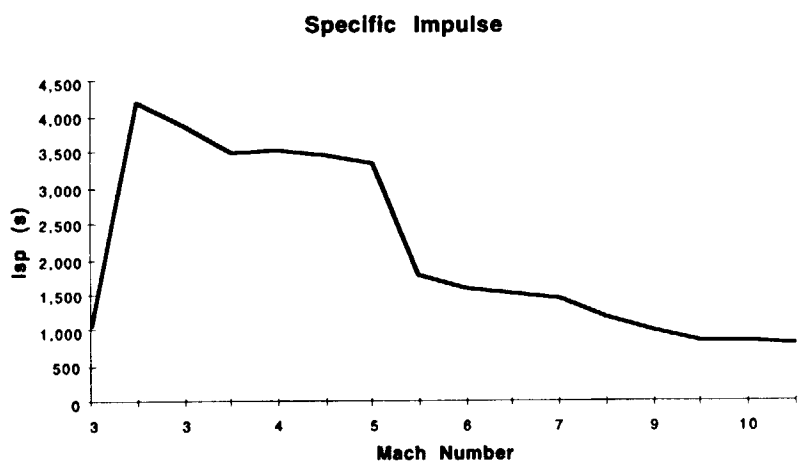

Engine Summary

Thrust (sls,each):	10,300 lbs
Isp (sls):	344 sec.
T/We (inst):	20
Ws/Wp (sls):	2.9
Mtr (A/B):	Mach 10
Max Phi:	1.0

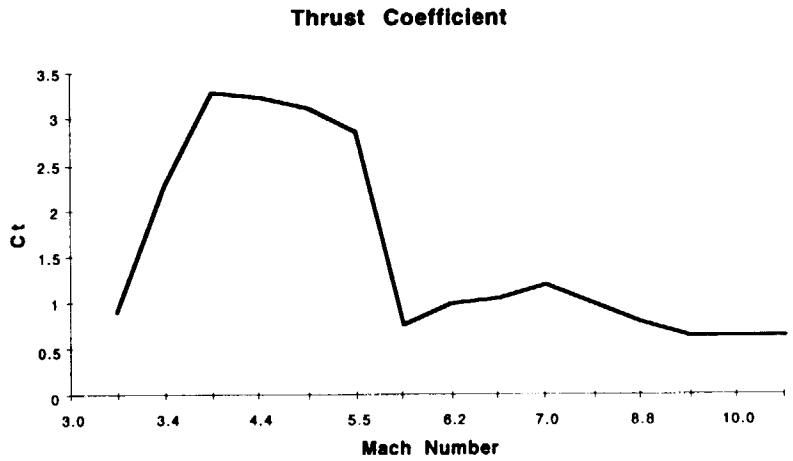

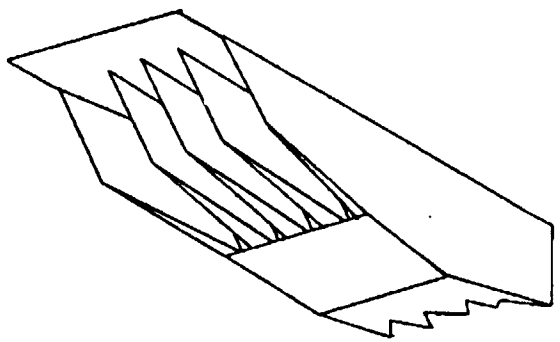

LOX/LH2 Ejector Scramjet (ESJ)

Fastrac-Derived U/S Engine

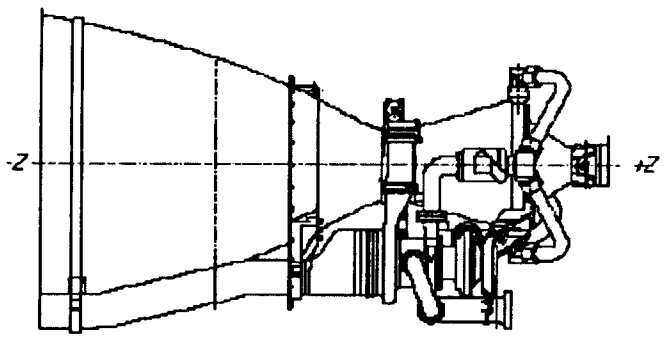

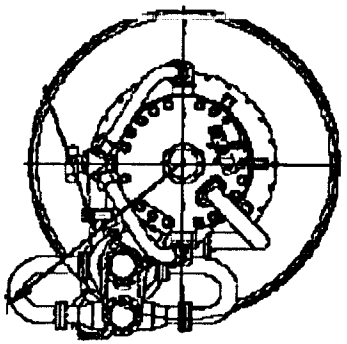

- Used on rocket upper stage
- LOX/RP propellants
- Gas generator cycle
- 1700 lb. thrust (vac.)
- 328 sec. specific impulse (vac.)
- 50:1 area ratio nozzle
- Expendable config. (~$580k ea.)

Leverages MSFC low cost Fastrac development effort

Other Stargazer Technologies

- Structural Materials (booster)
  - Lightweight, reusable graphite/epoxy propellant tanks (LOX and LH2)
  - Advanced metal matrix composites (Titanium-aluminide)
- Thermal Protection Systems (booster)
  - Ultra-high temperature ceramics (UHTC/SHARP)
  - Lightweight ceramic tiles (AETB/TUFI-derived) and blankets (TABI)
  - Active cooling required only in ESJ engine
- Subsystems
  - Autonomous flight control system (booster autofly, autoland)
  - High rate electromechanical actuators (booster)
  - High power density fuel cells (booster)
  - Lightweight avionics, light power distribution, fiber cabling, VHM (booster)
  - Low production cost avionics suite (upper stage)

Stargazer Recurring Cost

Recurring Cost Breakdown

Propellant Cost	$0.021 M
Labor Cost	$0.250 M
LRU Hardware Cost*	$0.033 M
Upper Stage**	$0.670 M
Site Fee	$0.050 M
Insurance Cost	$0.100 M

* Maintenance hardware for booster
** Average for first year of operation

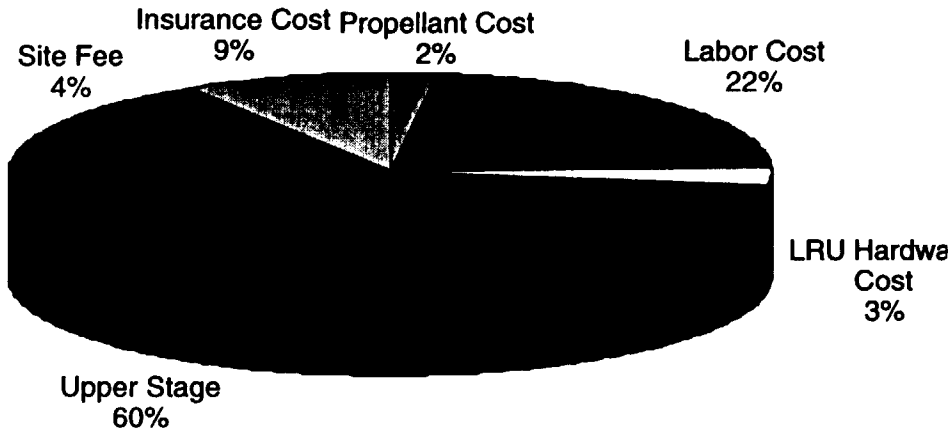

Estimated Recurring Cost per Flight = $1.125M

Meets $1.5M/flight goal. Higher flight rates could lead to even lower upper stage production costs.

Stargazer Non-Recurring Cost

DDT&E Cost Breakdown

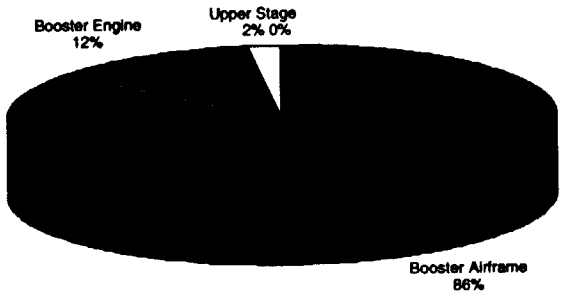

Booster Airframe	$1,045 M
Booster Engine	$150 M
Upper Stage	$24 M

*Does not include Fastrac development costs.

TFU Cost Breakdown

Booster Airframe	$204 M
Booster Engines (4)	$220 M
Upper Stage	$1 M

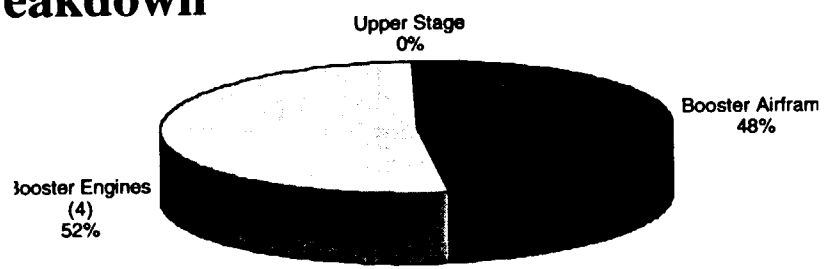

Total Non-Recurring Cost = $1.327B (includes $60M for facilities)

Stargazer Concept Summary

- Meets Bantam payload requirements
- Meets cost per flight objectives
- Exploits advanced technologies (RBCC, Fastrac, TPS, materials)
- Flyback RBCC booster enables single base operations and faster turnaround
- Up front investment in reusability (higher non-recurring cost) results in lower recurring costs per flight relative to ELVs

Stargazer: *Staging Mach Number Trades*

Laura A. Ledsinger

Ph.D. Student

Space Systems Design Lab

Georgia Institute of Technology

Marshall Summer Student

July/August, 1998

Project Goal

Optimize the staging Mach number of the TSTO Bantam-X Concept:

Stargazer

Stargazer Staging Mach Number Trades

Stargazer *Configuration*

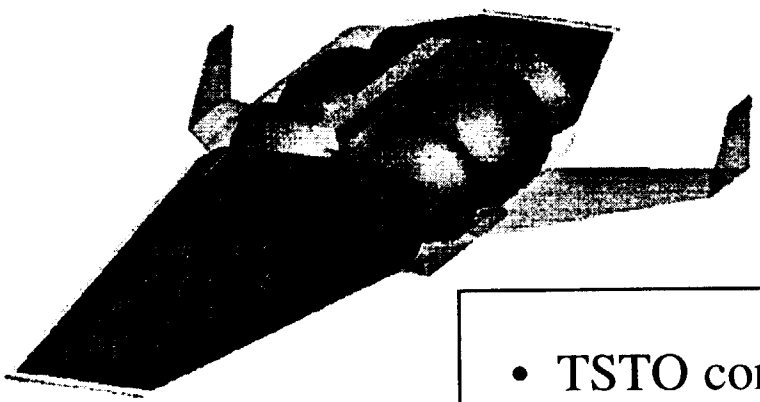

- TSTO configuration
- Horizontal takeoff & landing
- Reusable booster, expendable upper stage
- Four ejector scramjet, RBCC engines
- Autonomous flight (no crew)
- 300 lb to 200 nmi. circ. x 28.5°

Stargazer Staging Mach Number Trades

Flight Profile

- Fully reusable LOX/LH2 booster
- Autonomous flight (no crew)
- Powered flyback (ramjet mode)
- Expendable LOX/RP upper stage

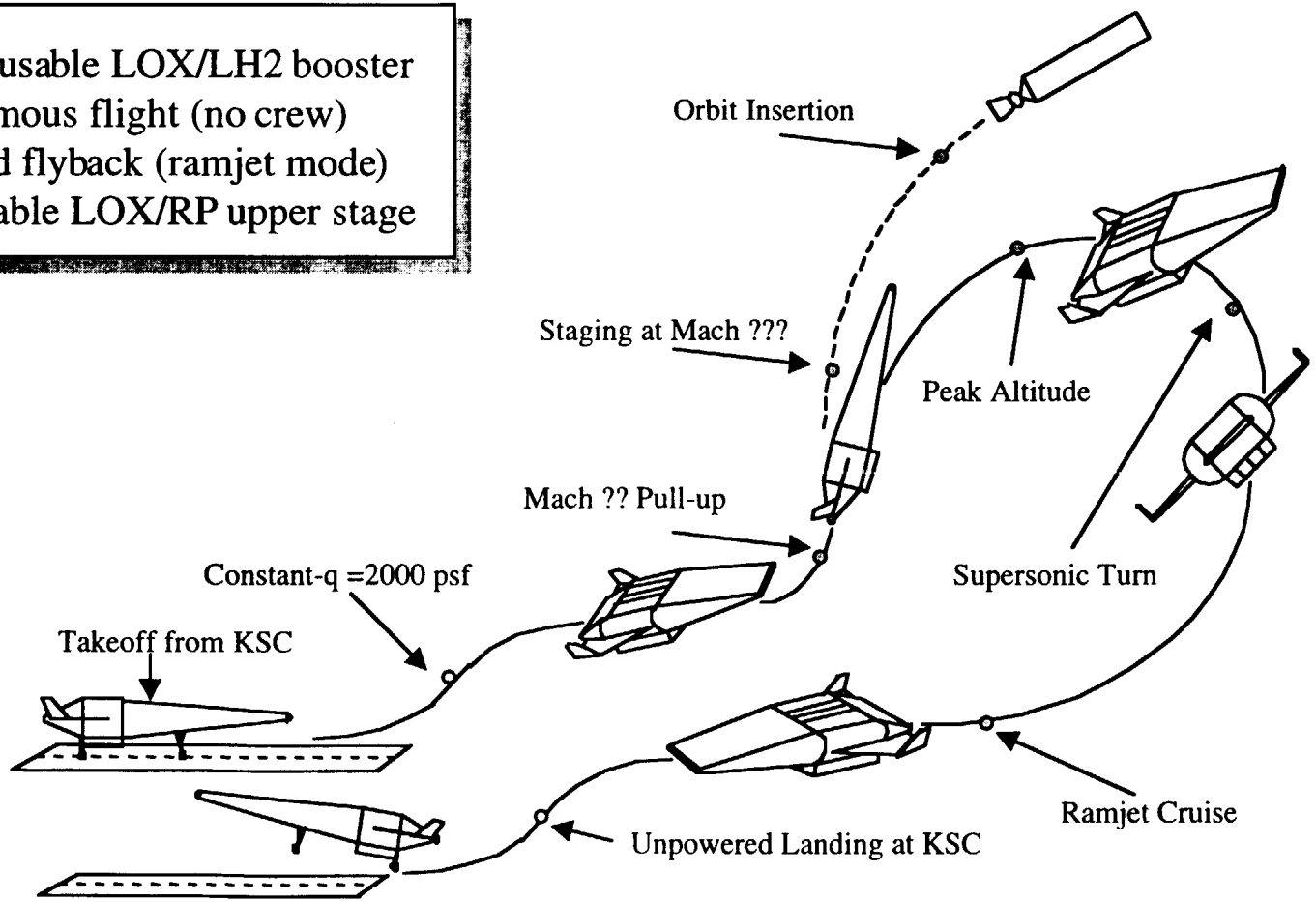

Stargazer Staging Mach Number Trades

Project Question

- Optimize staging Mach number with respect to ???
  - Dry Weight of the Booster
  - Dry Weight of the Upper Stage
  - DDTE/TFU Costs
  - Recurring Cost per Flight

And the Answer Is...

- Recurring Cost per Flight
  - Bantam-X goal
  - Booster dependency
  - Upper Stage dependency
  - Trade-off between the two

- Optimize staging Mach number w.r.t. **minimizing** recurring cost per flight

Recurring Cost per Flight Components

- Recurring Cost includes:
  - Expendable Upper Stage Cost (configuration dependent)
  - Propellant Cost (configuration dependent)
  - LRU Hardware Cost (configuration dependent)
  - Labor Cost ($250,000 per flight)
  - Insurance Cost ($100,000 per flight)
  - Site Fee ($50,000 per flight)

Weights vs. Staging Mach Number

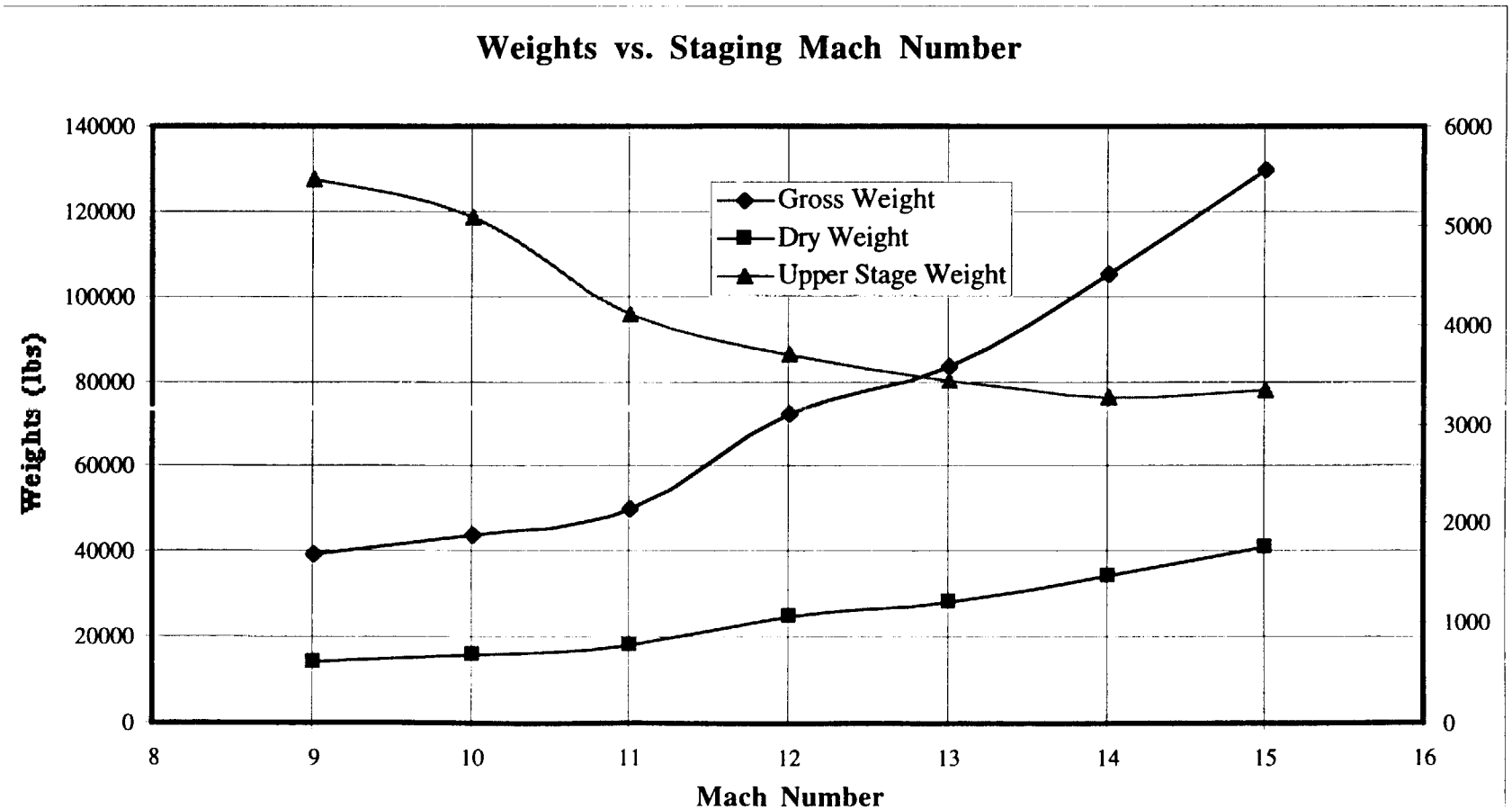

Stargazer Staging Mach Number Trades

Preliminary

LAL:8/98:15

The Iteration Process

Stargazer Staging Mach Number
Trades

LAL:8/98:8

Design Structure Matrix

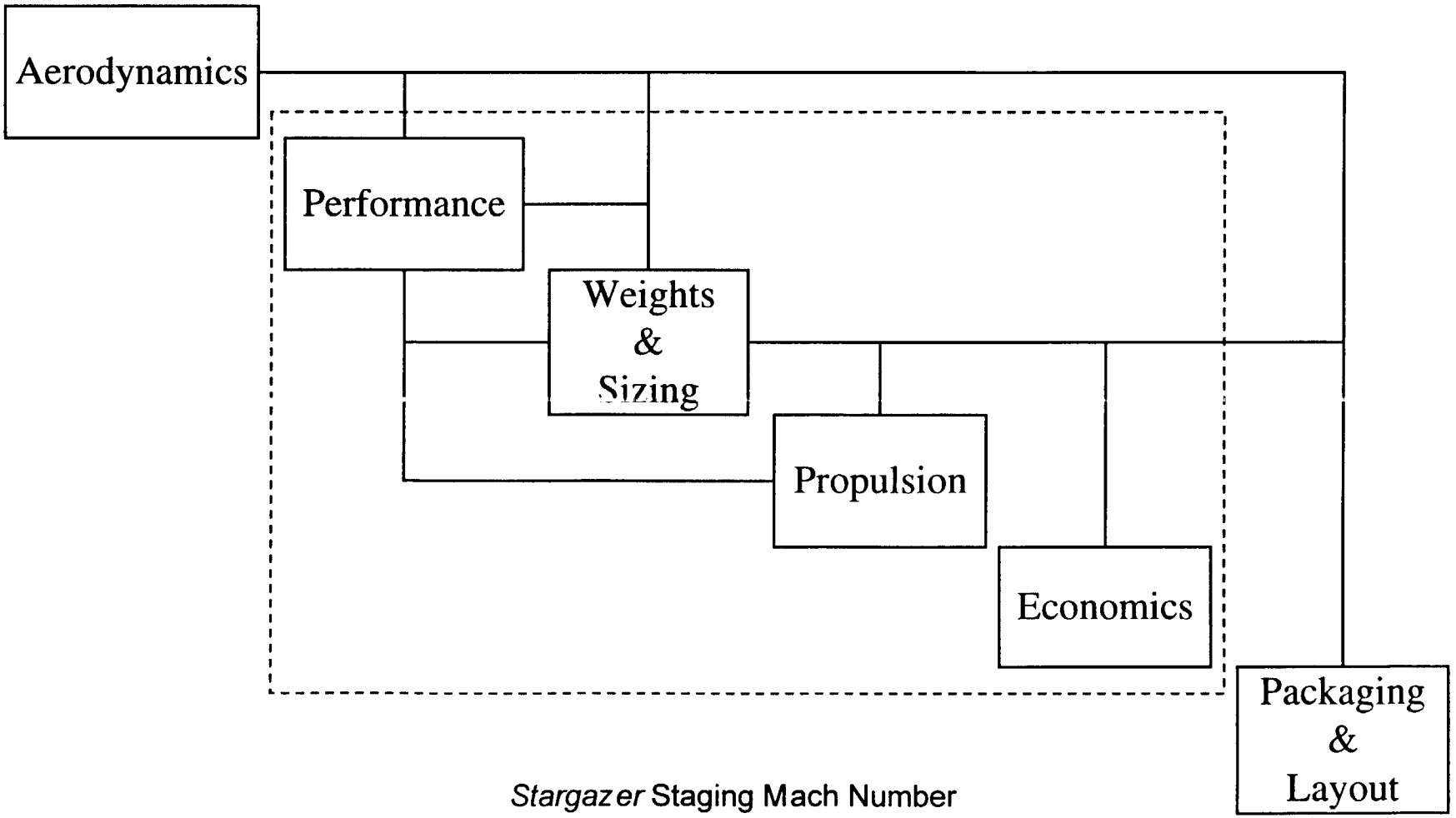

Stargazer Staging Mach Number Trades

Preliminary

LAL:8/98:9

Design Structure Matrix

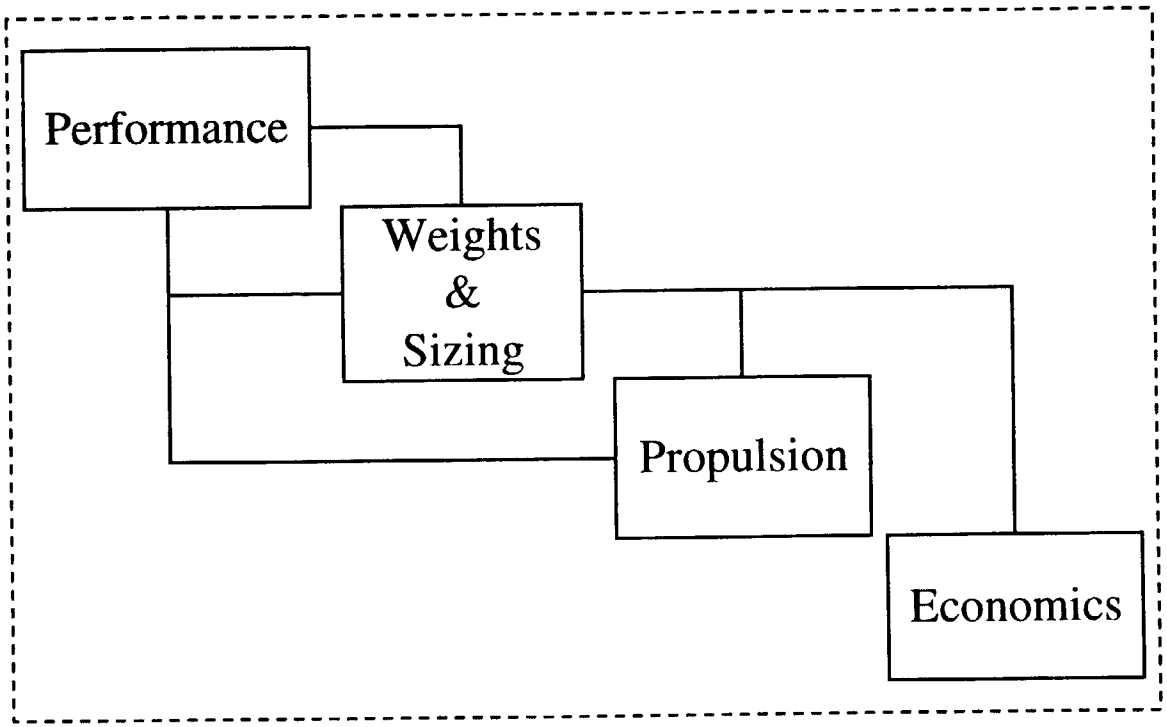

Stargazer Staging Mach Number
Trades

Disciplines & Programs

- Program to Optimize Simulated Trajectories (POST)
  - FORTRAN code (NASA/Lockheed-Martin)
  - Equation of Motion Integration/Event-Oriented
- Weights and Sizing
  - Excel Spreadsheet (GA Tech)
  - Based on Dr. Ted Talay's (NASA Langley) WER's

Disciplines & Programs (con.)

- Simulated Combined-Cycle Rocket Engine Analysis Module (SCCREAM)
  - HTML/C++ code (GA Tech)
  - Conceptual tool for RBCC analysis
- Cost and Business Analysis Module (CABAM)
  - Excel Spreadsheet (GA Tech)
  - Based on NASCOM CER's

POST in Depth

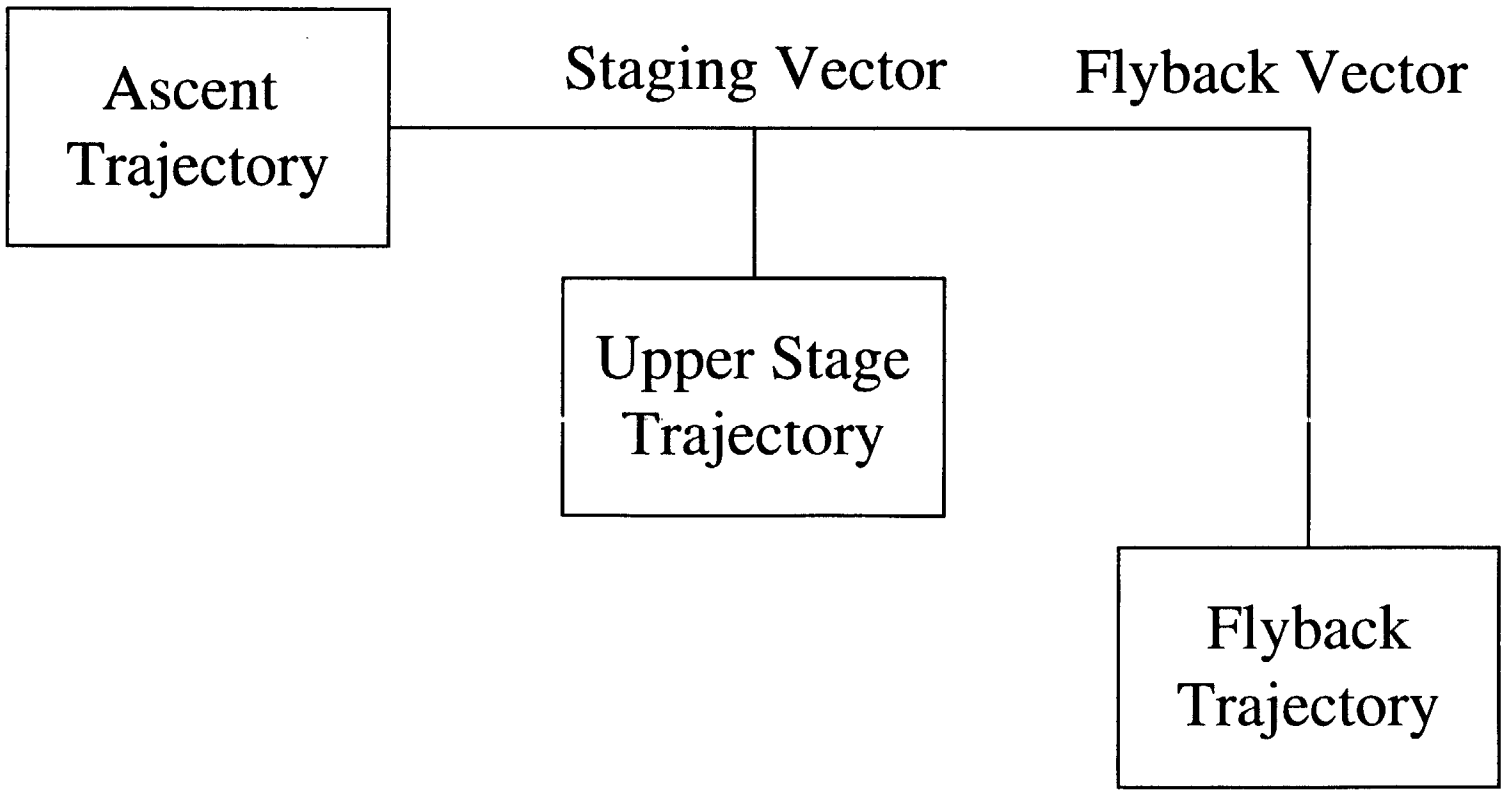

Stargazer Staging Mach Number Trades

The Results

Note: The results given here were revised since the original presentation on August 26, 1998. Due to updates in RBCC engine and upper stage cost modeling, the optimized staging Mach number changed from 11 to 14 as reported in the next few slides.

Weights vs. Staging Mach Number

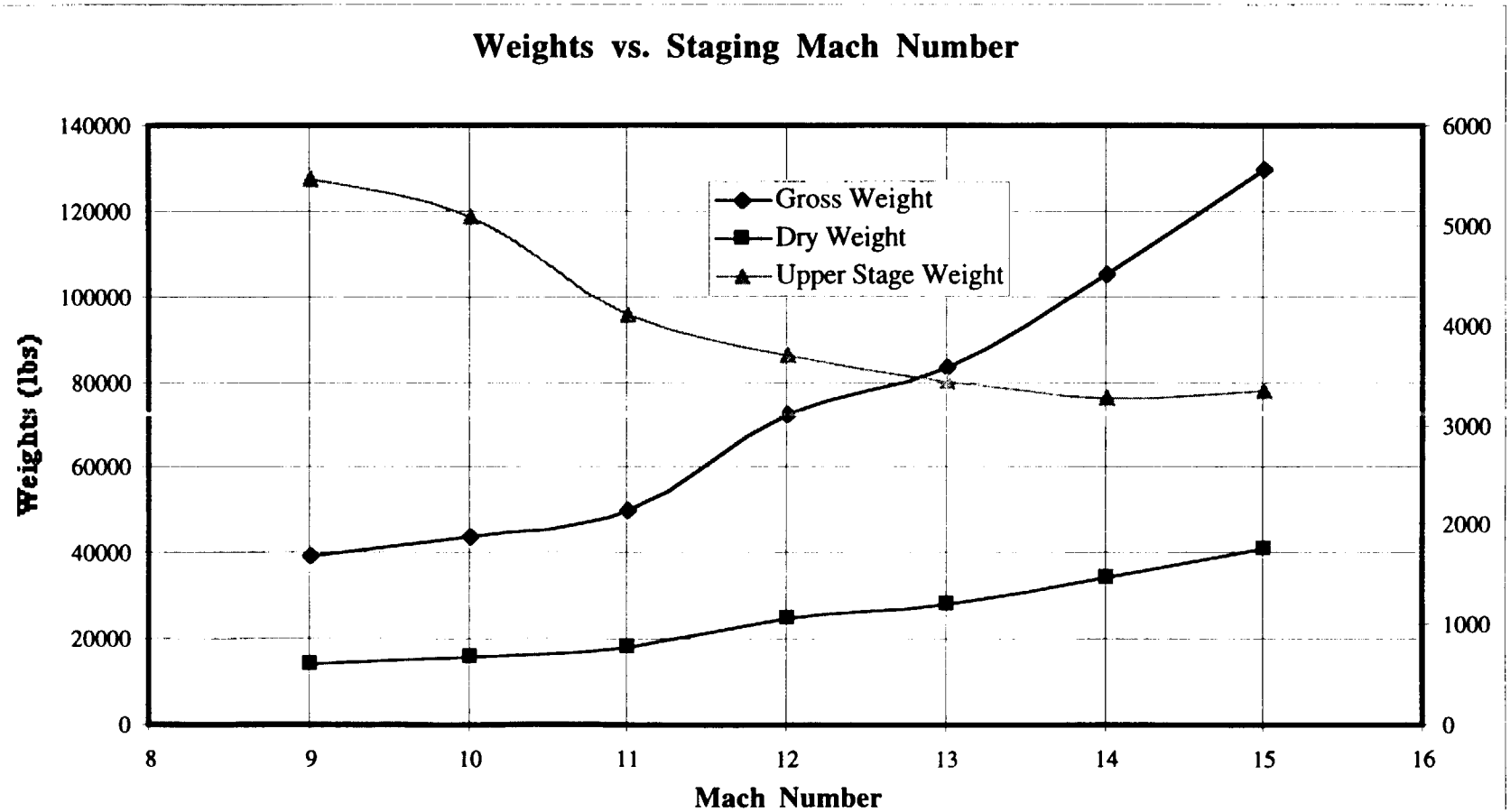

Stargazer Staging Mach Number Trades

Preliminary

LAL:8/98:15

Recurring Cost vs. Staging Mach Number

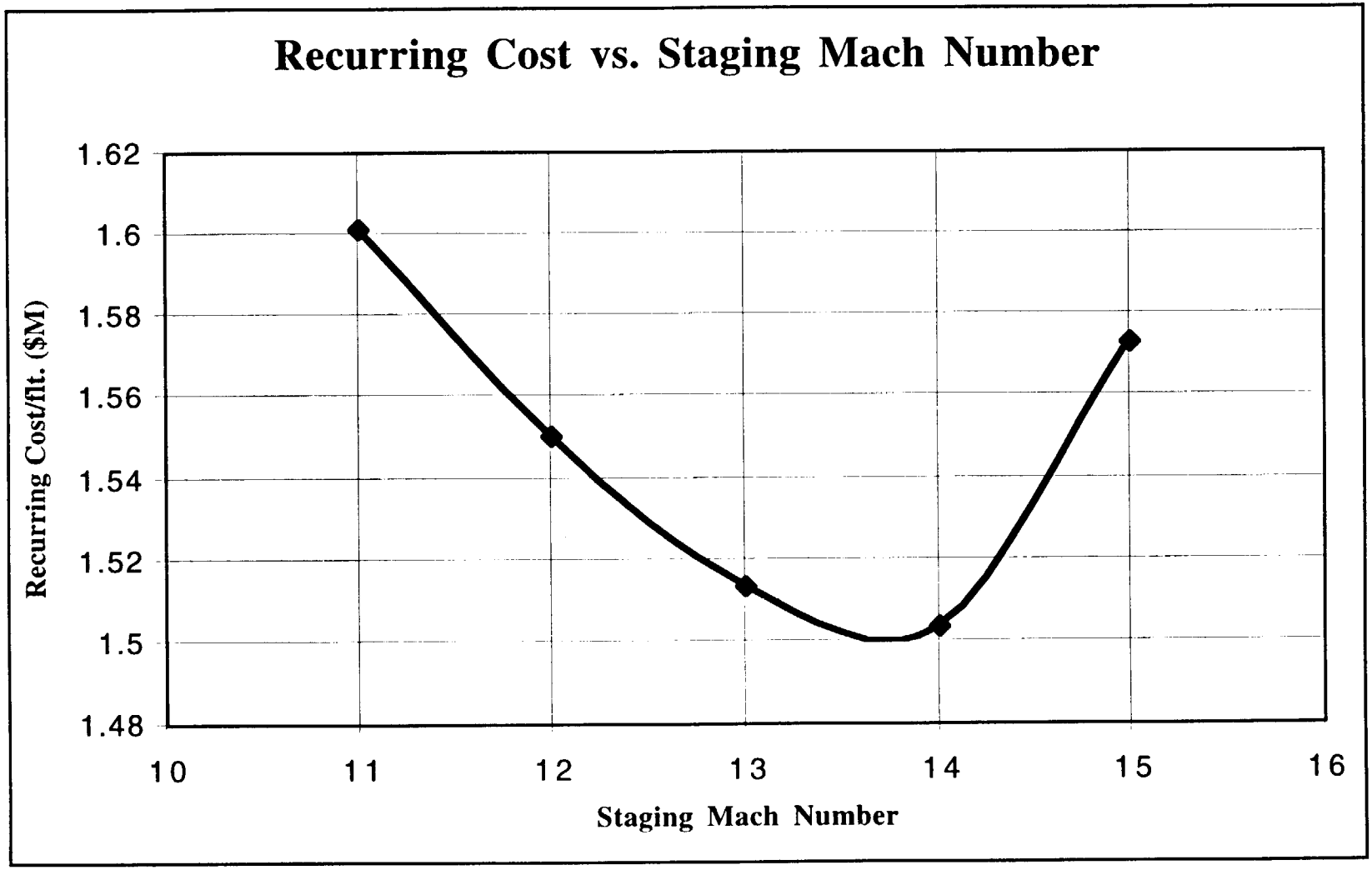

Stargazer Staging Mach Number Trades

Preliminary

LAL:8/98:16

Conclusions

- Staging at Mach 14 results in lowest recurring cost per flight
  - Decreased booster ascent fuel
  - Decreased booster flyback fuel
  - Only small change in upper stage mass

Bantam Argus Vehicle

Bantam-X Class SSTO Reusable RBCC Booster with Magnetic Levitation Launch Assist

Preliminary Results

Space Systems Design Lab

School of Aerospace Engineering
Georgia Institute of Technology
Atlanta, GA

Bantam Argus Concept

Key Technical Features

- Reusable Aerodynamic Booster
  - HTHL configuration
  - potential for other launch uses
  - advanced materials & TPS used
- Supercharged Ejector Ramjet RBCC Engines
  - LOX/LH2 propellants
  - peak A/B at Mach 6
- Magnetic Launch Assist
  - Launch speed ~ 800 fps

Key Programmatic Features

- Highly Reusable RBCC Booster
  - very little maintenance required
  - long life components
  - Skunkworks-style flying prototype
- 'Bantam Corp.' Operations
  - launch/landing from KSC
  - two new buildings constructed
  - only 40 ground personnel req'd
  - low recurring costs/flt.

Bantam Argus Concept

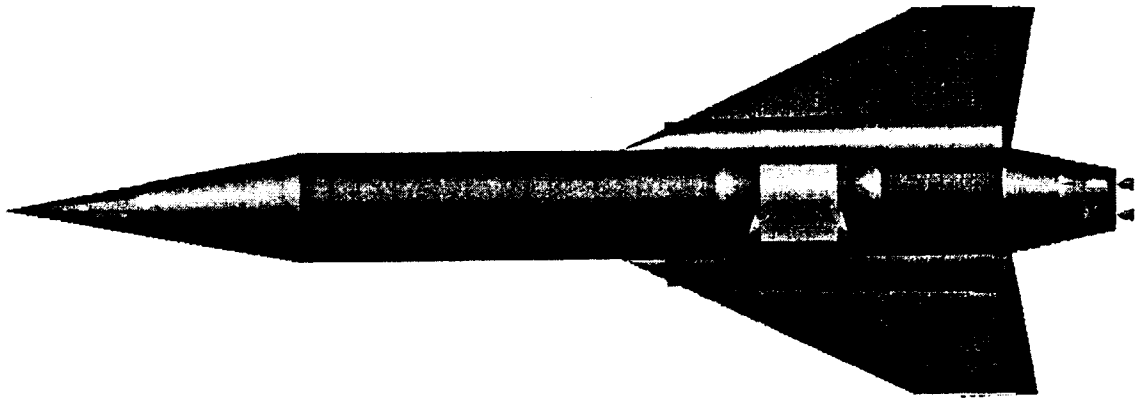

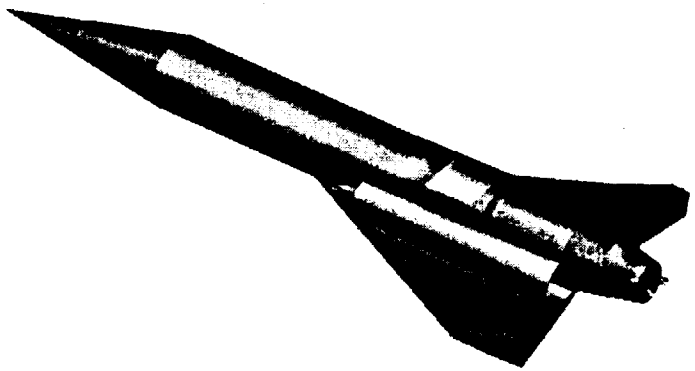

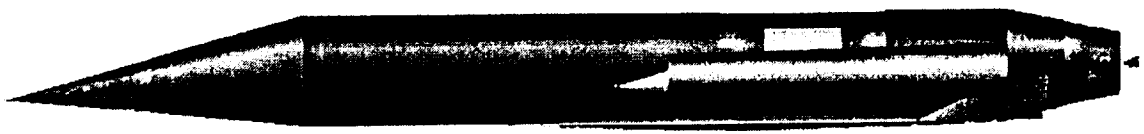

Bantam Argus Mission

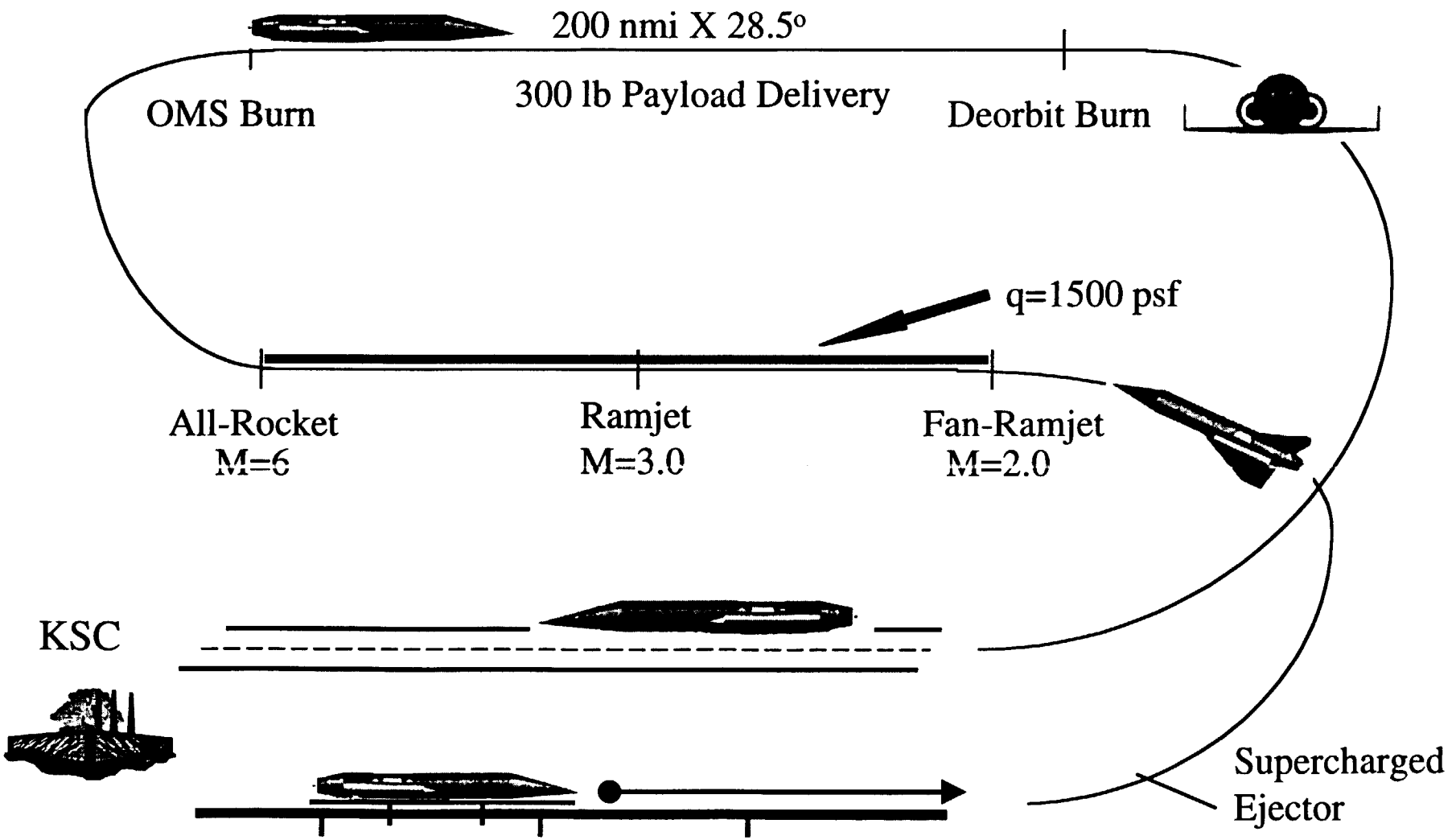

Weight Statement

1.0 Wing Group	3,528
2.0 Tail Group	401
3.0 Body Group	8,784
4.0 Thermal Protection	2,180
5.0 Landing Gear/Maglifter Attach Points	1,431
6.0 Main Propulsion (LOX/LH2 SERJ RBCC)	6,915
7.0 RCS Propulsion	249
8.0 OMS Propulsion	213
9.0 Primary Power	762
10.0 Electrical Conversion & Dist.	2,263
12.0 Surface Control Actuation	237
13.0 Avionics	1,600
14.0 Environmental Control	1,859
16.0 Dry Weight Margin	4,563
Dry Weight	**34,986**
19.0 Cargo (up and down)	300
20.0 Residual Propellants	256
21.0 OMS/RCS Reserve and Landing Propellants	243
Landed Weight	**35,786**
22.0 RCS Entry Propellants (ΔV = 25 fps)	66
Entry Weight	**35,852**
23.0 RCS/OMS Propellants (on-orbit)	1,752
25.0 Ascent Reserve and Unusable Propellants	1,239
26.0 Inflight Losses and Vents	359
Insertion Weight	**39,200**
27.0 Ascent Propellants	165,152
Gross Liftoff Weight	**204,352**
28.0 Startup Losses	597
Maximum Pre-launch Weight	**204,949**

Dry Weight Breakdown

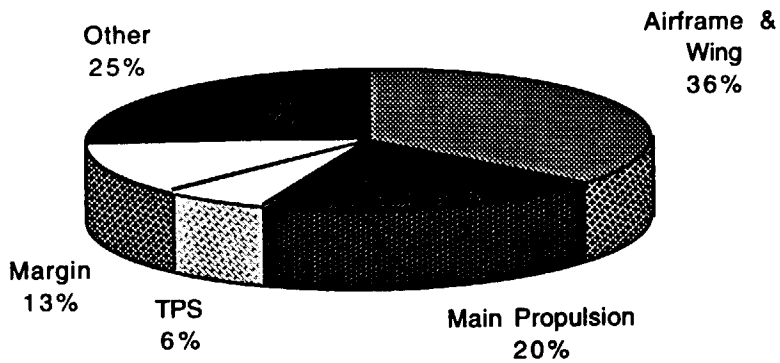

Gross Weight Breakdown

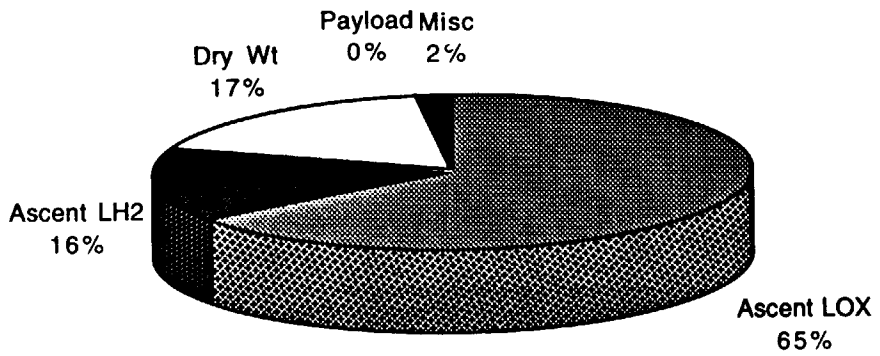

Recurring Cost

Cost Breakdown

Propellant Cost	$0.046 M
Labor Cost	$0.250 M
LRU Hardware Cost	$0.100 M
Site Fee	$0.050 M
Insurance Cost	$0.100 M

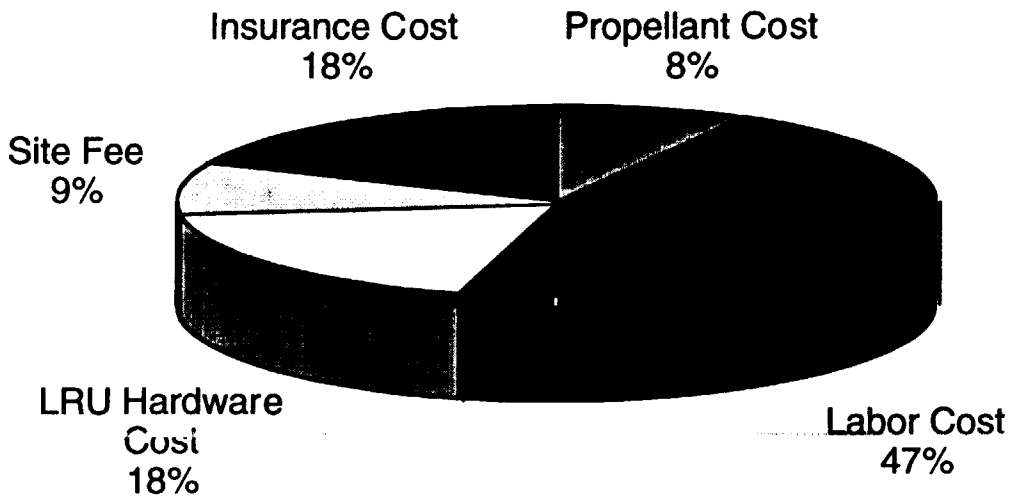

Recurring Cost per Flight = $0.546 M

Non-Recurring Cost

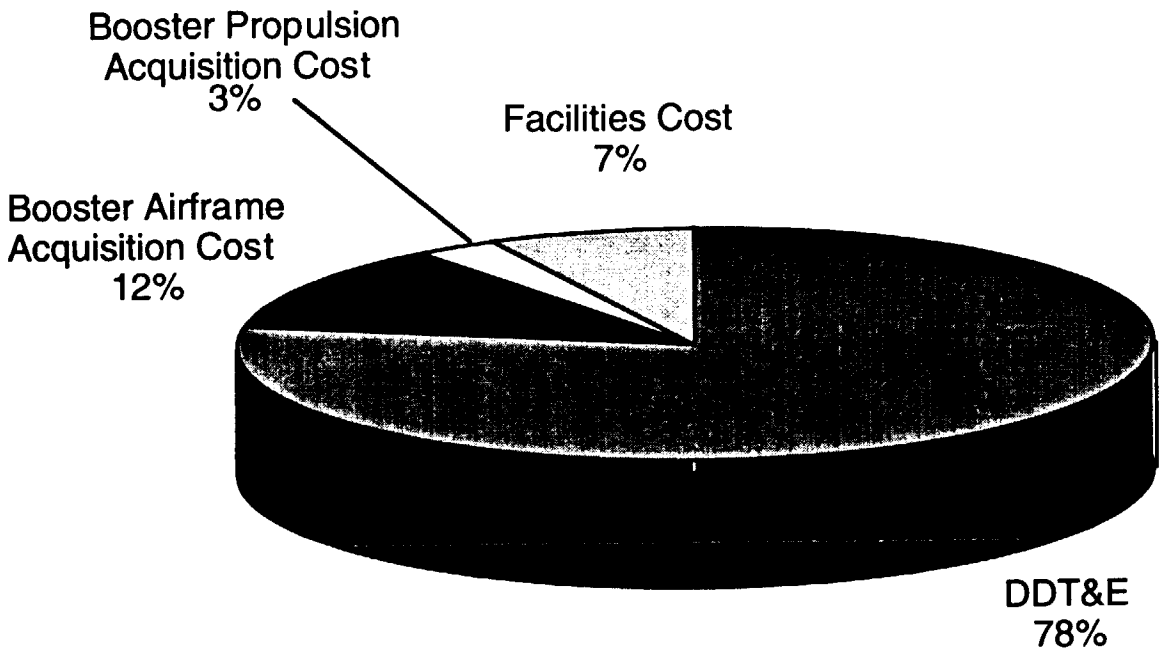

Total Non-Recurring Cost = $3.551 B

Payload Trade Study

Increasing the payload 5 times increases gross weight by only 9% and lowers recurring cost to 366 $/lb.

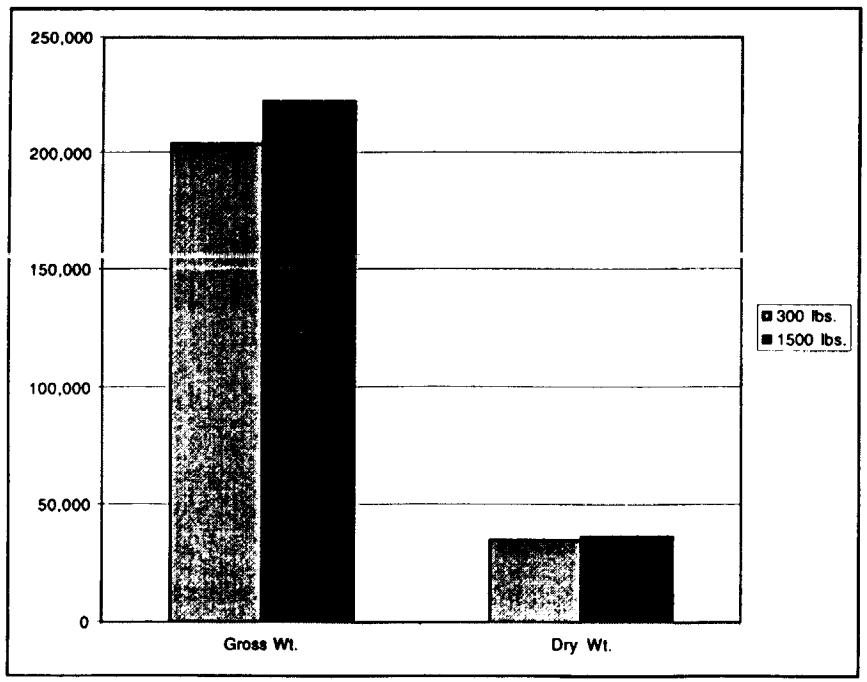

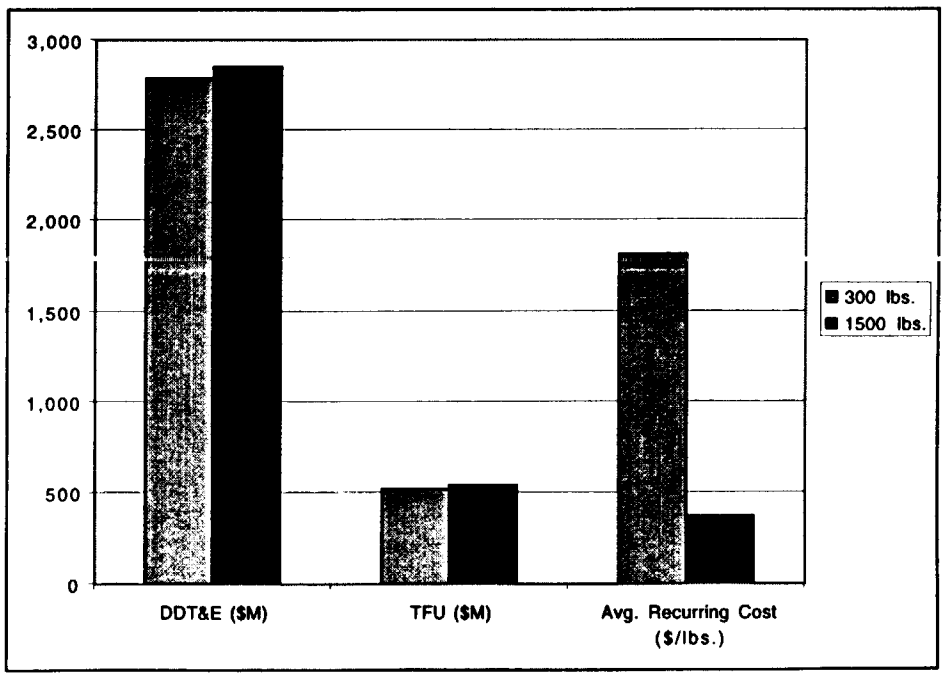

NAG8-1302 Report Attachments

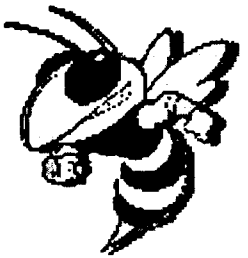

- SCCREAM Development
  - SCCREAM summary slides (Bradford, 1998 AIAA JPC)
  - 1998 and 1997 technical papers (Bradford/Olds)
- *Hyperion* Vehicle
  - Current *Hyperion* status slides (SSDL team/Bradford, 1/99)
  - RBCC vehicle "Honest Assessment" slides (Olds, 2/98 RBCC Workshop)
  - RBCC vehicle "Better Direction" slides (Olds, 1998 NASA summer stay)
  - 1997 *Hyperion* trade studies (Bradford, 1997 summer internship)
- 1998 Bantam-X Support
  - 1998 LOX/LH2 *Stargazer* overview slides (SSDL team/Ledsinger, 1/99)
  - *Stargazer* staging Mach number trade study (Ledsinger, 1998 summer internship)
  - 1998 *Bantam Argus* overview slides (SSDL team/Way, 6/98)
- 1998 Mars Exploration Support
  - Mars Mission trajectory evaluation slides (Poston, 1998 summer internship)

Human Mars Mission
Transportation Analysis

Tara Poston
Georgia Institute of Technology
August 28, 1998

Outline

- Trajectory Analysis
  - Propulsive or Aerobraking Mars Orbit Capture?
  - Benefits of Type I Cargo Trajectories
  - Mars Entry Speed Analysis
  - Enveloping 2014, 2016, & 2018 Missions
  - 2026 - 2041 Opportunities
- Vehicle Sizing

Tara Poston
Georgia Inst. of Technology
August 28, 1998

Propulsive or Aerobraking?

Flights to Mars Categorized By Opportunity (MOC w/ Prop. ΔV)

Mission Type	Launch Year	TMI Date (m/d/yy)	TMI ΔV (m/s)	Velocity Losses* (m/s)	Mars Arrival Date (m/d/yy)	Outbound Flight Time (days)	MOC ΔV (m/s)	Velocity Losses* (m/s)	Mars Stay Time (days)	Mars Departure Date (m/d/yy)	TEI ΔV (m/s)	Return Time (days)	Return Date (m/d/yy)	Total Mission Duration (days)	Dep. C_3 (km^2/s^2)	Total Major Mission ΔVs (TMI+MOC+TEI) (m/s)
Cargo 1	2009	10/13/09	3,747	107	09/02/10	324	812	2	—	—	—	—	—	—	10.28	4,560
Cargo 2	2009	10/13/09	3,749	108	09/02/10	324	812	2	—	—	—	—	—	—	10.28	4,561
Piloted	2009	11/09/09	4,322	223	06/07/10	210	1,837	62	496	10/16/11	1,567	199	05/02/12	905	20.86	5,889
Cargo 1	2011	11/09/11	3,684	102	09/11/12	307	928	3	—	—	—	—	—	—	8.97	4,612
Cargo 2	2011	11/09/11	3,686	103	09/11/12	307	928	3	—	—	—	—	—	—	8.97	4,614
Piloted	2011	12/14/11	4,182	201	07/11/12	210	1985	81	509	12/02/13	1,580	186	06/06/14	905	18.11	5,762
Cargo 1	2013	12/05/13	3,717	111	09/25/14	294	1170	7	—	—	—	—	—	—	9.50	4,887
Cargo 2	2013	12/05/13	3,718	112	09/25/14	294	1171	7	—	—	—	—	—	—	9.50	4,889
Piloted	2014	01/23/14	4,096	184	08/11/14	200	1978	80	544	02/06/16	1,567	156	07/11/16	900	16.48	5,663
Cargo 1	2016	01/11/16	3,847	136	10/12/16	275	1482	16	—	—	—	—	—	—	11.88	5,329
Cargo 2	2016	01/11/16	3,848	137	10/12/16	275	1483	16	—	—	—	—	—	—	11.88	5,331
Piloted	2016	03/20/16	4,077	180	09/06/16	170	1946	76	595	04/24/18	1,567	126	08/28/18	891	16.15	5,644
Cargo 1	2018	05/11/18	3,631	99	12/01/18	204	1060	5	—	—	—	—	—	—	7.84	4,691
Cargo 2	2018	05/11/18	3,632	100	12/01/18	204	1060	5	—	—	—	—	—	—	7.84	4,692
Piloted	2018	05/17/18	3,666	100	11/13/18	180	1147	13	577	06/12/20	1,567	156	11/15/20	913	8.58	5,233
Cargo 1	2020	07/26/20	3,930	131	02/17/21	206	872	3	—	—	—	—	—	—	13.90	4,802
Cargo 2	2020	07/26/20	3,932	132	02/17/21	206	872	3	—	—	—	—	—	—	13.90	4,804
Piloted	2020	07/29/20	3,955	134	01/25/21	180	1045	9	542	07/21/22	1,580	200	02/06/23	922	14.40	5,534
Cargo 1	2022	08/31/22	3,982	138	08/15/23	349	890	3	—	—	—	—	—	—	14.93	4,873
Cargo 2	2022	08/31/22	3,984	140	08/15/23	349	890	3	—	—	—	—	—	—	14.93	4,874
Piloted	2022	09/19/22	4,272	192	04/07/23	200	1319	20	506	08/25/24	1,574	200	03/13/25	906	20.41	5,846
Cargo 1	2024	10/01/24	3,800	113	08/30/25	333	806	2	—	—	—	—	—	—	11.35	4,607
Cargo 2	2024	10/01/24	3,802	114	08/30/25	333	807	2	—	—	—	—	—	—	11.35	4,608
Piloted	2024	10/26/24	4,335	219	05/24/25	210	1682	46	495	10/01/26	1,580	199	04/18/27	904	21.26	5,914

* Velocity losses are included in TMI & TEI ΔVs

08/04/98

Tara Poston
Georgia Inst. of Technology
August 28, 1998

Propulsive or Aerobraking?

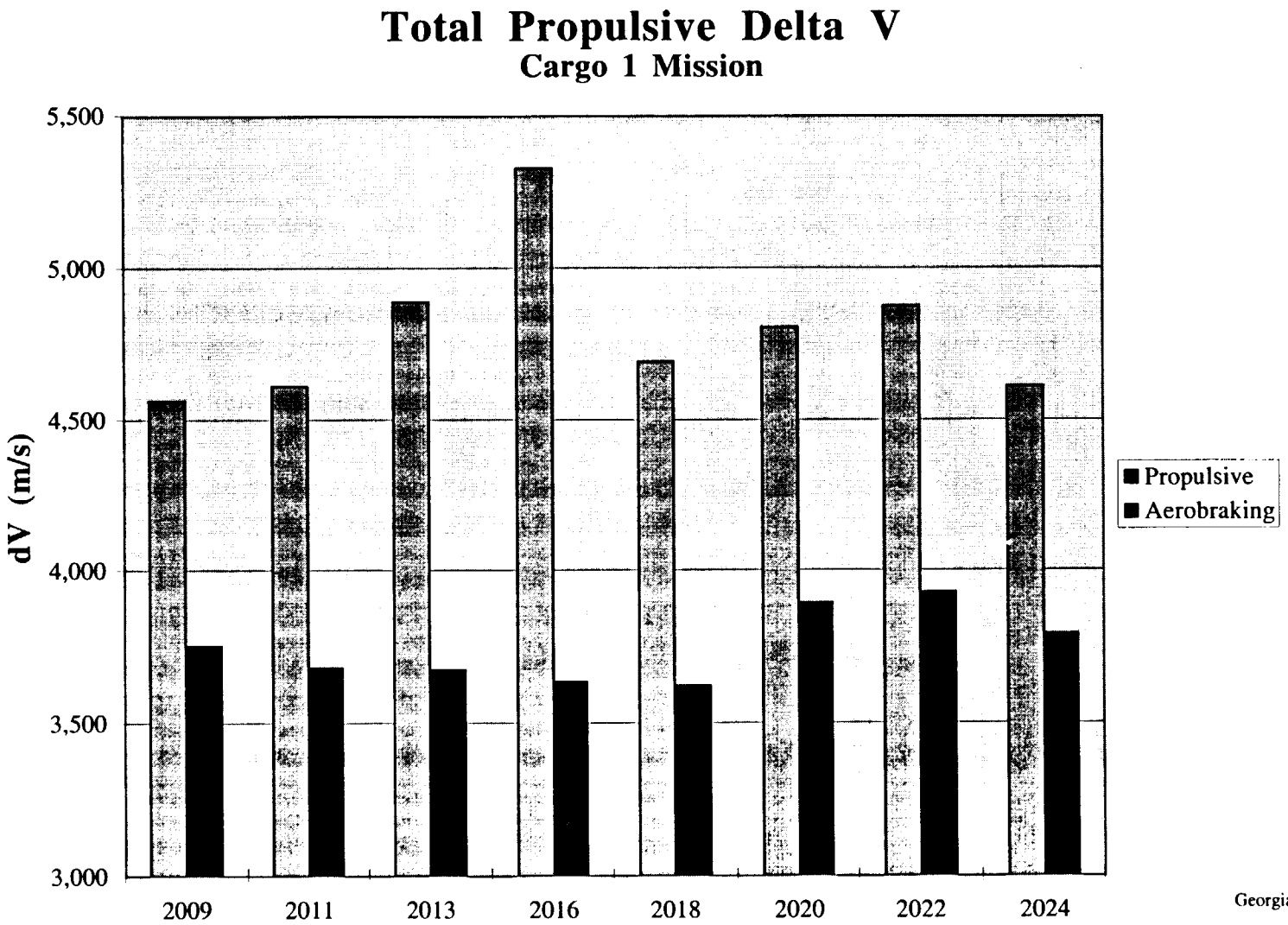

Tara Poston
Georgia Inst. of Technology
August 28, 1998

Propulsive or Aerobraking?

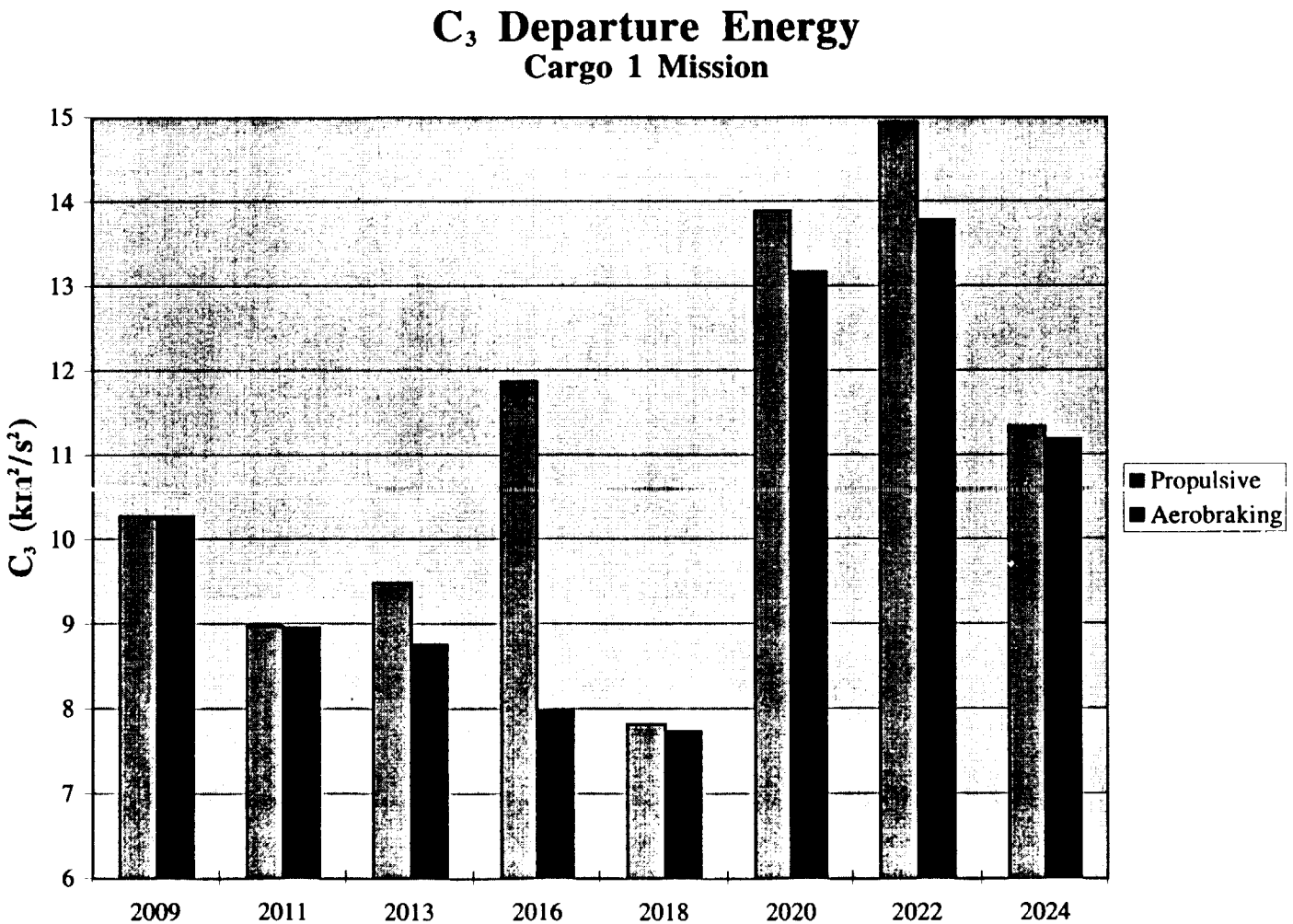

Tara Poston
Georgia Inst. of Technology
August 28, 1998

Propulsive or Aerobraking?

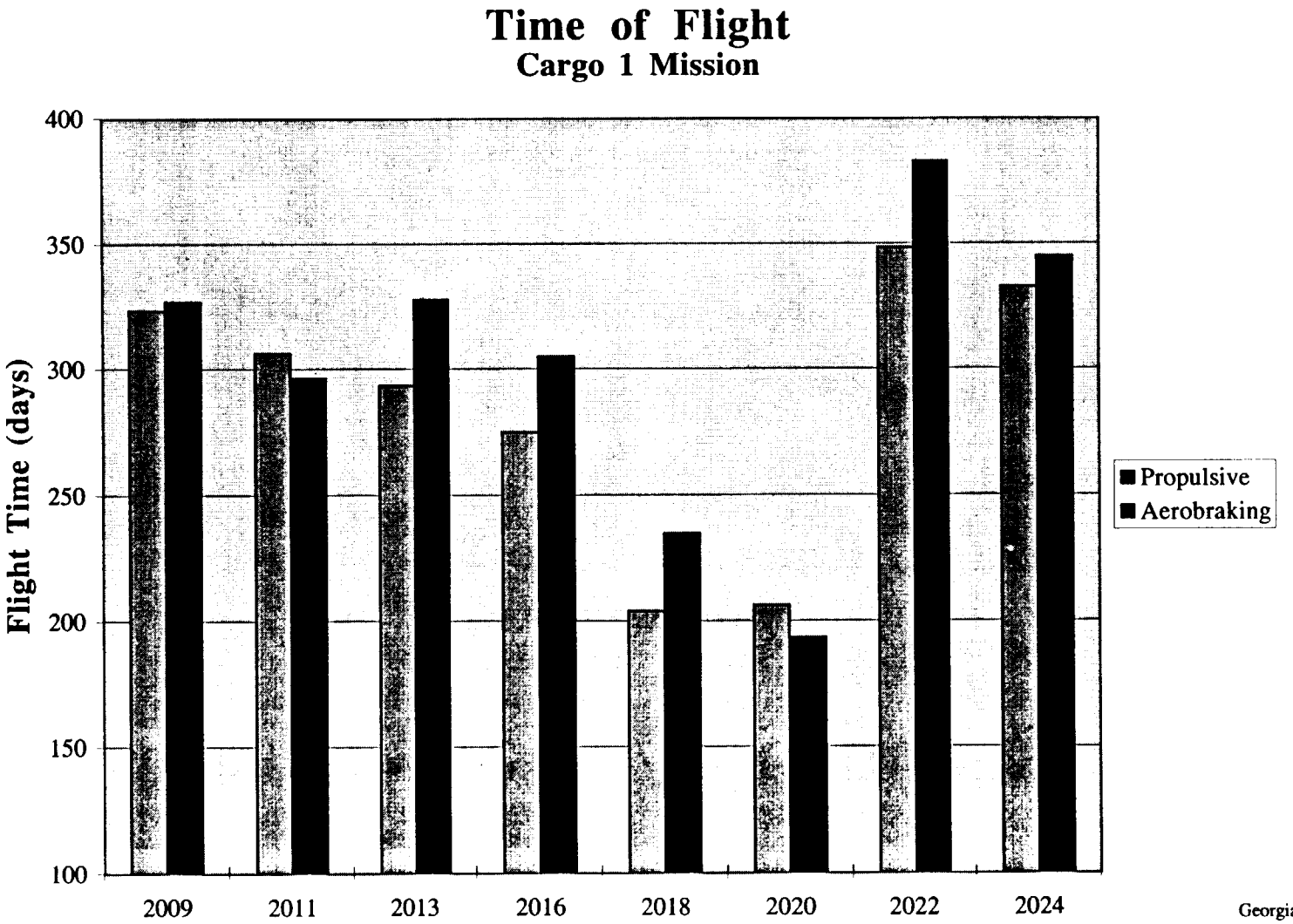

Tara Poston
Georgia Inst. of Technology
August 28, 1998

Propulsive or Aerobraking?

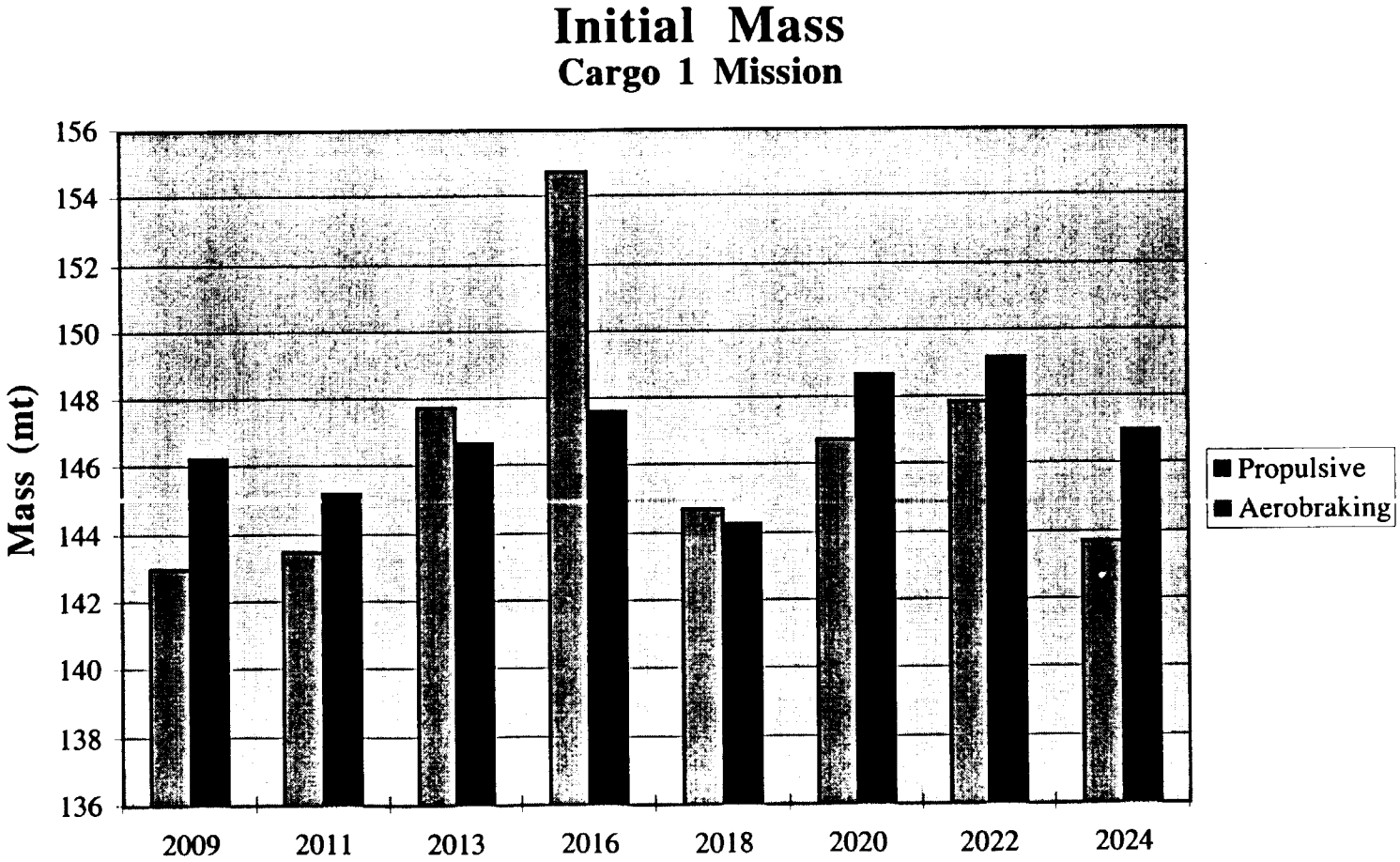

Note: A 10.6 mt Aerobrake was used for all Aerobraking cases except 2013 (11.6 mt/6.6 Km/s) & 2016 (12.7 mt/7.3 Km/s).

Tara Poston
Georgia Inst. of Technology
August 28, 1998

Benefits of Type I Cargo Trajectories

Additional Surface Time

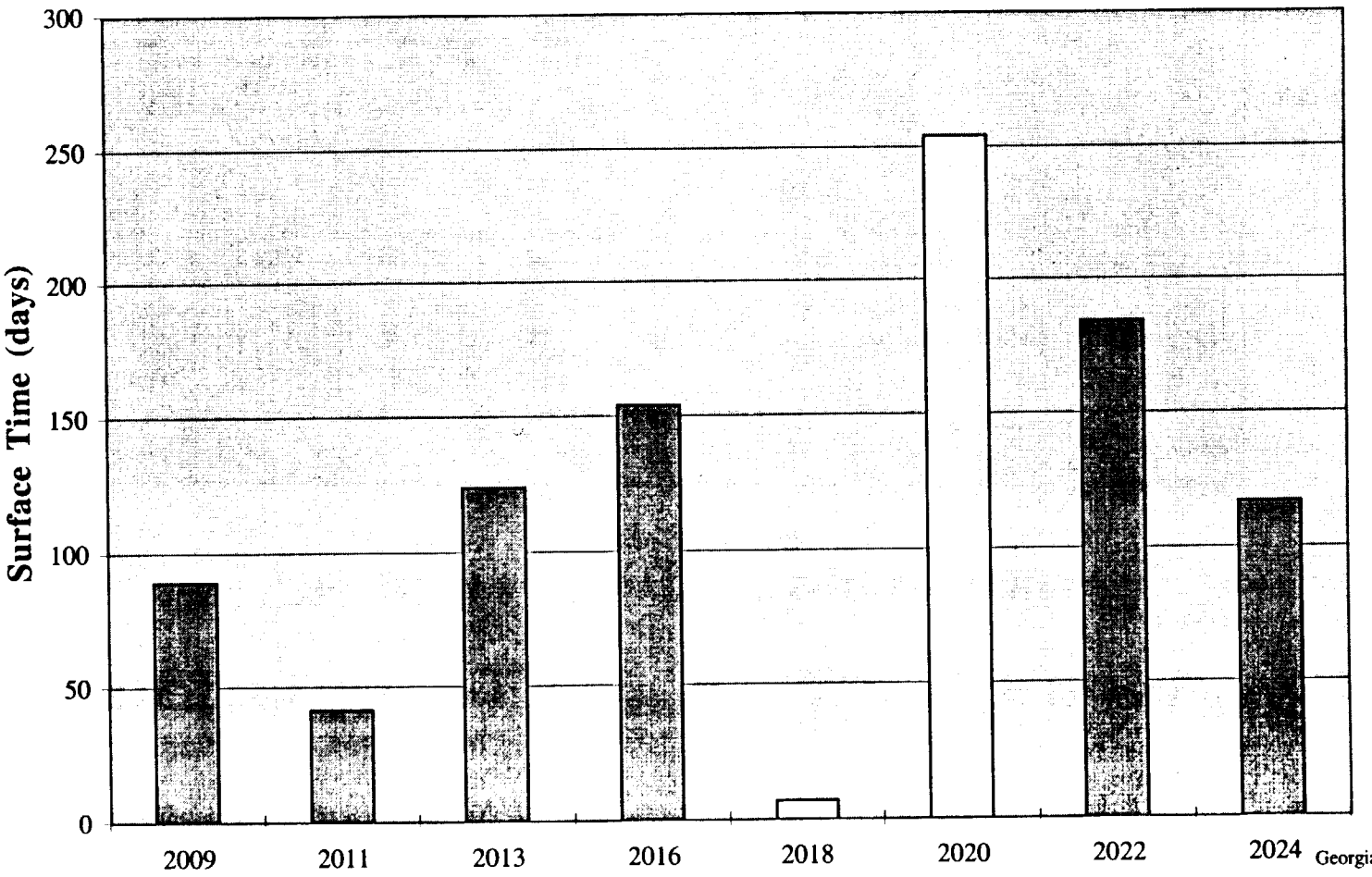

Tara Poston
Georgia Inst. of Technology
August 28, 1998

Benefits of Type I Cargo Trajectories

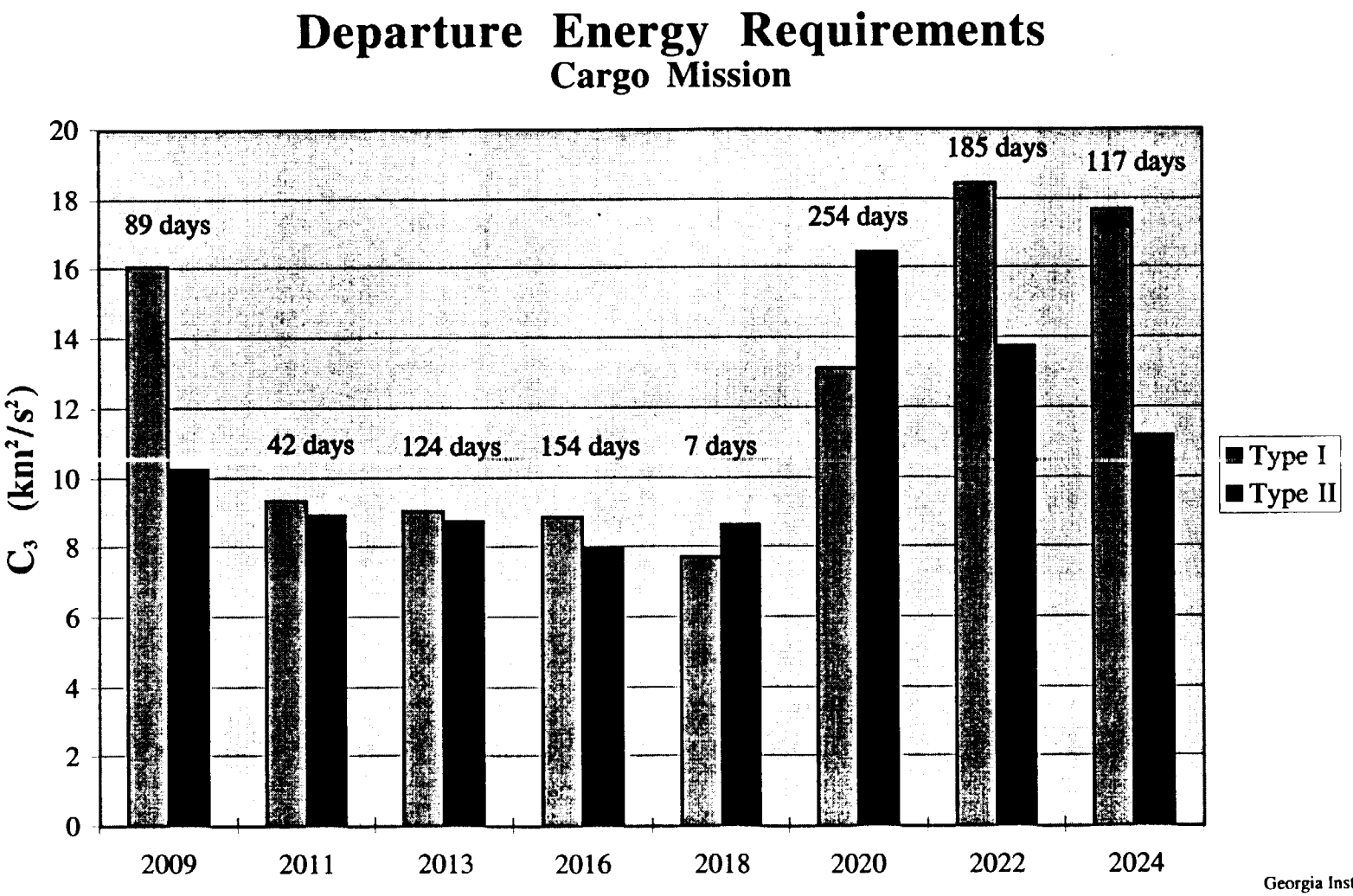

Tara Poston
Georgia Inst. of Technology
August 28, 1998

Benefits of Type I Cargo Trajectories

Flights to Mars Categorized By Opportunity (MOC w/ A/B)

Type I Trajectory vs. **Type II Trajectory**

Trajectory Type	Mission Type	Launch Year	TMI Date (m/d/yy)	TMI ΔV (m/s)	Velocity Losses* (m/s)	Mars Arrival Date (m/d/yy)	Outbound Flight Time (days)	Dep. C_3 (km^2/s^2)	Comments	Departure V∞ Earth (km/s)	Arrival V∞ Mars (km/s)	Arrival Velocity @ Mars (km/s)
II	Cargo 1	2009	10/14/09	3,752	112	09/06/10	327	10.27	Optimal min init mass	3.205	2.470	5.515
I	Cargo 1	2009	10/25/09	4,046	152	06/09/10	227	16.09	Forced Type I trajectory	4.011	4.051	6.382
	Type I Benefit			-294		89						
II	Cargo 1	2011	11/08/11	3,686	104	08/31/12	297	8.95	Optimal min init mass	2.991	2.751	5.647
I	Cargo 1	2011	11/16/11	3,706	107	07/20/12	247	9.36	Forced Type I trajectory	3.059	3.867	6.267
	Type I Benefit			-21		42						
II	Cargo 1	2013	12/31/13	3,677	104	11/24/14	328	8.78	Optimal min init mass	2.963	4.418	6.621
I	Cargo 1	2013	12/27/13	3,691	105	07/23/14	208	9.04	Forced Type I trajectory	3.007	5.340	7.269
	Type I Benefit			-13		124						
II	Cargo 1	2016	03/21/16	3,638	99	01/20/17	305	7.99	Optimal min init mass	2.826	5.368	7.289
I	Cargo 1	2016	02/20/16	3,682	104	08/19/16	181	8.87	Forced Type I trajectory	2.979	5.297	7.237
	Type I Benefit			-44		154						
II	Cargo 1	2018	05/06/18	3,670	103	01/16/19	255	8.64	Forced Type II trajectory	2.939	3.472	6.031
I	Cargo 1	2018	05/18/18	3,625	98	01/09/19	236	7.74	Optimal min init mass	2.782	3.263	5.914
	Type I Benefit			45		7						
II	Cargo 1	2020	08/24/20	4,067	155	10/09/21	411	16.50	Forced Type II trajectory	4.062	3.803	6.228
I	Cargo 1	2020	07/19/20	3,899	131	01/28/21	193	13.17	Optimal min init mass	3.630	2.857	5.699
	Type I Benefit			169		254						
II	Cargo 1	2022	09/14/22	3,930	135	10/02/23	383	13.79	Optimal min init mass	3.714	3.074	5.811
I	Cargo 1	2022	09/08/22	4,166	171	03/31/23	204	18.42	Forced Type I trajectory	4.292	3.653	6.137
	Type I Benefit			-236		185						
II	Cargo 1	2024	10/05/24	3,799	118	09/15/25	345	11.19	Optimal min init mass	3.345	2.541	5.548
I	Cargo 1	2024	10/13/24	4,129	165	05/21/25	220	17.72	Forced Type I trajectory	4.209	4.106	6.417
	Type I Benefit			-331		117						

* Velocity losses are included in TMI ΔVs

Tara Poston
Georgia Inst. of Technology
August 28, 1998

Mars Entry Speed Analysis

2014 Mars Entry Speed

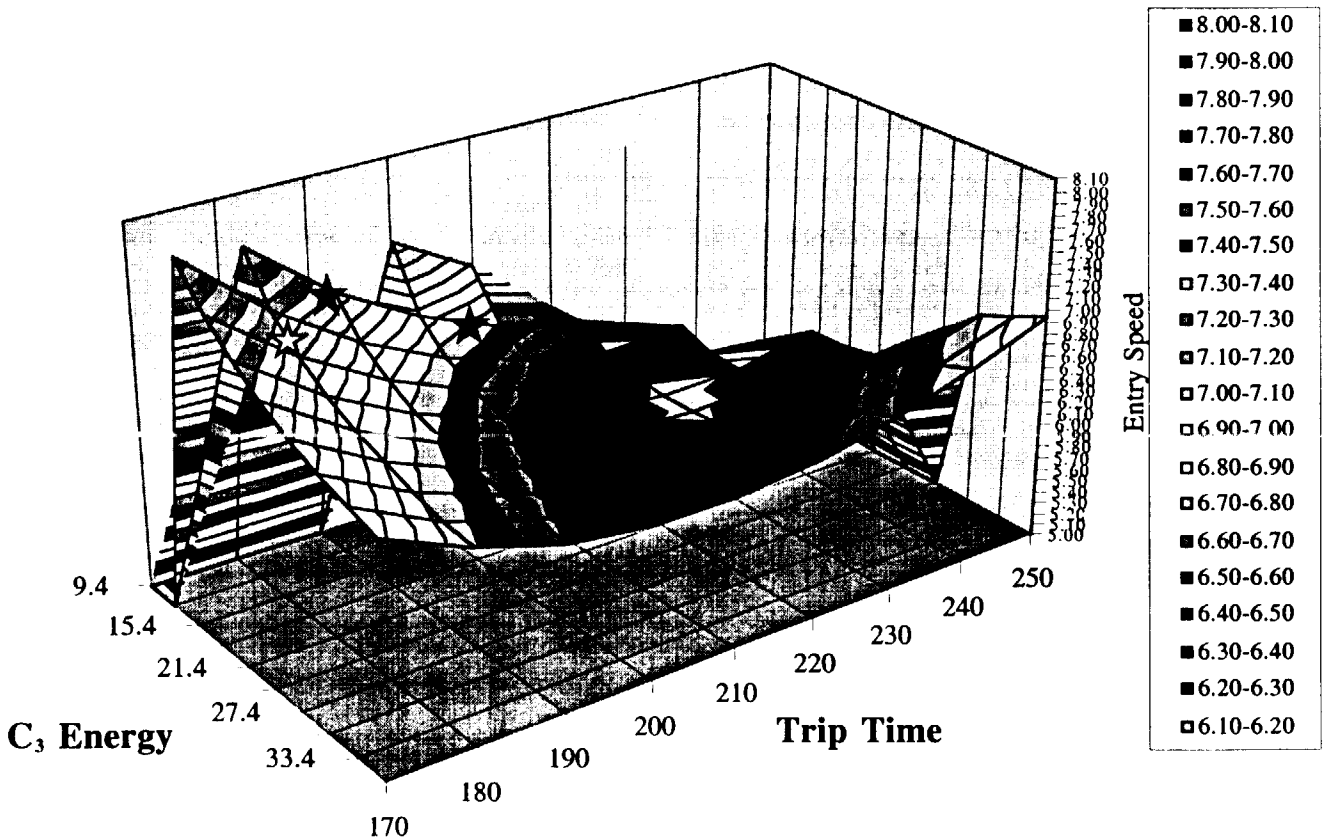

☆ 178 Days & C_3 = 17.8 Km^2/s^2

Payload=57mt

Tara Poston
Georgia Inst. of Technology
August 28, 1998

Enveloping 2014, 2016, & 2018 Piloted Missions

- Limitations:
  - 206 day maximum flight time
  - 12.83 km^2/s^2 maximum C_3
  - 7.36 km/s maximum Mars entry speed
- Additional Limit (shaded)
  - 180 day maximum flight time
- Findings:
  - All opportunities can be enveloped with initial limitations.
  - 2014 opportunity cannot be made in 180 days without relaxing other limitations.

2014	Flight Time	C_3 Energy	Mars Arrival Speed
No Restrictions	208	9.04	7.27
Min C_3	206	**9.06**	7.33
Min. Trip Time	**187**	12.83	7.36
Min Arrival Spd.	206	12.83	**6.64**
Min C_3	180	**16.43**	7.36
Min Arrival Spd.	180	12.83	**7.77**
2016			
No Restrictions	181	**8.87**	7.24
Min. Trip Time	**158**	12.83	7.36
Min Arrival Spd.	206	12.83	**6.18**
Min C_3	180	**8.88**	7.26
Min Arrival Spd.	180	12.83	**6.47**
2018			
No Restrictions	235	7.74	5.91
Min C_3	206	**7.83**	5.76
Min. Trip Time	**129**	12.83	7.36
Min Arrival Spd.	203	7.84	**5.75**
Min C_3	180	**8.11**	5.91
Min Arrival Spd.	180	10.14	**5.81**

Tara Poston
Georgia Inst. of Technology
August 28, 1998

Enveloping 2014, 2016, & 2018 Piloted Missions

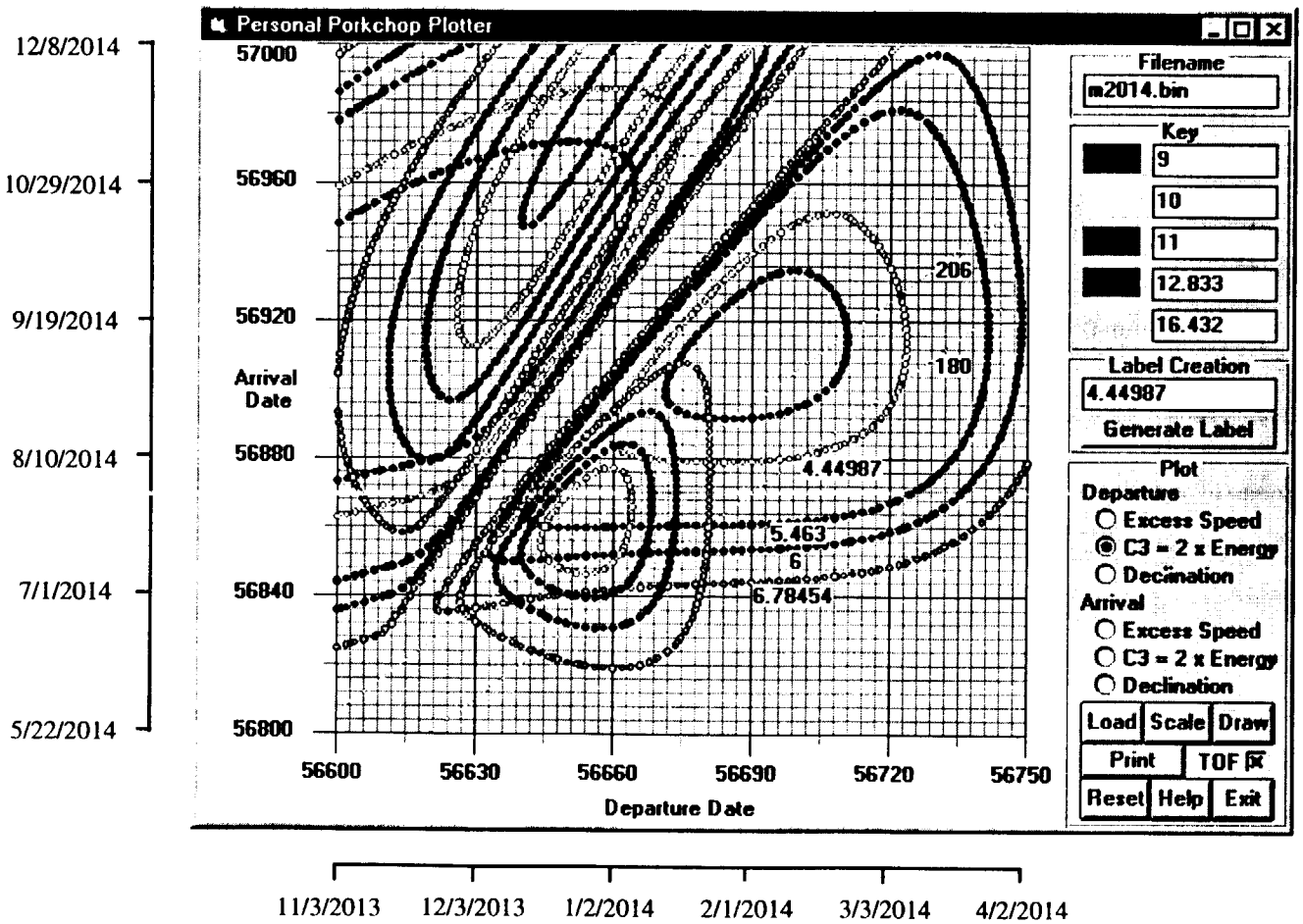

Tara Poston
Georgia Inst. of Technology
August 28, 1998

2026 - 2041 Opportunities

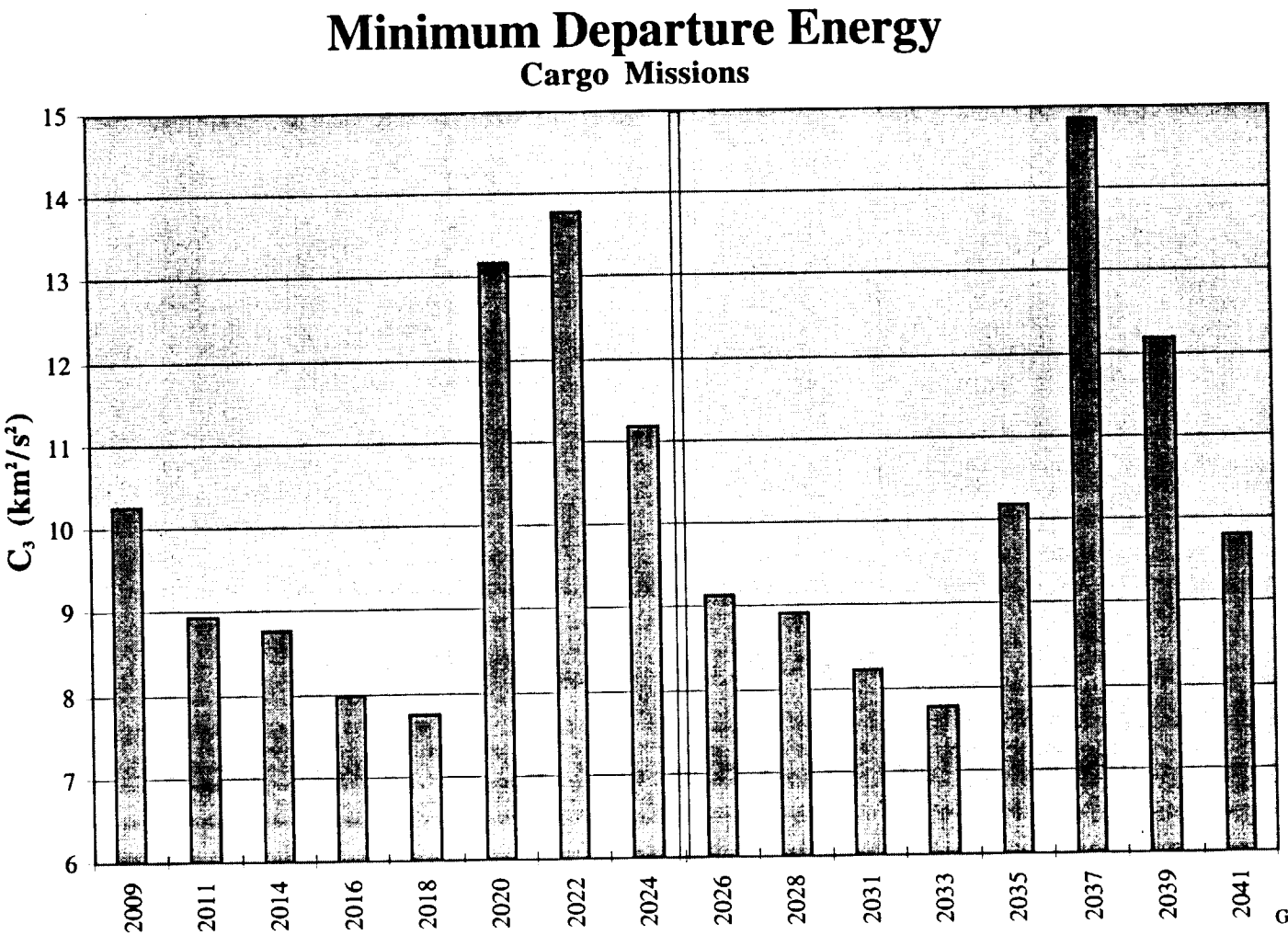

Tara Poston
Georgia Inst. of Technology
August 28, 1998

2026 - 2041 Opportunities

Cargo Mission Duration

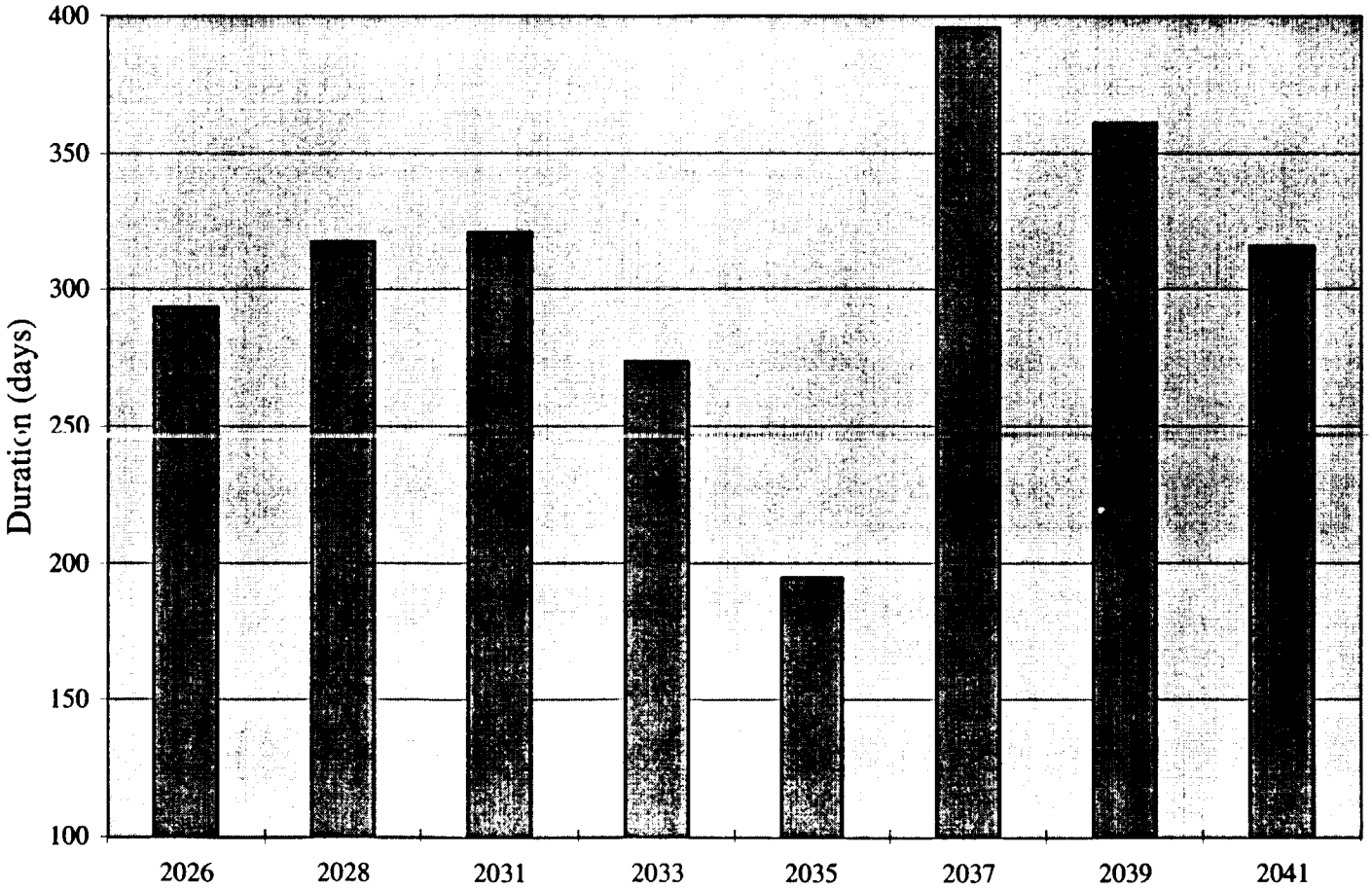

Tara Poston
Georgia Inst. of Technology
August 28, 1998

2026 - 2041 Opportunities

Optimal Type I Departure Energy
Piloted Missions

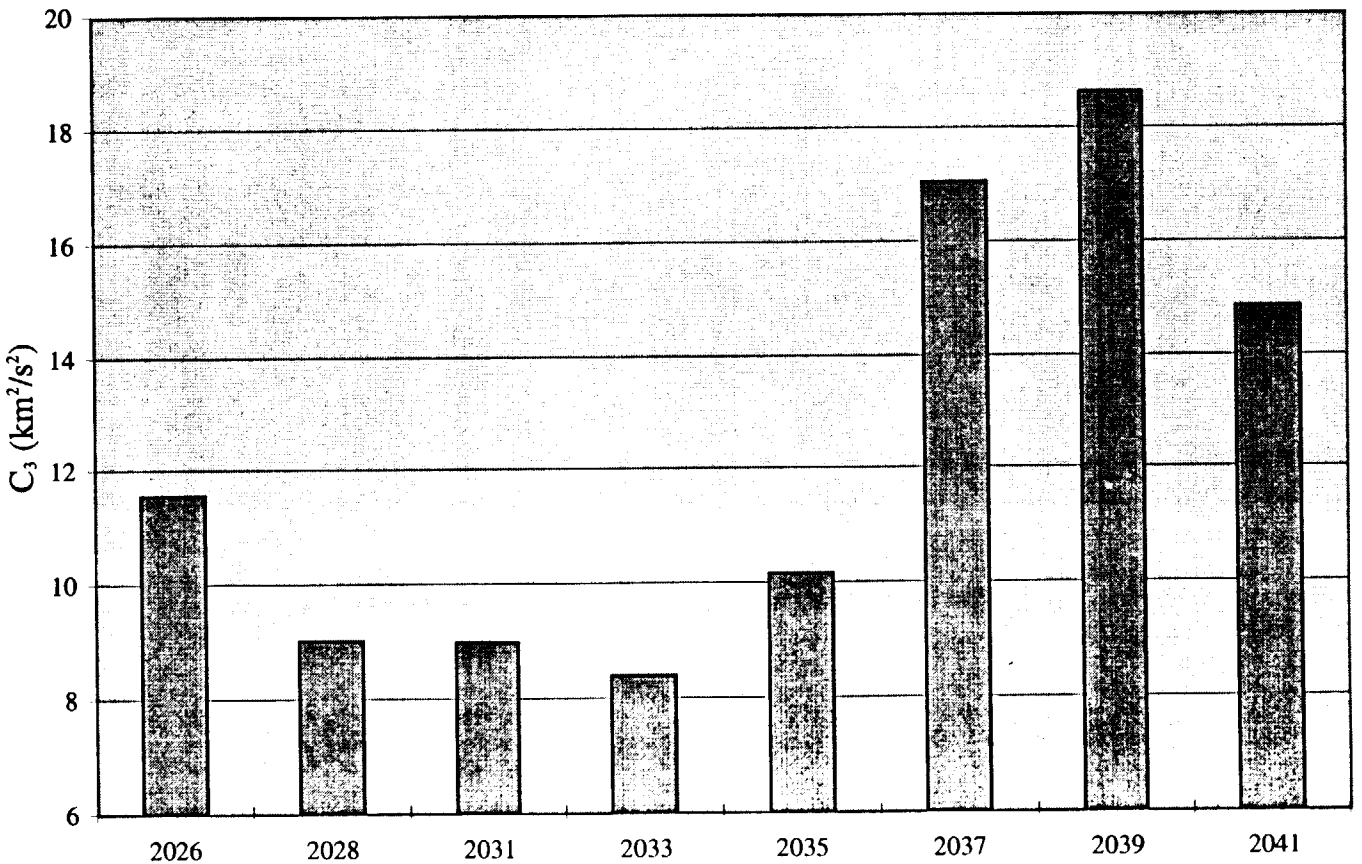

Tara Poston
Georgia Inst. of Technology
August 28, 1998

2026 - 2041 Opportunities

Optimal Type I Mission Duration

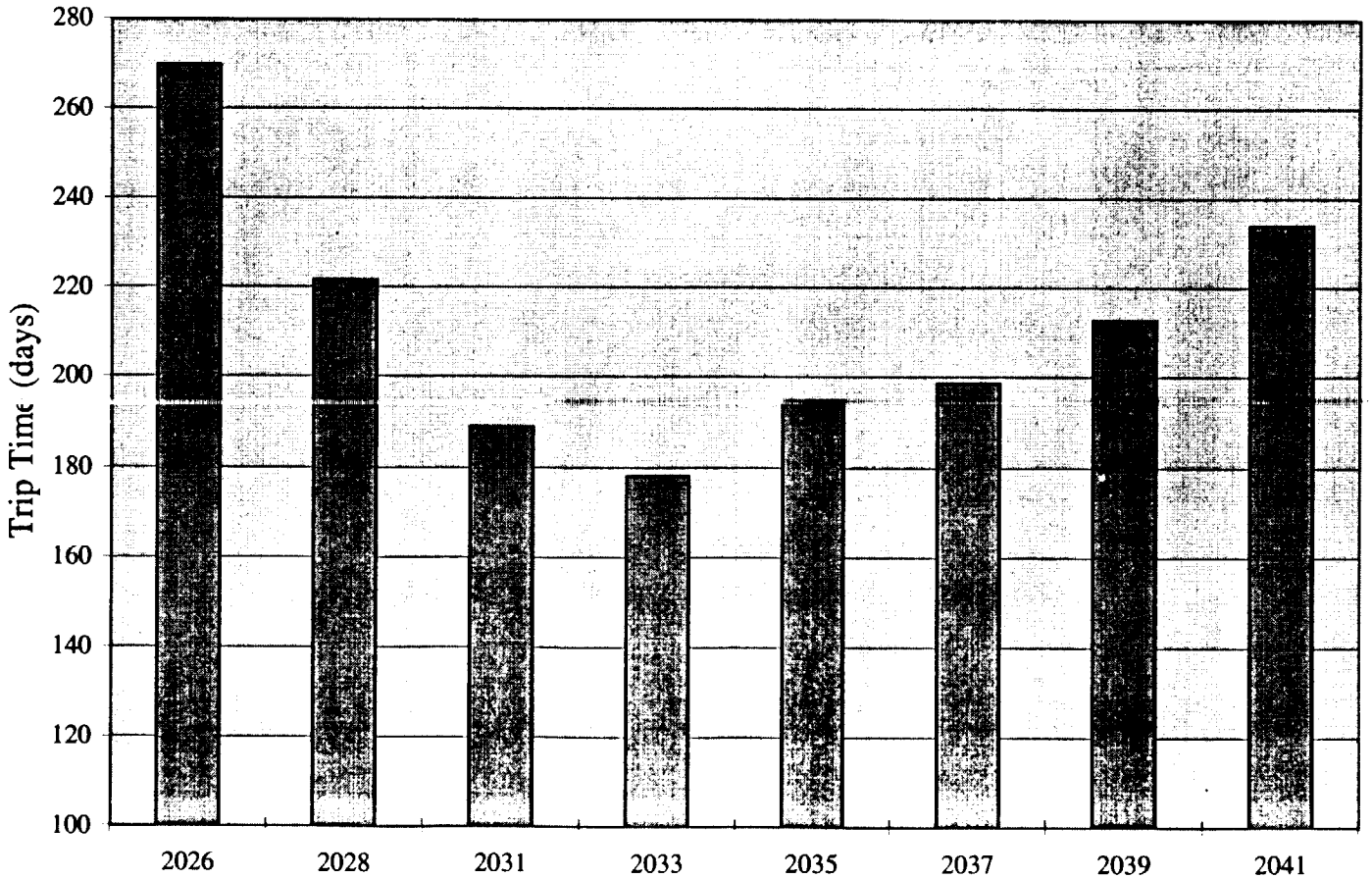

Tara Poston
Georgia Inst. of Technology
August 28, 1998

2026 - 2041 Opportunities

Additional Departure Energy Required for 180 Day Piloted Mission

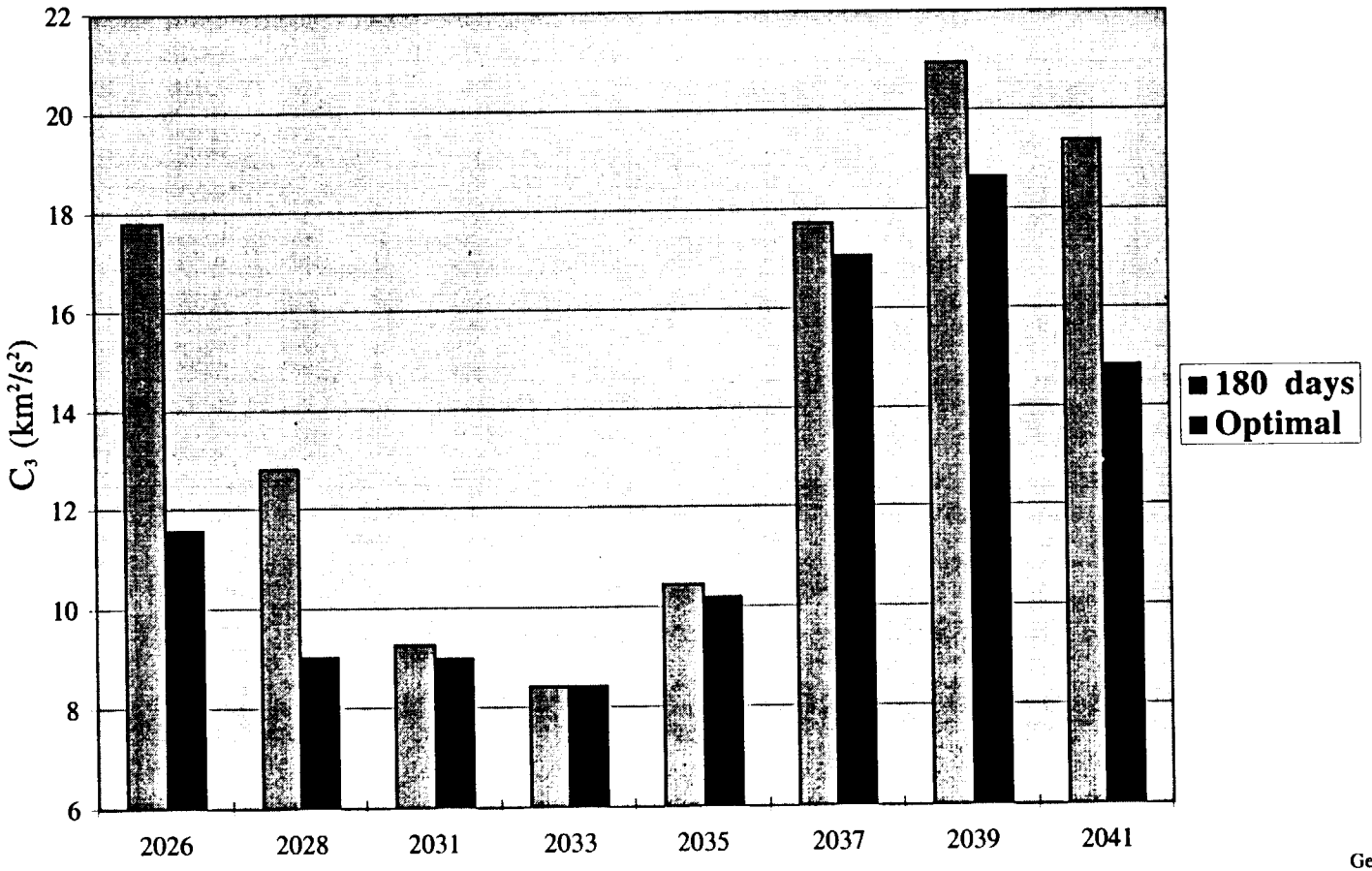

Tara Poston
Georgia Inst. of Technology
August 28, 1998

2026 - 2041 Opportunities

Flights to Mars Categorized By Opportunity

Mission Type	Launch Year	TMI Date (m/d/yy)	TMI ΔV (m/s)	Velocity Losses* (m/s)	Mars Arrival Date (m/d/yy)	Outbound Flight Time (days)	Mars Stay Time (days)	Mars Departure Date (m/d/yy)	TEI ΔV (m/s)	Return Time (days)	Return Date (m/d/yy)	Total Mission Duration (days)	Dep. C_3 (km^2/s^2)	Total Major Mission ΔVs (TMI+TEI) (m/s)
Cargo 1	2026	10/30/26	3,681	91	08/20/27	294	-----	-----	-----	-----	-----	-----	9.14	3,681
Cargo 2	2026	10/30/26	3,690	101	08/20/27	294	-----	-----	-----	-----	-----	-----	9.14	3,690
Piloted	2026	11/19/26	4,135	167	05/18/27	180	536	11/04/28	1630	180	05/03/29	896	17.80	5,764
Piloted	2026	10/27/26	3,819	121	07/24/27	270	415	09/11/28	851	265	06/03/29	950	11.58	4,670
Cargo 1	2028	12/02/28	3,670	90	10/16/29	318	-----	-----	-----	-----	-----	-----	8.93	3,670
Cargo 2	2028	12/02/28	3,680	99	10/16/29	318	-----	-----	-----	-----	-----	-----	8.93	3,680
Piloted	2028	12/21/28	3,881	129	06/19/29	180	546	12/17/30	1232	180	06/15/31	906	12.81	5,113
Piloted	2028	12/09/28	3,691	106	07/19/29	222	470	11/01/30	789	248	07/07/31	940	9.05	4,480
Cargo 1	2031	02/23/31	3,636	86	01/10/32	321	-----	-----	-----	-----	-----	-----	8.24	3,636
Cargo 2	2031	02/23/31	3,646	96	01/10/32	321	-----	-----	-----	-----	-----	-----	8.24	3,646
Piloted	2031	01/30/31	3,703	107	07/29/31	180	570	02/18/33	912	180	08/17/33	930	9.27	4,615
Piloted	2031	01/28/31	3,689	105	08/05/31	189	541	01/27/33	782	218	09/02/33	948	9.00	4,471
Cargo 1	2033	04/28/33	3,614	84	01/27/34	274	-----	-----	-----	-----	-----	-----	7.78	3,614
Cargo 2	2033	04/28/33	3,623	93	01/27/34	274	-----	-----	-----	-----	-----	-----	7.78	3,623
Piloted	2033	04/05/33	3,659	102	09/30/33	178	594	05/17/35	1097	180	11/13/35	952	8.41	4,757
Piloted	2033	04/05/33	3,659	102	09/30/33	178	585	05/08/35	1,060	198	11/22/35	961	8.41	4,720
Cargo 1	2035**	06/23/35	3,733	96	01/04/36	195	-----	-----	-----	-----	-----	-----	10.19	3,733
Cargo 2	2035**	06/23/35	3,693	106	01/04/36	195	-----	-----	-----	-----	-----	-----	10.19	3,693
Piloted	2035	06/24/35	3,762	114	12/21/35	180	572	07/15/37	1,604	180	01/11/38	932	10.45	5,366
Piloted	2035	06/23/35	3,749	112	01/04/36	195	551	07/08/37	1,545	195	01/19/38	941	10.19	5,294
Cargo 1	2037	09/06/37	3,963	122	10/07/38	396	-----	-----	-----	-----	-----	-----	14.85	3,963
Cargo 2	2037	09/06/37	3,976	136	10/07/38	396	-----	-----	-----	-----	-----	-----	14.85	3,976
Piloted	2037	08/23/37	4,132	166	02/19/38	180	549	08/22/39	1,841	180	02/18/40	909	17.74	5,973
Piloted	2037	08/21/37	4,097	160	03/08/38	199	514	08/04/39	1,485	220	03/11/40	933	17.07	5,582
Cargo 1	2039	09/27/39	3,831	107	09/22/40	361	-----	-----	-----	-----	-----	-----	12.18	3,831
Cargo 2	2039	09/27/39	3,842	118	09/22/40	361	-----	-----	-----	-----	-----	-----	12.18	3,842
Piloted	2039	10/04/39	4,298	195	04/01/40	180	537	09/20/41	1,897	180	03/19/42	897	20.97	6,195
Piloted	2039	10/01/39	4,178	174	05/01/40	213	469	08/13/41	985	270	05/10/42	952	18.64	5,163
Cargo 1	2041	10/20/41	3,714	94	09/01/42	316	-----	-----	-----	-----	-----	-----	9.81	3,714
Cargo 2	2041	10/20/41	3,724	104	09/01/42	316	-----	-----	-----	-----	-----	-----	9.81	3,724
Piloted	2041	11/07/41	4,216	180	05/06/42	180	534	10/22/43	1747	180	04/19/44	894	19.37	5,963
Piloted	2041	11/01/41	3,984	143	06/23/42	234	432	08/29/43	881	269	05/24/44	935	14.85	4,865

* Velocity losses are included in TMI & TEI ΔVs

** Type I trajectory

07/28/98

Tara Poston
Georgia Inst. of Technology
August 28, 1998

Vehicle Sizing - Single MLV Mission

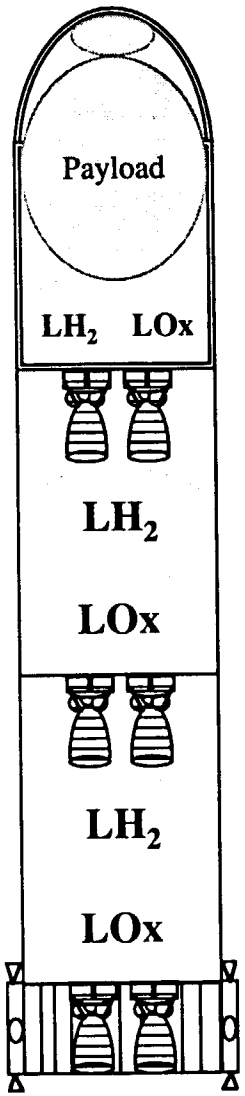

m_{ab} = 5.3 mt
$m_{parachute}$ = 0.7 mt
Surface Pyld = 13.5 mt

Descent Stage (2 RL-10s):
m_{dry} = 4.1 mt
m_p = 3.4 mt

Mars Orbit Payload (w/o A/B) = 21.3 mt

TMI Stage 2 (2 RL-10s):
m_{dry} = 4.1 mt
m_p = 21.2 mt

TMI Stage 1 (2 RL-10s):
m_{dry} = 4.1 mt
m_p = 21.2 mt
$m_{interstage}$ = 2.5 mt

One Magnum Stack Mass = 80 mt

Assumptions

- 80 mt = Magnum launch capability
- Aerobrake mass = 20% of Mars orbit mass
- C_3 = 10.27 km^2/s^2
- 2 stages for 2 burn Chemical TMI
  - Stage 1 jettisoned prior to stage 2 burn
- 2 RL10B-2 engines on each stage:
  - Isp = 466 sec
  - Thrust = 24.75 klb_f per engine
  - Mass = 0.31 mt per engine

Results

- Mass in Mars orbit = 26.6 mt
- Payload Mass on Martian surface = 13.5 mt

Tools Used

- COPA - Computerized Orbital Performance Analysis
- MAnE - Mission Analysis Environment

Tara Poston
Georgia Inst. of Technology
August 28, 1998

Vehicle Sizing - Dual MLV Mission

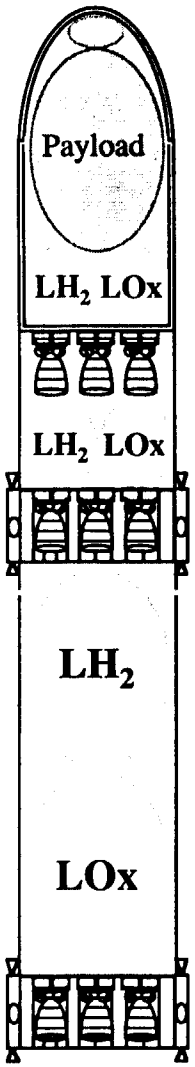

m_{ab} = 10.6 mt
$m_{parachute}$ = 0.7 mt
Surface Pyld = 29.5 mt

Descent Stage (3 RL-10s):
m_{dry} = 4.2 mt
m_p = 6.8 mt

Mars Orbit Payload (w/o A/B) = 42.6 mt

TMI Stage 2 (3 RL-10s):
m_{dry} = 3.6 mt
m_p = 20 mt
$m_{interstage}$ = 2.5 mt

TMI Stage 1 (3 RL-10s):
m_{dry} = 11.6 mt
m_p = 65.9 mt
$m_{interstage}$ = 2.5 mt

Two Magnum Stack Mass = 160 mt

Assumptions

- 80 mt = Magnum launch capability
- Aerobrake mass = 20% of Mars orbit mass
- C_3 = 10.27 km^2/s^2
- 2 stages for 2 burn Chemical TMI
  - Stage 1 jettisoned prior to stage 2 burn
- RL10B-2 engines on each stage:
  - Isp = 466 sec
  - Thrust = 24.75 klb_f per engine
  - Mass = 0.31 mt per engine

Results

- Mass in Mars orbit = 53.2 mt
- Payload Mass on Martian surface = 29.5 mt

Tools Used

- COPA - Computerized Orbital Performance Analysis
- MAnE - Mission Analysis Environment

Tara Poston
Georgia Inst. of Technology
August 28, 1998

Summary

- Trajectory Analysis
  - Propulsive or Aerobraking Mars Orbit Capture?
    Aerobraking was more efficient in most cases
  - Benefits of Type I Cargo Trajectories
    More surface time at the expense of additional TMI ΔV
  - Mars Entry Speed Analysis
    A complex optimization of departure energy, trip time, & entry speed
  - Enveloping 2014, 2016, & 2018 Missions
    Max C_3 = 12.83, Max Trip Time = 206 days, & Max Entry Speed = 7.36 km/s
  - 2026 - 2041 Opportunities
    A characterization of the next "15 year" cycle
- Vehicle Sizing
  13.5 mt to Martian surface with 1 Magnum
  29.5 mt to Martian surface with 2 Magnums

Tara Poston
Georgia Inst. of Technology
August 28, 1998